Master Thesis

im Rahmen des Universitätslehrganges „Geographical Information Science & Systems“ (UNIGIS MSc) am Interfakultären Fachbereich für GeoInformatik (Z_GIS) der Paris Lodron-Universität Salzburg zum Thema

Impact assessment of oil exploitation in Upper Nile State, South Sudan, using multi-temporal Landsat data

vorgelegt von

Alexander Mager

U1532, UNIGIS MSc Jahrgang 2011

Zur Erlangung des Grades
„Master of Science (Geographical Information Science and Systems) – MSc (GIS)“

Gutachter:
Ao. Univ. Prof. Dr. Josef Strobl

Gilching, 07.08.2013

Acknowledgements

This study was carried out in cooperation between *Bonn International Center for Conversion* (BICC) and the Department *GeoRisks and Civil Security* of the *German Remote Sensing Data Center* (DFD) of the *German Aerospace Center* (DLR).

I would like to thank Elisabeth Schöpfer, Kristin Spröhnle, Stella Hubert, Lars Wirkus, Elke Graewert and Lena Guesnet for their support, advice and patience.

Thanks to Fabian Selg for preceding work which was of great benefit.

Martin Petry provided great maps and shared valuable information for which I am grateful.

A very special thank you goes to Elmar Csaplovics for digging up Harrison and Jackson's 1958 classic study on the ecology of Sudan. I was deeply impressed and I am very grateful for his kind act.

Erklärung

“Ich versichere, dass ich die beiliegende Diplomarbeit ohne Hilfe Dritter und ohne Benutzung anderer als der angegebenen Quellen und Hilfsmittel angefertigt und die den benutzten Quellen wörtlich oder inhaltlich entnommenen Stellen als solche kenntlich gemacht habe. Diese Arbeit hat in gleicher oder ähnlicher Form noch keiner Prüfungsbehörde vorgelegen.“

Gilching, den 07.08.2013

Abstract

This study examined the spatial impacts of oil exploitation in Melut County, South Sudan, at six points in time between 1999 and 2011. Oil is the most important source of revenue for the South Sudanese government. The history of oil exploration and production in the area was characterized by bloodshed, displacement and other grave human rights violations as it unfolded against the backdrop of a vicious civil war. By means of geo-spatial techniques such as remote sensing and GIS analysis, changes in land use for farming, population growth and the expansion of oil fields were observed and the relationships between them was analyzed. Six points in time – 1999, 2002, 2004, 2006, 2009, 2011 – were chosen to mine Landsat-5 and -7 satellite data for features in order to map the state of the area and as a base for further analysis. Two very high resolution scenes from 2004 and 2012 were also applied to explore reported population growth in the town of Paloich. Three features were chosen to be extracted and analyzed: cropland, oil well pads and roads. Feature extraction consisted of on-screen digitization as well as classification approaches. With regard to the latter, pixel- and object-based classification of land cover was performed as a base for further object-based classification of cropland areas and oil well pads. While the land cover classifications reached high levels of accuracy, the classification of cropland and oil well pads was challenging. Digitized vector data was used instead for GIS analysis of the relationship and interplay between features. Apart from a sharp decline in cropland areas between 1999 and 2002, agricultural lands increased steadily over time and more than doubled in size. Oil infrastructure grew enormously in size throughout the whole time series with 555 oil well pads identified in 2011, compared to a single one in 1999. GIS analysis revealed that causal connections between the increase in all three types of features is likely but can ultimately not be assessed from satellite data alone. Very high resolution imagery and especially ground-truth data is strongly needed to further investigate the complex interplay between population growth, development of infrastructure and land use changes. The results were presented in 19 maps, providing an overall picture of the developments in the area of interest.

Table of Contents

List of Figures

List of Tables

List of Abbreviations

AOI	Area of Interest
CDE	Centre for Development and Environment
CNPC	China National Petroleum Corporation
CPA	Comprehensive Peace Agreement
DLR	German Aerospace Center
ESA	European Space Agency
ETM+	Enhanced Thematic Mapper Plus
ECOS	European Coalition on Oil in Sudan
FAO	Food and Agricultural Organization
GI	Geo-Information
GIS	Geo-Information System
GPCP	Global Precipitation Climatology Project
HR-2	High Resolution-2
JRC	Joint Research Centre
MSS	Multi Spectral Scanner
NASA	National Aeronautics and Space Administration
OBIA	Object-Based Image Analysis
ONGC	Oil and Natural Gas Corporation Limited
PDOC	Petrodar Operating Company
SLC	Scan Line Corrector
SPLM/A	Sudan People's Liberation Movement/Army
SRTM	Shuttle Radar Topography Mission
TM	Thematic Mapper
UN IMWG	United Nations (Sudan) Information Working Group
USGS	United States Geological Survey
VHR-1	Very High Resolution-1

1 Introduction

South Sudan is the most oil-dependent country in the world. More than 98% of the state budget is oil revenue (World Factbook, 2013). South Sudan is also the world's youngest country. A referendum in 2011 ended decades of bloody north-south conflict and sealed the split from Sudan. The young nation faces massive problems. The country as a whole is underdeveloped and suffers widespread poverty. A lack of infrastructure means that abundant natural resources cannot be tapped. South Sudan's fertile lands could feed "most of sub-Saharan Africa" (Economist, 2013, p.33).

The development of the oil fields took place against the backdrop of Sudan's second civil war which lasted from 1983 to 2005. It was ended by the adoption of the Comprehensive Peace Agreement (CPA) that foresaw a five-year period of autonomy for the south followed by a referendum. The discovery of oil added a major economic component to the civil war and deepened the divide between north and south. The central government in Khartoum tried to achieve full control of the oil fields, a majority of which is located in the south. Thousands of people were evicted from their homes in order to secure undisturbed development of the fields. Villages were destroyed, people killed and thousands forcefully displaced. Others fled the violence. Lands were confiscated. The areas around oil fields became no-go zones. Apart from the bloodshed, oil field development led to big-scale environmental problems. Crop patterns changed, poorly constructed roads led to drain blocks which caused draughts and floods and polluted ponds pose a danger for humans and animals alike (BICC, 2013; ECOS 2006; ECOS 2009).

Since 2011, the Bonn International Center for Conversion (BICC) has been working on a project named "Socio-economic repercussions of Chinese oil investments in South Sudan". It aims at analyzing the impacts of oil production in Melut and Maban Counties and their conflict-provoking potentials. By conducting interviews with the local population as well as politicians and oil managers, BICC researchers studied both positive and negative effects of oil production (BICC, 2013).

This study aims at supporting the work of BICC by adding a geo-spatial component. Geo-spatial technologies such as Remote Sensing and Geographical Information Systems (GIS) provide powerful tools for the analysis of activities and their impacts on a landscape. Especially multi-temporal satellite image analysis makes observation of features and associated changes possible. By covering wide areas, remotely-sensed data enables the monitoring of vast

territories to get an overall picture. This enhanced view backs the work done locally on specific sites and incorporates it into an overall spatial framework.

The study provides an overview of oil-related developments in Melut County for the period from 1999 to 2011. The object is to map human activity and to assess its impacts in the area of interest. In order to document the development of the oil fields and impacts on their surroundings, six points in time were chosen for comparison (see chapter 4 for details). The study asks the following questions: What changes can be observed? What spatial connections exist between those observed changes? Can they be explained with existing knowledge about events related to oil production?

In order to answer the questions, a two-step approach is taken. First, feature extraction is performed using various techniques. Second, the extracted features are being used to map the state of the area of interest at the aforementioned points in time and to analyze the relationships between them. Taken together, an overall picture of the situation and its development over time emerges.

Prins Engineering, working for the European Coalition on Oil in Sudan (ECOS, 2006), compared Landsat satellite data for the years 1999, 2000, 2001 and 2005 for parts of Melut County. The author found changes in agricultural use, settlement patterns and hydrology which confirmed findings gained through interviews conducted by ECOS in the area. While this study follows a similar approach, it widens the scope with regard to the relationship between oil infrastructure and land use change. Prins focused more on cropland pattern change only. Research on the impacts of oil extraction on the Russian landscape using Landsat data has been conducted by Sergey and Oganes (2009) and Aksyonov (2006). Even though they focus on oil spills which is not of concern for this study, they also captured oil infrastructure from satellite data and analyzed the possibilities and limits of doing so. Some of their findings were confirmed (see chapter 4.1). Russia was also the focus for Hese and Schmullius (2009) who, amongst other features, classified oil well pads from Landsat-5 data. A likewise approach was followed in this study leading to similar results. Selg (2013) followed a similar approach by analyzing very high resolution imagery. The author investigated object-based classification of oil infrastructure in detail.

The subject of the thesis is applied GI-Science. It does not investigate a single specific methodological problem in depth but shows how a variety of GI methods can be applied to solve a problem. Those methods include data capture, pixel- and object-based image analysis, GIS analysis and different forms of visualization.

2 South Sudan

South Sudan is a land-locked country in east-central Africa. Its north-south extent reaches from 3.49°N to 12.25°N while it stretches from 23.44°E to 35.95°E in east-west direction, covering an area of 644,329 km². The northern and central part of the country is characterized by low lying plains that rise to the highlands in the south where the country's highest peak, Kinyeti, 3,187 m above sea level, can be found. A massive swamp named Sudd is located in the center and is being fed by the White Nile, the main river crossing the country from south to north. The climate is characterized by seasonal rainfall and hot temperatures (World Factbook, 2013).

Figure 1: South Sudan

Different types of low and high rainfall savanna cover a substantial part of South Sudan. Woodlands are present in the south with some highland areas covered by montane vegetation (Harrison and Jackson, 1958).

South Sudan has a population of 11 million people from more than a dozen ethnic groups. It is one of the world's most underdeveloped countries with the majority of people living off subsistence agriculture (World Factbook, 2013). Maternity mortality is the world's highest with 2,054 per 100,000 births. With only 1% of the people having access to electricity, "'This place makes Afghanistan look developed'" as the Economist (2013, p.33) quoted a foreign helper. Even though South Sudan has abundant natural resources, the country is unable to exploit them due to a lack of infrastructure. If the country was able to tap its vast resources, the state could overcome its dependence on oil revenue which accounts for more than 98% of state budget (World Factbook, 2013).

As an independent country, South Sudan came into being on July 09, 2011, as a result of a referendum. An overwhelming majority of 98% of the electorate voted for secession and sealed the split from Sudan (World Factbook, 2013).

Sudan itself gained independence from Britain in 1956. Two long civil wars dominate Sudan's post-independence history. The second conflict, raging from 1983 until 2005, when the final North/South Comprehensive Peace Agreement (CPA) was signed, led to an estimated death toll of more than 2 million. The peace agreement of 2005 included a five-year autonomy for the South followed by a referendum on independence. The main reason for Sudan's bloody history in the 20th century was domination of non-Muslim, non-Arab southern Sudanese by Muslim, Arab northern Sudanese in terms of politics and economics (World Factbook, 2013). The main protagonists in the second civil war were the Government of Sudan and the Sudan People's Liberation Movement/Army (SPLM/A) which became the army of South Sudan after independence. It struggled for a democratic and secular state and finally for independence. Since secession, tensions persist between the two countries. On-going disputes concern oil revenue sharing, transport fees for South Sudan's use of Sudan's export pipelines, the unresolved status of the disputed region Abyei or the alleged South Sudanese backing of rebel groups fighting the government in Khartoum (BICC, 2013; Bloomberg, 2013).

2.1 Oil in Sudan

Oil was found in 1978 by the American company Chevron with a second major discovery three years later (ECOS, 2009, p.18). Chevron wanted to start oil production in the 1980s but cancelled its engagement due to civil war related fighting in oil areas (Shankleman, 2011, p.2). In 1993, small companies started to produce oil. In 1996 Sudan received large-scale investment in its yet to fully develop oil industry when the China National Petroleum Corporation (CNPC)

began to finance the development of oil fields and related infrastructure such as pipelines and export terminals. Other Asian companies like the Malaysian-owned Petronas and the Indian-owned Oil and Natural Gas Corporation Limited (ONGC) followed. Oil production began to surge. From a modest 2,000 barrels per day in 1993, extraction increased to 490,000 barrels a day in 2009. Sudan and South Sudan combined account for 0.6 percent of world oil production (Shankleman, 2011, p.3). As soon as oil was discovered, the struggle for control of it began. The division between the north and south of the country was widened by the fact that most of the oil fields are located in the south. The conflict between north and south was fueled by an important economic component. To achieve full control of the southern oil fields, the central government, with the help of southern militias, forcefully displaced thousands of people from the fields. “For over two decades, oil stood at the center of warfare. During the last years of the war, when oil production started, the oil fields became the main battlegrounds.” (ECOS, 2009, p.29). Grave human rights violations were committed. To enable oil companies to produce undisturbed, the local population was severely thinned out and a so called “cordon sanitaire” was erected around the production facilities (ECOS, 2009, p.6).

Figure 2: Oil concession areas in Sudan
The map was taken from ECOS (2007).

Since most of the oil fields are located in the south but the main infrastructure components – pipelines, refineries, Red Sea export terminal – are situated in the north (Figure 2), sharing of oil revenue was one of the key components in the CPA of 2005 (Shankleman, 2011, p.1). The not yet fully demarcated border between the two countries also crosses some oil fields. Disputes concerning transport fees for the use of Sudan's pipelines for South Sudanese oil led the government in Juba to unilaterally shut down oil production in early 2012. South Sudan also captured the Heglig oil field in Sudan. Both sides settled the dispute in March 2013 with oil production resuming in April and early May (BICC, 2013; Chicago Tribune, 2013).

2.2 Area of Interest

The area of interest (AOI) is located in Upper Nile state, one of South Sudan's ten states (Figure 3, Figure 4). It includes Melut County as well as parts of the counties Renk, Maban, Baliet, Fashoda, Manyo and a very small area in the north-western corner that belongs to Sudan (Figure 46). The size of the AOI is approx. 10,500 km² (104 km x 101 km).

Figure 3: Location of AOI (red square)

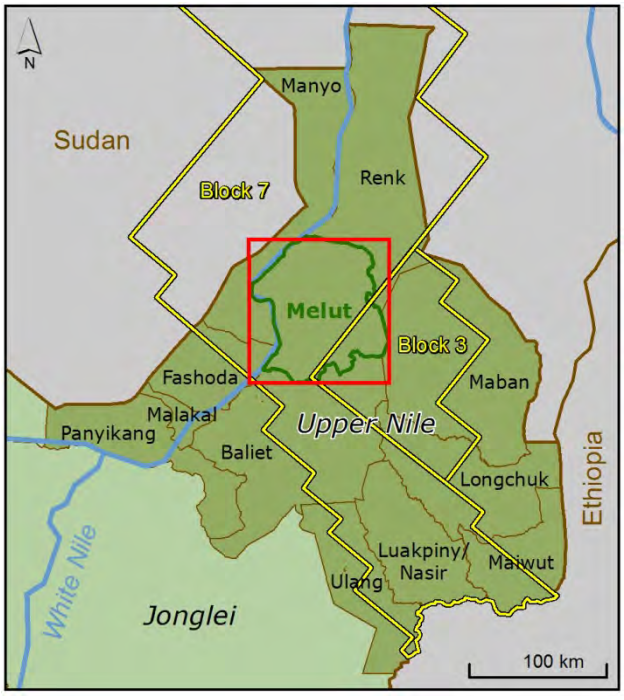

Figure 4: Counties of Upper Nile State

Even though the AOI comprises parts of neighboring counties, Melut County is the focus area of this study (please note that the northern top of Melut County is not part of the AOI (Figure 5). Reasons are given in chapter 3.4.1. Even though the county covers an area of 6,951 km² (BICC, 2013, p.30), the actual size of the dataset containing Melut County's borders measures only 6,945.53 km². After subtraction of the northern top, which has a size of 26.97 km², 6,918.56 km² remain. This is the number all calculations are based on in this study when referring to Melut County. The difference to the number given by BICC is 32.44 km² which is small enough to be neglected. The overall outcome of the study will not be affected.)

Melut County's western border is formed by the White Nile. Seasonal streams, Khor in Arabic, cross the area in east-western direction. Melut and its neighboring counties are part of a flat, clay plain. During the rainy season which lasts from June to October, the southern and central parts of the area get swampy (ECOS, 2006, p.7). November to May constitutes the dry season. The climate is hot with annual mean temperatures between 26° and 28° Celsius. Annual mean rainfall ranges between 600 and 800 mm (UNEP, 2007, p.40) (see chapter 5.6.1 for precipitation data analysis). According to Harrison and Jackson (1958), the AOI is part of two ecological zones: the north and center belong to "Low Rainfall Woodland Savannah". This area has been further characterized as being covered with "Acacia seyal-Balanites Savannah, alternating with grass areas". The south of the AOI is part of the larger "Flood Region" with higher rainfall than the north.

According to the 2008 census, 49,242 persons live in Melut County. The census data is generally regarded as underestimating the real number of inhabitants. The two major towns of the county are Paloich and Melut with 16,215 and 14,554 inhabitants in 2008, respectively. BICC (2013, pp.30-32) estimates the number of persons living in Melut County to be approx. 70,000 for mid-2013. Population seems to grow. The main ethnic group is the Dinka (BICC, 2013, pp.31-33). According to the 2008 census, 38% of Melut Counties inhabitants still live off farming. The average size of cultivated land per household is 2 hectares. (SSNBS, 2010, p.88) In the past, the majority of people lived off a combination of agricultural activities and pastoralism. The main crops are millet and sorghum. Tapping of gum Arabic trees provides another source of income. The land is used seasonally for a variety of activities and in different ways. During the dry season, pastoralists migrate with their cattle to wet areas along the main rivers where they live in temporary houses. At the beginning of the rainy season, those temporary settlements are left again for migration back to dryer grazing areas. During the rainy season, people work in rainfed agriculture on the higher planes. Some sub-sections of the Dinka do not migrate at all but stay permanently near the river banks for fishing, hunting and

agriculture. Some other people regard the wet season settlements as their primary homes (BICC, 2013, p.33; ECOS, 2006, p.7; Prins, 2010, p.4).

These patterns of living were disturbed by oil exploitation. Research by Bol (2012 cited in BICC 2013, p.34) found that "oil-related activities disturbed and disrupted the life in more than two-thirds (325) of 476 villages in Blocks 3 and 7." (See Chapter 2.2.1 for more detail.)

Melut County is divided into seven payams, the second-lowest administration level in South Sudan (BICC, 2013, p.30). The names of the payams are in some cases based on the main settlement they contain but not in every case. The name in brackets indicates the main settlement: Melut (Melut), Paloich (Paloich), Galdora (Galdora / Khor Adar in Arabic), Thiangrial (Thiangrial), Wonamum (Athieng), Gomochok or Bimachuk (Pariak) and Panomdiet (Panomdiet) (Petry, 2013c). See chapter 5.1 for some explanations regarding place names in the area of interest.

2.2.1 Oil exploitation and conflict in Melut County

The AOI lies in concession blocks 3 and 7 (Figure 2, Figure 4). In 1981, the Adar Yale oil field in Block 3 was discovered by Chevron (ECOS, 2009, p.18) but extraction was cancelled for security reasons as explained above. Oil production in Adar Yale began in 1997. In 2003, Petrodar, which exploits the oil fields in the AOI, announced major findings in block 7 and 3 with the Paloich field being the most important one (ECOS, 2011, pp.19-20). Petrodar Operating Company (PDOC) is a consortium of various Asian companies with CNPC and Petronas of Malaysia being the members with the biggest share. Exploration of the Paloich field began in 2001. In 2006, the Melut Basin Pipeline was opened which runs from the Paloich and Adar Yael oil fields in northern direction to Port Sudan. In the same year, full production started on the Adar Yale and Paloich fields (BICC, 2013, p.20).

In order to create the aforementioned "cordon sanitaire" around the oil fields, the government of Sudan forcefully displaced thousands of people in Melut and Maban Counties. Hundreds of villages were affected by the construction of oil well pads, roads, ponds and other infrastructure. Some villages vanished completely (ECOS, 2011, p.20; BICC, 2013, p.34). "The wave of destruction peaked in 1999-2002, preceding and coinciding with the development of the oil fields." (ECOS, 2006, p.19). Sudanese troops, supported by Government-backed southern Dinka militias, attacked villages, sometimes even using helicopter gunships or bomber aircraft. At that point, the SPLA did not present a threat to the oil fields (ECOS, 2006, p.19). In 2000-2001, 48 villages were allegedly destroyed (ECOS, 2006, p.14). Thousands of

displaced people settled in towns such as Paloich and Melut. After the CPA was signed in 2005, displaced people and refugees started to return in great numbers. Many found their villages destroyed (ECOS, 2006, p.19). Apart from death and destruction, the development of the oil fields caused environmental problems and changed socio-economic patterns of life (BICC, 2013, p.34). Environmental problems included drain blocks caused by poorly constructed roads which disrupt the natural flow of water and lead to flooding in some areas with droughts in others. These in turn caused changes in crop patterns (ECOS, 2006, p.22). Road construction had a negative impact on agricultural production. The Petrodar pipeline prevented cattle from crossing it (Wesselink, 2006, p.4). Ground water levels were reportedly falling in some areas. Whether or not oil production was responsible remains unclear. Ponds for disposal of "produced water", a by-product of oil extraction, posed a risk to humans and animals alike. Sometimes during the rainy season the pools (Figure 6) overflew, flooding the adjacent areas with oil-polluted water (BICC, 2013, p.40, p.53).

Positive effects could also be observed. As by-products of oil field development, the construction of roads, the increase of electricity supply and mobile coverage networks brought benefits to an underdeveloped region (ECOS, 2006, p.22). Positive socio-economic change like market integration took place, though yet on a very small scale only (BICC, 2013, p.35).

3 Remote Sensing

This chapter introduces selected remote sensing concepts as well as the data that was used for this study.

3.1 Classification

Apart from visual interpretation, which can be arduous but usually yields good results, classification of satellite data is the most important way of obtaining information from imagery. It is based on the categorization of pixels into classes according to different characteristics they possess. Various approaches such as spectral pattern recognition, spatial pattern recognition or temporal pattern recognition exist. For this study, one spectrally oriented approach – supervised pixel-based classification – was applied. The above mentioned techniques examine the characteristics of single pixels in a multi-dimensional feature space. A different way of information-extraction starts with the idea of segmenting imagery into homogenous objects consisting of single pixels. In a second step, these objects are classified according to criteria such as color or shape, i.e. spectral and spatial characteristics. The approach just described is called object-based classification or object-based image analysis (OBIA) and has been applied in this study as well (Lillesand, 2008, pp.545-547; p.581).

3.1.1 Pixel-based classification

Various techniques exist to separate single pixels into classes according to spectral characteristics with unsupervised and supervised classification being the most prominent ones. Unsupervised classification aims at grouping pixels with similar spectral characteristics into cluster. A variety of mathematical models, such as Maximum-Likelihood, Minimum-Distance-to-Means or Parallelepiped, have been developed to realize this. Supervised classification differs by utilizing training data to define classes before the actual classification process. While unsupervised classification categorizes pixels on a purely mathematical base, supervised classification uses training areas to numerically describe the spectral attributes of the classes aimed at. The pixels will then be put into the class they most closely resemble according to a mathematical model or algorithm (Lillesand, 2008, p.549; Albertz, 2007, pp.158-161).

The algorithm applied in this study is the Maximum-Likelihood approach. It is based on the assumption that “the distribution of the cloud of points forming the category training data is Gaussian (normally distributed)” (Lillesand, 2008, p.554). Lillesand (2008, p.554) calls this assumption to be “generally reasonable for common spectral response distribution”. The

algorithm then computes the probability of a pixel belonging to a specific class. Maximum-Likelihood is considered to be computationally intensive but at the same time to yield good results (Albertz, 2007, p.159). It is “the most widely used method for the classification of land cover” (Frohn et al., 2009).

3.1.2 Object-based classification

According to Blaschke and Strobl (2001), “Human perception does not observe, nor do we actually think in pixels”. Human beings perceive objects instead. As the spatial resolution of satellite data continued to improve, the problem arose that objects of interest were no longer represented by single pixels (Figure 6). Homogenous groups of an ever increasing number of pixels represent real life objects. Single pixels in very high resolution satellite data usually belong to the same class or object of interest (Blaschke and Strobl, 2001; Blaschke, 2010). Pixel-based classification approaches did not take this into account nor did they consider contextual information. OBIA offers means to overcome the shortcomings of traditional pixel-based approaches. Before the actual classification process starts, segmentation is performed, i.e. division of the image into homogenous and hopefully “semantically significant groups” (Blaschke, 2010). Apart from possessing additional spectral information, e.g. minimum and maximum as well as mean values, segments contain spatial information. That means they can be addressed by spatial characteristics such as their size, shape or relationship to neighboring objects which allows for a wide range of classification possibilities compared to single-value pixels (Blaschke, 2010).

Even though OBIA was developed to cope with challenges posed by very high resolution satellites such as IKONOS, GeoEye or QuickBird, object-based approaches have successfully been applied to Landsat TM and ETM+ data. Frohn et al. (2009) mapped wetlands in Florida, reaching a much higher overall/producer’s/user’s accuracy and kappa coefficients (see chapter 3.3) for the object-based classifications compared to the pixel-based maximum-likelihood algorithm. Magalhaes et al. (2012) transferred Frohns method to classify wetlands in Brazil, resulting in object-based classification outcomes that represented the shape and distribution of the wetlands better than the classification results of a maximum-likelihood approach. The opposite result – maximum-likelihood classification yielding better results than an object-based one – was the finding of the approach of Dorren (Maier and Seijmonsbergen, 2003) in order to map forests in a mountainous Austrian region with Landsat-5 TM data. Even though the pixel-based classification reached a slightly higher level of accuracy, OBIA classification provided better overall results as stated by local foresters.

3.2 Indices

The information contained in single band pixel values is limited. Several methods have been developed to mine satellite data for much more information. These techniques are based on differences and ratios between bands. The resulting parameters are called indices. The following four indices were applied.

The Normalized Difference Vegetation Index (NDVI) utilizes the fact that green vegetation strongly correlates with reflectances in the infra-red spectral bands. Rouse et al. (1974) monitored vegetation systems in the Great Plains of the United States and defined the NDVI as

$$\frac{NIR - RED}{NIR + RED}$$

with NIR and RED being the reflectances in the near-infrared and red spectral bands. The NDVI has been applied and studied extensively.

Baret and Guyot, (1991) compared NDVI with other indices and reported reduced reliability in sparsely vegetated areas, especially when soils appear very bright. To overcome these shortcomings, vegetation indices that account for soil properties were developed such as the Soil Adjusted Vegetation Index (SAVI) (Huete, 1988). SAVI was tested but finally not applied in this study since it was found not to improve classification results. Qi et al. (1994) proposed a Modified Soil Adjusted Vegetation Index (MSAVI). It is based on SAVI but modified to allow for greater vegetation sensitivity which the authors define as the "'vegetation signal' to 'soil noise' ratio". MSAVI was used in this study for object-based classification and is computed as

$$\frac{2NIR + 1 - \sqrt{(2NIR + 1)^2 - 8(NIR - RED)}}{2}$$

with NIR and RED being the reflectances in the near-infrared and red spectral bands.

Bare Soil Index (BSI) and Burned Area Index (BAI) were also applied. BSI enhances "bare soil areas, fallow lands and vegetation with marked background response" (Azizi, Najafi and Sohrabi, 2008) and is computed as

$$\frac{(Mean\ NIR + Mean\ GREEN) - Mean\ RED}{(Mean\ NIR + Mean\ GREEN) + Mean\ RED}$$

with Mean representing the mean values of the corresponding spectral bands.

Burned Area Index, which has been developed for Mediterranean areas, is very sensitive to charcoal signals of burned areas. The index was defined by Martin in 1998 as

$$\frac{1}{(0.1 - Mean\ RED)^2 + (0.06 - Mean\ NIR)^2}$$

with Mean representing the mean values of the corresponding spectral bands. Chuvieco (Martin and Palacios, 2002) compared it to NDVI, SAVI and GEMI and found BAI to better identify burned areas than any of the other indices. Though the Southern Sudanese landscape differs significantly from Mediterranean lands, BAI led to very satisfying results in burned area detection (see chapter 5.2 – 5.4).

3.3 Accuracy Assessment

In order to be able to judge the quality of a classification it is necessary to perform an accuracy assessment. As Congalton (1991) put it: "'It looks good is not a valid accuracy statement.'" Instead, ground truth data collection is necessary for a comparison with classification results (Congalton, 1991). If ground truth data is not available, a second data source that is assumed to be correct can be used as a reference data set instead. The standard way of presenting classification results is the error matrix. While its rows contain the classification results, its columns represent the reference data. An error matrix represents the relation between classified and reference data. Table 5 – Table 8 show examples for matrices. Three statistical measures can be derived from an error matrix: Overall accuracy, user's accuracy and producer's accuracy. The first one, overall accuracy, is the sum of correctly classified pixels divided by the total number of pixels in the matrix. User's accuracy provides information about errors of inclusion. To calculate it, the number of correctly classified pixels in a class is divided by the total number of sample pixels from the same class. User's accuracy is a measure of commission. To give an example, a user's accuracy of 60% for Wetland means that only 60% of the areas called Wetland are actually Wetland (Congalton, 1991). By contrast, producer's accuracy indicates errors of exclusion, so called omission errors. The number of correctly classified pixels in a class is divided by the total number of pixels of the same class as derived from the reference data. Transferred to the Wetland example, a producer's accuracy of 60% means that the probability of a reference pixel being correctly classified is 60% for the Wetland class (Congalton, 1991; Lillesand, 2008, pp.589-590).

Another important measure to evaluate the quality of a classification is Kappa. Kappa analysis leads to a *KHAT* (k) statistic. The values for k usually range between 0 and 1 even though

values between -1 and 1 are mathematically possible. It is a measure of the difference between an observed classification and a random assignment of pixels. A kappa value of 0.87 indicates that a classification is 87% better than a classification based on chance. The lower the kappa value, the more does an observed classification resemble a purely random one (Lillesand, 2008, p.590).

3.4 Earth Observation Data

This chapter introduces the types of satellite data that were utilized in this study: Landsat-5 TM, Landsat-7 ETM+, QuickBird-2 and WorldView-2.

3.4.1 Landsat

The main data sources for this study were Landsat-5 TM and Landsat-7 ETM+ images (see chapter 4). NASA started its Landsat program in the 1970s. The first satellite was launched in 1972. Many more followed with Landsat-8 being the most recent one. It was shot into space in February 2013. Images were made available from June 2013 on. Landsat satellites are often referred to as “work horses” due to the amount of imagery they capture and their longevity which usually exceeds projected life span. The satellites’ near polar orbits are repetitive, circular and sun-synchronous. Sun-synchronicity refers to the daily crossing of the equator at the same time. The repetition rate, i.e. the time needed until one spot on the earth’s surface is being flown over again, for both Landsat-5 and -7 is 16 days. One full orbit takes about 99 minutes. The satellites carry different instruments to capture images for a variety of applications. The main difference between the Thematic Mapper (TM) instrument on-board of Landsat-5 and Landsat-7’s Enhanced Thematic Mapper Plus (ETM+) instrument is the addition of a panchromatic 15 m band for ETM+. Apart from that, the thermal band of Landsat-7 has a finer resolution of 60 m compared with Landsat-5’s 120 m thermal band (USGS 2013b; Albertz, 2007; Lillesand, 2008). Table 1, which is based on Albertz (2007, p.243), provides an overview regarding the satellites’ specifications.

Landsat-5 / Landsat-7		
	Landsat-5 TM	**Landsat-7 ETM+**
Year of launch	1984	1999
Altitude	705 km	705 km
Repetition rate	16 days	16 days
Swath width	185 km	185 km
Pixel resolution	30 m x 30 m	30 m x 30 m
Bands	1 0.45 – 0.52 µm	1 0.45 – 0.52 µm
	2 0.52 – 0.60 µm	2 0.52 – 0.60 µm
	3 0.63 – 0.69 µm	3 0.63 – 0.69 µm
	4 0.76 – 0.90 µm	4 0.76 – 0.90 µm
	5 1.55 – 1.73 µm	5 1.55 – 1.73 µm
Thermal band	6 10.4 – 12.5 µm	6 10.4 – 12.5 µm
Panchromatic band		8 0.52 – 0.90 µm (15 m x 15 m)

Table 1: Landsat satellite specifications

In May 2003, Landsat-7's scan line corrector (SLC) failed which resulted in data gaps and pixel duplications in the imagery. Various approaches to fill the gaps have been proposed (Lillesand, 2008, p.415).

The area of interest is completely covered by Landsat paths 173 and 172 of row 53 (Figure 5). A very small area in the northern part of Melut County was left out since including it would have resulted in using additional data from path 173 of row 52.

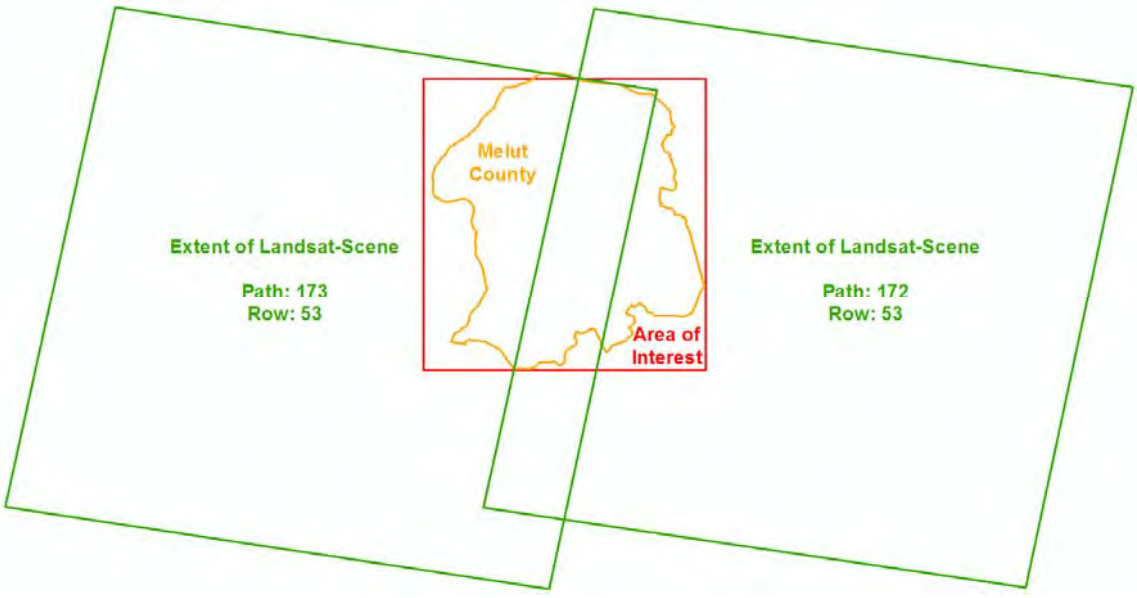

Figure 5: Extents of Landsat scenes

As described above in the introductory chapter, a time series consisting of six points in time was developed. The dates were chosen based on data availability as well as significance with regard to events in the AOI. Chapter 4 examines this in detail. Two images were needed for every point in time. Because of the SLC's failure in 2003, additional data (marked with an asterisk in Table 2) was used for 2004 and 2006 to fill the gaps in the imagery. Table 2 provides an overview. White and blue color was applied in the table for easy distinction between the six points in time.

Landsat data			
Sensor	**Path / Row**	**Acquisition Date**	**Resolution**
Landsat 7	172 / 053	29.11.1999	15 m (pansharpened)
Landsat 7	173 / 053	06.12.1999	15 m (pansharpened)
Landsat 7	172 / 053	23.12.2002	15 m (pansharpened)
Landsat 7	173 / 053	30.12.2002	15 m (pansharpened)
Landsat 7	172 / 053	26.11.2004*	15 m (pansharpened)
Landsat 7	172 / 053	12.12.2004	15 m (pansharpened)
Landsat 7	173 / 053	03.12.2004*	15 m (pansharpened)
Landsat 7	173 / 053	19.12.2004	15 m (pansharpened)
Landsat 7	172 / 053	18.12.2006	15 m (pansharpened)
Landsat 7	172 / 053	04.02.2007*	15 m (pansharpened)
Landsat 7	173 / 053	25.12.2006	15 m (pansharpened)
Landsat 7	173 / 053	10.01.2007*	15 m (pansharpened)
Landsat 5	172 / 053	18.12.2009	30 m
Landsat 5	173 / 053	09.12.2009	30 m
Landsat 5	172 / 053	06.01.2011	30 m
Landsat 5	173 / 053	13.01.2011	30 m

Table 2: Used Landsata data

Landsat-5 data was available for 2009 and 2011 which were used to keep the number of images that contain gaps, as in 2004 and 2006, to a minimum.

For pre-processing, a tasseled cap transformation was performed on all images using *ERDAS Imagine 2011*. Kauth and Thomas (1976) developed a tasseled cap transformation for Landsat-Multi Spectral Scanner (MSS) data to improve identification of agricultural crops. It is based on the discovery of "data structures inherent to a particular sensor" (Crist, 1986) after which the data is being rotated in order to establish a viewing perspective that allows for best observation of those data structures. The transformation must be adjusted to each sensor. For Landsat TM data, it results in a three-band feature space where the first band corresponds to brightness, the second band corresponds to greenness and the third band is called wetness and relates to soil and surface moisture (Lillesand, 2008, p.535). This applies for ETM+ data, too. For this study, the third band was of great help to identify human-made structures with very little or no surface moisture such as oil well pads.

A second pre-processing step consisted of pan-sharpening of Landsat-7 data which includes a panchromatic band with a resolution of 15 m. This band was merged with a layer stack of the bands 1-2-3-4-5-7 to produce color images which in turn feature a resolution of 15 m instead of 30 m (Lillesand, 2008, p.414). A variety of pan-sharpening techniques exist. Extensive testing led to the employment of the Hyperspherical Color Space Resolution Merge algorithm implemented in *ERDAS Imagine 2011*.

Atmospheric correction was not applied. Song et al. (2001) convincingly illustrated that atmospheric correction is unnecessary for maximum likelihood classification of a single date image with training data and testing data being from the same image. Although the authors examined effects of atmospheric correction on Landsat TM data only, no atmospheric correction was performed on the ETM+ images as well.

The 2002 and 2009 scenes were chosen for land cover classification. Subsets of them were mosaicked to fit the AOI. A variety of techniques was proposed to fill the gaps in SLC-off Landsat imagery such as interpolation of neighboring scan lines or the mosaicking of the imagery with scenes from alternative acquisition days (Lillesand, 2008, p.419; USGS 2013c). None of these methods was applied to fill gaps in the 2004 and 2006 images since the imagery concerned was only used for manual on-screen vector digitization using *ArcMap*. In *ArcMap*, the relevant images were simply displayed on top of alternative scenes (Table 2, asterisk).

3.5.1 Data: QuickBird-2 and WorldView-2

According to the classification of remotely-sensed data with regard to spectral resolution as applied by the European Space Agency (ESA, 2013), Landsat-5 and -7 data belongs to the category of High Resolution-2 (HR-2) imagery. This class features spectral resolutions between 10 m and 30 m. Satellite sensors with a much finer resolution exist. If the imagery's resolution is better than 1 m, it falls into the ESA category Very High Resolution-1 (VHR-1). QuickBird-2 and WorldView-2 with resolutions of 0.61 m and 0.5 m are examples for VHR-1 data. Both satellites are commercial systems, operated by private companies. Their superior resolution enables a wide range of earth observation applications (Figure 6). QuickBird-2 was launched in 2001 with WorldView-2 going into space in 2009. Because of their high resolution, swath width is much smaller compared to Landsat: 18 km for QuickBird-2 and 16.4 km for WorldView-2 (Satellite Imaging Corporation, 2013; DigitalGlobe, 2013).

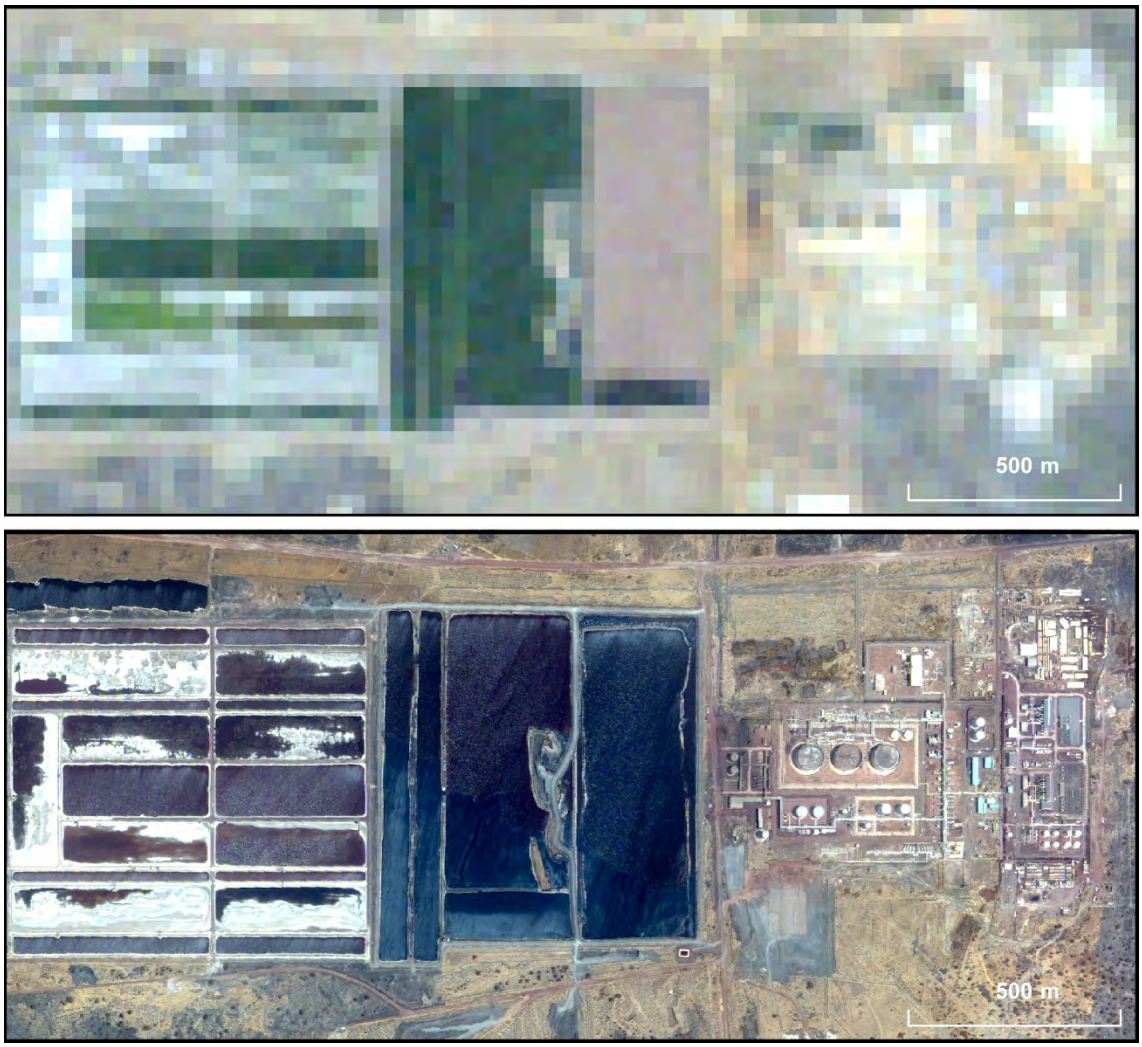

Figure 6: Landsat-5 (30 m) vs. WorldView-2 (0.5 m)
Infrastructure of the Paloich oil field, from left to right: Pools for waste water disposal, field processing facility, power plant

A QuickBird-2 scene, acquired on November 07, 2004, and a WorldView-2 scene from March 24, 2012 were used to map changes with regard to population in the town of Paloich. Ortho-rectification and pan-sharpening on both images was performed in-house by DLR.

4 Methodology

An overview of the final workflow is given below (Figure 7). The workflow consists of three main steps: Feature extraction, feature analysis and visualization. Each workflow element is being discussed in detail in the corresponding chapter. Feature extraction aims at creating a database of features that serves two purposes. Mapping the state of the oil fields for every point in time is one purpose. The second one is to use the features to analyze their spatial connections and to explore interaction and relatedness between them. GIS techniques are used for this step. The outcomes of the mapping and the analysis approach will then be visualized to generate the overall picture as described in the introductory chapter of the study.

During the course of this study, the workflow concept was modified substantially. Original plans were based on the assumption that the object-based classification of cropland and oil well pads would yield satisfying results to use them for GIS analysis. As chapter 5 explains, this was not the case. In the end only digitized features were used for further GIS analysis. The same applies for initially planned change detection analysis between land cover classifications which were found not to be meaningful and therefore discarded. Chapters 5.2 and 5.3 further elaborate on this. In the end only two dates - 2002 and 2009 - were chosen for exemplary object-based and pixel-based land cover classification.

Landsat data was chosen for two reasons. The first reason was its free availability. The second reason was full coverage of the entire area of interest over the whole period of interest. Even though very high resolution data would have been desirable to work with and would have surely resulted in a higher level of accuracy regarding some results of this study, associated costs prevented its use.

The six points in time were chosen based on events that occurred in the AOI as well as data availability. Some dates were set from the beginning: 1999, 2002, 2004 and 2011. The first one – 1999 – was of interest because it showed the state of the area before oil production started. The second point in time – 2002 – supposedly not only showed the first stages of oil field expansion but also the effects of the heavy fighting that took place between 1999 and 2002 as explained in chapter 2.2.1. In the year 2004, displaced people and persons that had fled the areas started to return to Melut County (BICC, 2013). The last date in the list – 2011 – was set as an endpoint of the time series upon design of the study in mid-2012. The fact that early 2011 was the last time for which Landsat-5 imagery of the area of interest was available also contributed to this decision. By choosing Landsat-5 images, working with a huge number of

SLC-off Landsat-7 scenes was avoided. The two remaining dates in-between – 2006 and 2009 – were then chosen by keeping the time interval of two to three years between dates.

Dry-season images were chosen. According to Action Against Hunger Southern Sudan (2008, p.13), the period from late November until January is the time of harvest in Melut County. Farmlands should therefore be identifiable whether or not they had already been harvested. If they had not been harvested yet, they would probably be identifiable because of spectral reflectances related to vegetation. After harvesting, they would contrast their surroundings in terms of color and shape. Acquisition dates of late November and early December were aimed at but could not in every case be ensured (see Table 2).

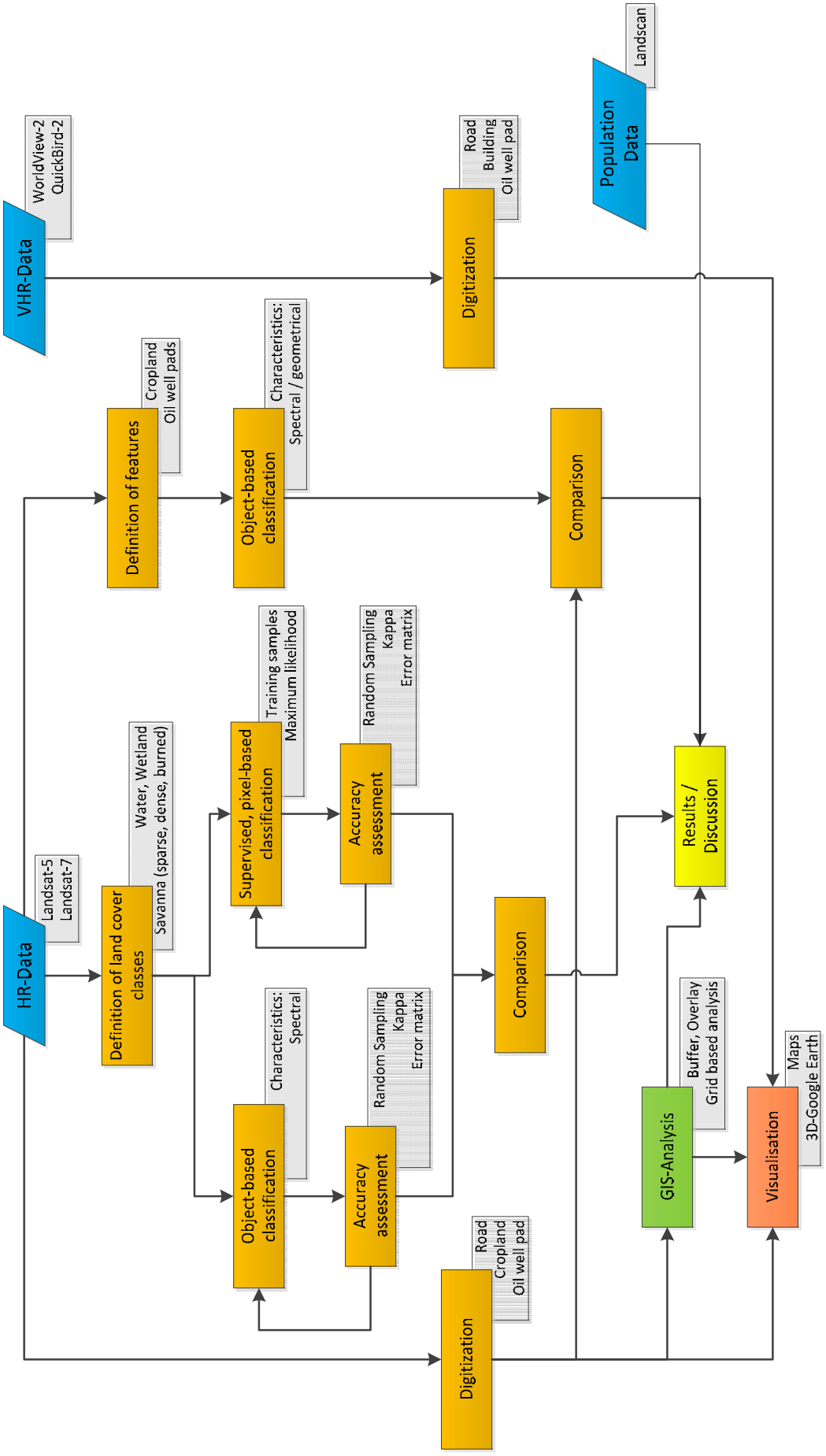

Figure 7: Workflow

4.1 Visual interpretation and manual extraction

Based on visual inspection of a variety of Landsat scenes, three features were found to be identifiable on 15 m and even 30 m resolution data: Cropland, roads and oil well pads.

Figure 47 shows examples of cropland, roads and oil well pads from the 2009 Landsat-5 scenes.

The feature class road covers a variety of features that are used for transport between different places. They include paved and unpaved roads, simple tracks as well as routes specifically built to connect oil well pads to the road network. The resolution of the satellite imagery did not allow for a distinction between different types of roads. Due to their long and narrow shape, roads were most often easily identifiable. A possible source of error was the fact that small oil pipelines, which often connect oil well pads and other oil extracting infrastructure, appeared very similar to roads. A comparison with very high resolution *Google Earth* data showed that some small roads were not visible on Landsat data. Some minor roads may therefore be missing.

Oil well pads are mostly unambiguous features. Measuring approx. 100 m in width and length, they are used to drill for oil. For the first step of construction, “the surface area needs to be cleansed of all vegetation and leveled in order to be prepared for drilling” (Selg, 2013, p. 37). While the smaller features they often contain, e.g. the well head or the so called ring main unit building, could not be identified on HR-2 imagery, the pad itself was in most cases recognizable because of its white color and squared shape. Whether the well was a producing one at the time of image acquisition could not be assessed from HR-2 data. Some pads serve purposes like water injection. Because of their inseparability regarding use, all captured pads were referred to as oil well pads. In the context of this study, the exact use of the pads was irrelevant since only the fact that a man-made structure had been erected was of interest. In Tasseled Cap Band 3, which indicates wetness, they stood out as very dark spots.

In this study the term cropland describes land that is used for agricultural purposes. It includes small and big scale farming. Small scale farming comprises rainfed agriculture being done without the help of motorized machinery. The plots of land that are cultivated this way are quite small. Capturing this type of cropland on Landsat imagery was much more challenging than capturing big fields where tractors are supposedly in use. Big scale farm lands have a distinctive shape and compactness that sets them apart from their surroundings even when

the use of NDVI or MSAVI does not yield good results because of low vegetation cover in the dry season. Figure 8 illustrates this with a subset of a Landsat-5 image.

Figure 8: Cropland
Band combination: Red: Band 4, Green: Band 3, Blue: Band 2

A lot of small scale farming takes place on the river banks and their immediate surroundings (Prins, 2010, p.4). A good indicator for this type of farming is the proximity of settlements on the river banks. As stated above in chapter 2.2, these settlements are located in more highly situated areas which are not prone to flooding during the wet season. By overlaying information on wetness (Tasseled Cap Band 3) with SRTM elevation data, potential settlement locations were identified and checked against *Google Earth* data. Figure 9 shows an example. The dark spot in the image on the left (red box, Landsat-5, Tasseled Cap Band 3) was identified as a settlement with the help of *Google Earth* imagery as pictured on the right. Single huts are visible.

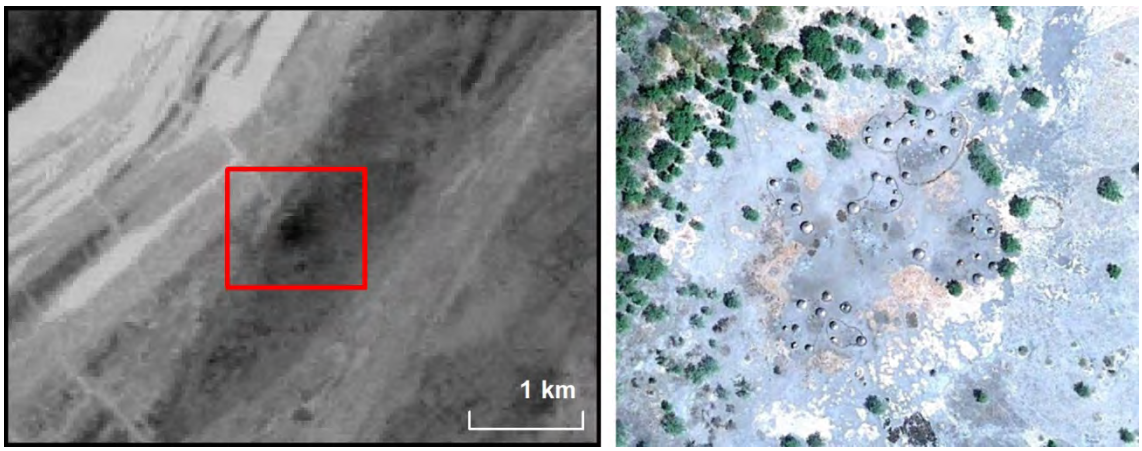

Figure 9: Small settlement on river bank

Areas close to these settlements like the white ones on the right hand side in Figure 9 are probably used for small scale farming. Prins (2010, p.7) classified any bright appearing area

with high reflectance along the river banks as cropland. Confirmation of those areas being cropland was not possible because in most cases *Google Earth* did not provide very high resolution imagery. In order to avoid capturing too many non-cropland areas as cropland, the described areas along the river banks were not extracted. The possibility exists that too little small-scale farm land was captured. In general, fallow fields could not be distinguished from cultivated fields. Since no ground-truth data or reference images were available, the size of captured cropland areas may differ from the actual size. It is assumed that a lot of small-scale farm lands were not captured while over-capture of big scale farm lands is possible. The latter is due to the aforementioned fact that separation between cultivated and fallow fields was not possible.

For every single one of the six points in time, cropland, roads, and oil well pads were digitized and stored in a file-geodatabase using *ESRI ArcMap10.1*. In case of ambiguity, *Google Earth* data was used to check on certain features. Unfortunately very high resolution *Google Earth* data was not available for the whole AOI. Misinterpretations may have occurred for every feature class with a higher likelihood in case of cropland and roads compared to oil well pads.

A second set of Landsat imagery (Table 3), dating from the rain season or the end of it, was used to assess the extracted data and to refine it.

Additional Landsat data			
Sensor	**Path / Row**	**Acquisition Date**	**Resolution**
Landsat 7	172 / 053	29.09.1999	15 m (pansharpened)
Landsat 7	173 / 053	04.11.1999	15 m (pansharpened)
Landsat 7	172 / 053	04.10.2002	15 m (pansharpened)
Landsat 7	173 / 053	27.10.2002	15 m (pansharpened)
Landsat 7	172 / 053	25.10.2004	15 m (pansharpened)
Landsat 7	173 / 053	16.10.2004	15 m (pansharpened)
Landsat 7	173 / 053	01.11.2004	15 m (pansharpened)
Landsat 7	172 / 053	13.09.2006	15 m (pansharpened)
Landsat 7	172 / 053	06.10.2006	15 m (pansharpened)
Landsat 7	172 / 053	16.11.2009	15 m (pansharpened)
Landsat 7	173 / 053	07.11.2009	15 m (pansharpened)
Landsat 7	172 / 053	11.11.2010	15 m (pansharpened)
Landsat 7	173 / 053	02.11.2010	15 m (pansharpened)

Table 3: Landsat imagery used for refinement of digitization

In their study on the environmental impact of the Russian oil and gas industry, Sergey and Oganes (2009) showed that Landsat-TM and –ETM+ data can be applied to identify oil well pads and roads. The authors evaluated the possibility to spot pipelines as “limited” (Sergey and Oganes, 2009). This study confirms their findings. While the Petrodar pipeline, running from the Paloich oil field in direction of the town of Renk, was identified, the pipeline from Adar to Paloich was not.

Exploration patterns (Figure 46, Figure 47) were captured as additional features. They remain after oil exploration activity stops and form giant grids of lines on the earth's surface which are also often referred to as "seismic lines". Selg (2013, pp.16-17) describes the exploration activities in detail. Field trips in 2013 by Petry (2013b) confirmed that exploration patterns were still visible in the area between the Muleeta oil field (Figure 46) and the White Nile. These patterns were not identified on the 2011 imagery which illustrates the limits of Landsat-5 data.

4.2 Land cover classification

This chapter explains how the remote sensing methodologies as explained in chapters 3.1 – 3.3 were applied for land cover classification.

4.2.1 Definition of land cover classes

In order to define appropriate land cover classes, existing land cover data was examined. Figure 65 and Figure 66 show land cover classes for six available data sets. One data set (CDE, 2008) was specifically designed for South Sudan. The rest covers at least several countries (FAO, 2003), the entire African continent (USGS, 2003a) or even the whole world (ESA, 2008; Food Policy Research Institute, 2002; JRC, 2004). All land cover data sets are dominated by various types of grasslands with sparse shrub cover, i.e. savanna, which is in accordance with the findings of Harrison and Jackson (1958). Some data sets show a high level of detail, e.g. FAO Africover and ESA Globcover. Since ground truth data was unavailable and very high resolution imagery for reference purposes only partially available via *Google Earth*, a simple classification schema on the basis of the CDE and USGS classes was adopted. After detailed visual inspection and initial unsupervised classification tests, five land cover classes were chosen: Water, Wetland (mostly river bank areas) and three subtypes of savanna. These include densely vegetated savanna (Savanna-Dense), sparsely vegetated savanna (Savanna-Sparse) and savanna areas which have been burned and not yet fully recovered (Burned Area). Because of their dark greyish and blackish color, the latter areas were relatively easy to identify. Pastoralists often set grazing areas on fire since they believe this will result in growth of higher quality grass (Graewert, 2012). Sparsely and densely vegetated savanna differ in their level of vegetation being present which can be assessed by using Landsat band 4 values and indices. Other possible land cover classes like settlements, open soil or various sub-types of savanna were dropped after initial classification attempts. Low resolution of the Landsat data as well as the rather small size of the areas covered by some of those classes, e.g. open soil, prevented their inclusion. The same applies for cropland which was not assigned a distinct land

cover class but later classified separately on the basis of the savanna classes. Pixel-based classification tests in order to classify cropland as a distinct land cover class resulted in poor outcomes. The spectral characteristics of the cropland areas were too similar to those of burned areas as well as sparsely vegetated and densely vegetated savanna. Spectral information alone was not sufficient enough to satisfactorily classify cropland. Based on this observation, OBIA was applied for classification of cropland. This way, spatial information like the shape of the fields could be included. The approach of Prins (2010, p.7) which is based on the assumption that every high-reflectance, i.e. bright, pixel indicates farming activities, was rejected, since no ground-truth data or very high resolution imagery for verification of this assumption was available.

4.2.2 Pixel-based classification

ERDAS Imagine 2011 was used to perform a supervised pixel-based classification on the 2002 and 2009 satellite scenes. Up to 40 training samples were selected for each class. Each sample consisted of 25 pixels (5 x 5). Training samples were set using a band combination of 4-3-2. Maximum likelihood, "the most common supervised classification method" (Richards and Jia, 1999, p.182), was employed as classification approach.

4.2.3 Object-based classification

The software *Definiens eCognition* was used to perform OBIA. A rule set was developed for the 2009 scenes, which was later modified to classify the 2002 mosaic. After initial multiresolution segmentation (Baatz, 2000), objects were classified as Water, Wetland and Burned Area, using thresholds for the Maximum difference, NDVI and Mean Green values (see Annex- Definiens eCognition rule sets-R1 for details). Visual inspection showed that any of the yet unclassified objects would fall into the classes Water or Wetland. A second cycle was necessary to classify the remaining objects which would be assigned to the Burned Area, Savanna-Sparse and Savanna-Dense class. A multiresolution segmentation was performed on the remaining unclassified objects in order to obtain smaller objects. The scale parameter was thus reduced from 10 as in the first cycle to a value of 5 for the second one. Shape and compactness values of 0.1 and 0.5 were deemed feasible and therefore maintained. Remaining objects were classified as Burned Areas with the help of the Burning Area Index. All of the yet unclassified objects would qualify as either Savanna-Sparse or Savanna-Dense. The image did not show natural breaks between those types of land cover but a wide and continuous range of infrared values (Band 4) indicating vegetation. A threshold was finally set with the help of the MSAVI index and brightness values, separating sparsely from densely vegetated savanna.

The 2009 rule set was then modified to fit the needs of the 2002 15 m-mosaic (see Annex-Definiens eCognition rule sets-R2 for details). Due to the difference in resolution, a single pixel in the 2009 image is equivalent to four pixels in the 2002 image. The latter image contains much more spectral information. The 2002 rule set reflects this by being more detailed than the 2009 rule set. The higher level of detail was also based on the fact that even though the image contains more pixels, the pixel's spectral values for Green, Brightness, NDVI and MSAVI were much more similar than in the 2009 image. Distinguishing visually between sparse and dense savanna was found to be challenging. Complexity was added by the fact that partially recovered burned areas and sparse vegetation differed only slightly in their spectral characteristics. Areas that were considered densely vegetated due to their texture featured very low NDVI and MSAVI values.

The basic structure of the 2002 set was not altered. It consists of two segmentation cycles, refining the objects of interest. Water and Wetland were completely classified during the first cycle but with different means compared to the 2009 set. The Bare Soil Index was applied to classify Wetland. A basic Burned Area classification was performed as well during the first cycle. The second cycle tried to classify the remaining objects which were much more similar in their spectral characteristics than the 2009 objects. The adopted strategy was to subtract objects that could be classified as either Burned Area or Savanna-Dense and to assign the rest to the Savanna-Sparse class. As mentioned above, separating burned areas from sparse vegetation was demanding. In the end, thresholds for NDVI-, MSAVI-, Burned Area Index-, SWIR1-, SWIR2, and Brightness-values were set to define objects as either Burned Area or Savanna-Dense.

4.2.4 Accuracy assessment

Chapter 3.3 emphasized the need for accuracy assessments to evaluate the quality of a classification. Since ground truth and reference data sets were unavailable, each classification was compared to the satellite image it was based on. A stratified random sampling approach was chosen to perform the accuracy assessment for the four land cover classifications described above. For each classification, a minimum of 50 sample points per class and a total of 500 sample points were randomly selected. The number of sample points increased with the total number of pixels per class, ranging from 50 in the least populated class (Water) to more than 200 in the Savanna-Sparse class. This approach follows the procedures suggested by Congalton (1991). *ERDAS Imagine 2011* was used to perform the accuracy assessments.

4.3 Object-based cropland classification

Based on the 2009 object-based land cover classification, a rule set was developed to classify cropland for 2009. The need for an object-based classification of cropland compared to a pixel-based approach has been justified in chapter 4.2.1. Table 4 shows the results of an overlay of the digitized cropland areas for the year 2009 with the OBIA land cover classification of the same year. Vector data derived from digitization was used as reference data for the classification. The table shows that 70.55% of digitized cropland vectors fall into the Savanna-Sparse category while another 16.09% were part of the Savanna-Dense class. Put together, the two savanna classes contain more than 86% of all cropland. In order to obtain good enough results quickly, a rule set was developed which excludes all Burned Area, Water, and Wetland areas from further examination regarding cropland.

Cropland – Land cover overlay		
Class	**Area in km²**	**Percentage of digitized Cropland**
Water	0	0
Wetland	0.13	0.03
Burned Area	57.83	13.33
Savanna-Dense	69.77	16.09
Savanna-Sparse	305.95	70.55

Table 4: Results of overlay of cropland on land cover classification

The rule set is shown in chapter 8.1 R3. It consists of three segmentation cycles. In the first cycle, Wetland and Water was classified. A thematic layer, the digitized road network, was introduced. It was later used in the third cycle for an exclusion of all objects further away than 250 pixels (7,500 m) from the road network. A GIS-based buffer analysis showed that 90.58% of all digitized cropland areas were located within this buffer distance. The second segmentation cycle refined the remaining objects and classified more objects as Burned Area. In contrast to this, the third cycle started with a new multiresolution segmentation which created bigger, not smaller objects. This was done by changing the scale parameter from 5 to 25. The reason for it was the fact that bigger objects in many cases very well represented whole fields used for farming. Besides the scale parameter, the values for shape and compactness were also altered to 0.6 and 0.2, to address the cropland's specific characteristics. After segmentation, a new class was used for the first time: Non-Cropland. Its purpose was to store all areas that do not contain cropland. The Cropland class itself was later filled with objects falling under a certain threshold of mean difference to red band values. At the last stage, the Cropland class was refined by eliminating non-cropland from it. This was

done with the help of the shape index – most cropland areas show a characteristic shape – and the Bare Soil Index as well as the aforementioned distance to the road network.

Because of the poor quality of the classification's results (See chapter 5.4), subsets were created instead of classifying the whole satellite scene. The subsets cover an area of 625 km² (25 km x 25 km) each. Figure 10 shows their location as well as the digitized cropland in blue color. Subset A contains cropland areas that are easy to distinguish from their surroundings because of color and shape when shown in band combination of 4-3-2. Some cropland areas from subset B are much more difficult to identify due to their similarity in appearance with burned areas and savanna. Figure 11 presents a detailed view with the cropland areas highlighted by a blue colored boundary.

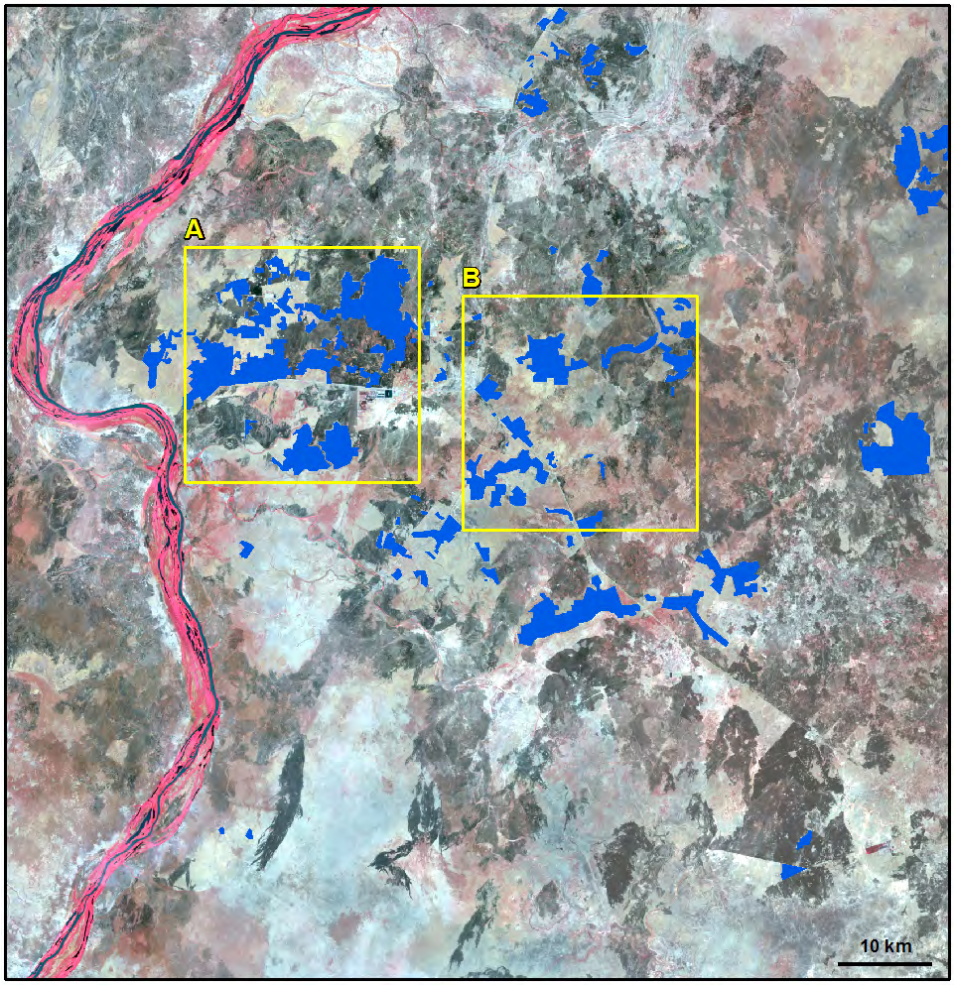

Figure 10: Subsets for cropland classification
Band combination: Red: Band 4, Green: Band 3, Blue: Band 2

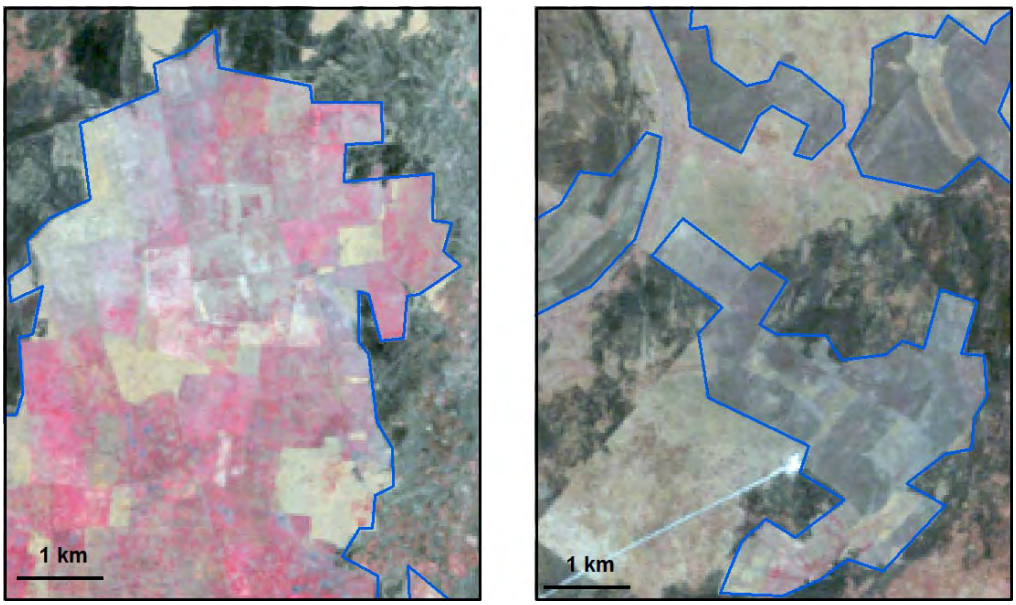

Figure 11: Detail view of Subset A (left) and B (right)
Band combination: Red: Band 4, Green: Band 3, Blue: Band 2

Rule sets for both subsets are presented in the Annex. For subset A, two segmentation cycles sufficed. With the help of vegetation-related indices like NDVI and MSAVI, many non-cropland areas were excluded. In the second cycle, geometrical characteristics like shape index, asymmetry, roundness, and the relation between length and width of an object were used to exclude non-cropland. The general approach was to exclude all obvious non-cropland areas in a first step, after which the remaining unassigned objects were put in the cropland class. During a final step, the cropland class was refined by eliminating non-cropland objects based on a mixture of geometrical and spectral characteristics. This approach was also applied for subset B, with the addition of a third cycle to create bigger objects as it was the case for the cropland classification of the entire scene.

4.4 Object-based oil well pad classification

A rule set was developed to test if oil well pads could be classified on the 30 m Landsat-5 data from 2009. Similar to the cropland classification, the road network was used as a thematic layer. A buffer of 25 pixels – 750 m – was applied since a GIS analysis revealed that 94% of all digitized oil wells in the 2009 image are situated in a maximum distance of 750 m to the road network. As described above, oil well pads are squared in shape and of a certain size: 100 m x 100 m which corresponds to 3 pixels in length and width. To make use of this, geometrical characteristics like area, rectangular fit, and the relation between length and width were employed to select potential oil well pads. Apart from these queries, brightness values were considered since oil well pads appear as very bright objects in a variety of band combinations.

4.5 GIS-Analysis

For GIS-analysis, digitized vector data of cropland areas, roads and oil well pads were used instead of the classification results. Reasons for this approach are given below in chapters 5.4 and 5.5. In a first step, basic statistic overview data was calculated. This included the size of cropland areas, road lengths and the number of oil well pads.

4.5.1 Cropland change analysis

In order to get a detailed insight into the development of cropland areas over time, the second GIS-analysis step consisted of cropland change detection. In his classic 1989 paper on change detection, Singh (1989) defined the technique as "the process of identifying differences in the state of an object or phenomenon by observing it at different times". While this definition and its further elaboration referred to satellite images as raster data, the underlying idea of highlighting differences and visualizing change can be applied to vector data as well. By employing a variety of GIS operations based on overlaying different data layers, new vector layer containing gained, lost and unchanged cropland areas were created. The steps listed below were performed in *ArcMap 10.1* using the relevant data sets for the change periods of 1999-2002, 2002-2004, 2004-2006, 2006-2009 and 2009-2011. (Pre-data refers to the earlier data set of a certain change period, e.g. 2004, while post-data describes the later data set of the same period, e.g. 2006. Italics mark *ArcGIS*-tools or –commands.)

- *Export* pre-data one time and post-data twice from geodatabase to shape file-format
- *Merge* all cropland areas in one of the two exported post-data sets and rename the file to *_merge.shp
- *Add field* to attribute table of the second post-data shape file named "Status" (Type: Text) and rename the file to *_change_detection.shp
- Overlay pre-data above post-data (*_change_detection.shp) and split post-data using the *Split Polygons*-tool
- *Select by Location*-query: Target features (post-data) *are within the source layer* feature (pre-data)
- Populate selected features' attribute field "Status" with "Unchanged"
- *Switch selection* and populate attribute "Status" with "New"
- *Clip* post-data (*_merge.shp) on pre-data using the *Discard the area that intersects* option
- *Append* the remaining areas of pre-data to post-data (*_change_detection.shp) and populate the "Status"-attribute with "Loss"

- Find and delete sliver-polygons
- Re-calculate the polygon's areas using *Calculate geometry*

The outcomes were visualized in maps (Chapter 8.2) and are being discussed below.

4.5.2 Correlation analysis between cropland and road network

In a third step, the relationship between different features was further investigated using *ArcGIS 10.1*. The connection between the road network and cropland areas was of significant interest since a lot of research literature (See chapter 2.2.1) states the negative effects of new roads on existing cropland areas in Melut County. Positive effects would constitute new roads making hitherto out-of-reach areas accessible. Three questions were asked: What is the distance between cropland areas and the road network for every year? Does the construction of new roads lead to the establishment of new cropland areas? Does the construction of new roads lead to loss of existing cropland?

To answer the first question, a buffer analysis was performed. Six buffers comprising distances of 500 m, 1,000 m, 2,500 m, 5,000 m, 10,000 m and 20,000 m were created for the entire road networks of every year of interest. This was done with the help of the *Multiple Ring Buffer*-tool. The buffers were used to split the cropland. To give an impression, Figure 12 uses bright colors to highlight parts of cropland areas that are situated within the same buffer distance. Bright green indicates areas that are between 1,000 m and 2,500 m away from the road network which is visualized with red color. Light blue areas lie outside the outermost buffer and are therefore more than 20,000 m away from any road. After splitting, the sizes of corresponding areas were summed up. Results are discussed below.

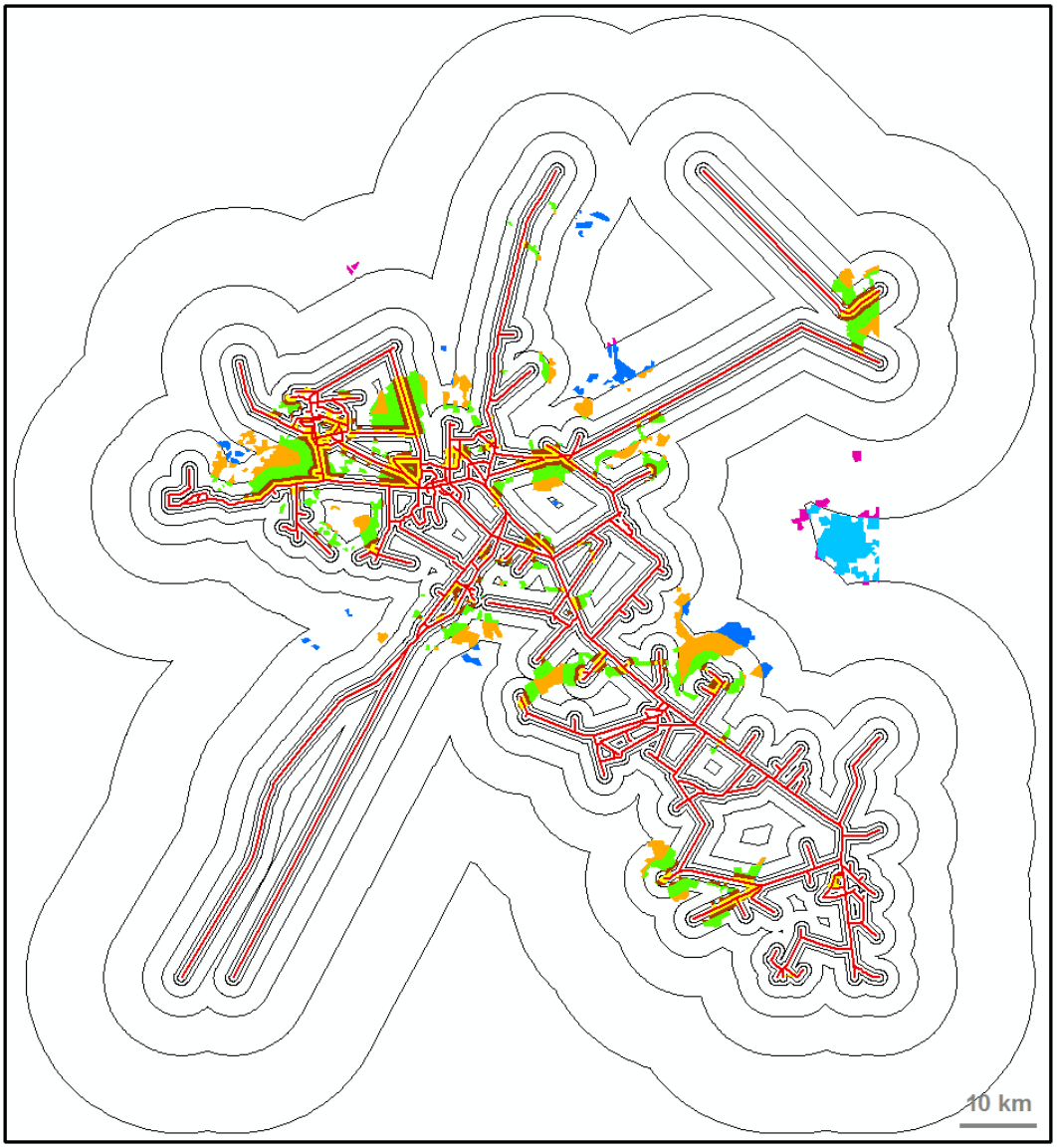

Figure 12: Multiple ring buffer and cropland (2011)

The second question concerns assumed positive effects of road construction. It needed to consider a change period rather than a single point in time. To answer it, a strategy very similar to the one just explained above was adopted. The same buffer distances were applied with the major difference that those buffers were created two times. Firstly for pre-data (e.g. road network as seen in 2004 for the 2004-2006 change period) and secondly for new roads (e.g. roads present in 2006 but not yet present in 2004). Because of this approach, cropland areas were split two times as well, using both buffer data sets.

The final question with regard to the cropland-road relationship asks whether or not existing cropland is being destroyed by the construction of new roads. Construction activities might swallow up lands previously used for farming. To investigate this, the buffer approach was discarded. Instead, a visual analysis was performed by overlaying new roads (as explained above) with lost cropland areas. This was done for all change periods, i.e. five times.

4.5.3 Oil field development

In order to examine and visualize the development of the four oil fields in the AOI, a grid-based approach was chosen. A cell-size of 1 km in width and length was applied for a grid covering the whole area of interest. The resulting grid comprises 10,200 cells and can be seen in Figure 63. For each cell, the number of contained oil well pads was counted. This operation needed to be performed six times to cover all points in time. It was done with the help of a spatial join between the oil well pad feature class and the grid-file. A new field called “Count” was created in the attribute table of the oil well pad feature class. It was populated with the value “1” for each oil well pad. As a next step, the grid was joined to the oil well pad feature class by using the *Join data from another layer based on spatial location*-option. After joining, the sum for each grid cell was calculated and a new file with the number of oil well pads present in each grid cell was created. This way, six grids were created that show the development of the oil fields when visualized appropriately. For their visualization, the number of oil well pads each cell contains was grouped into five classes: 0; 1; 2-3; 4-7; 8-10. This categorization was based on the distribution of the 2011 data as Figure 13 shows (please note that Figure 13 does not include grid cells with zero oil pads). No more than five classes were aimed at to ensure an easy to grasp visual picture. With the class “0” already reserved for grid cells with no pads at all, four classes remained to allocate data to. Grid cells containing a single oil well pad were put into a class of their own since they constitute the overwhelming majority of cells. Values of 2 and 3 were grouped together, as were values 4 to 7. The rest formed a distinct class, representing the grid cells with 9 and 10 oil well pads.

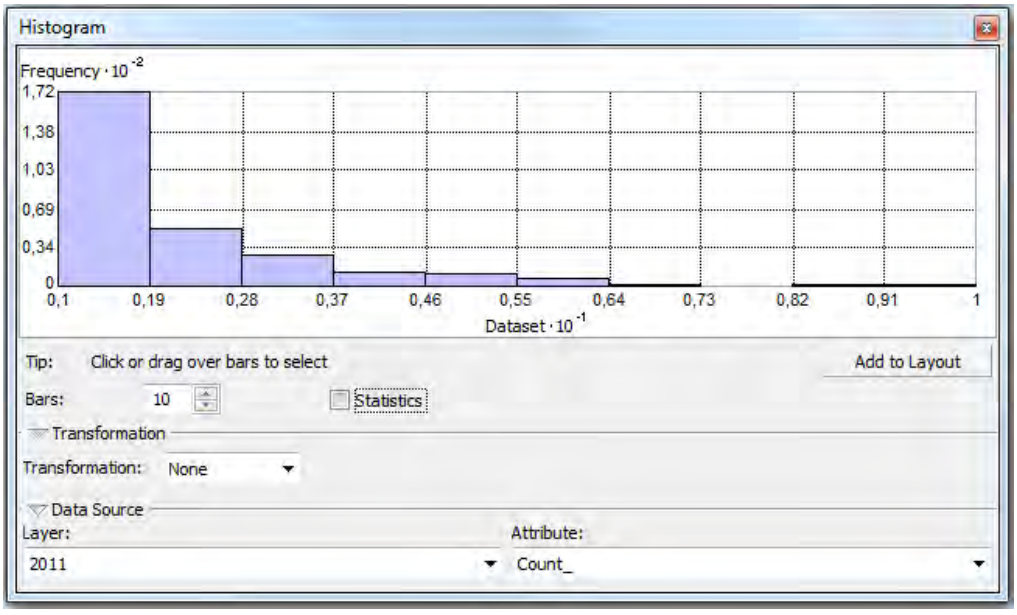

Figure 13: Histogram for 2011 oil well pads

The rapid growth of oil well pads raised the question whether their expansion led to loss of cropland areas. To answer this, a visual analysis similar to the one regarding new roads and lost cropland was performed. Lost cropland areas were placed on top of a grid like the one used for the oil field development analysis with the difference of showing cells with newly constructed oil well pads only. This was done for all five change periods.

4.5.4 Miscellaneous

Another overlay analysis combined digitized pipeline and exploration patterns with lost cropland areas.

Drain blocks were a source of changes in cropland patterns as stated by ECOS (2006, p.22). Drain blocks arise when natural water flows are disrupted by poorly constructed man-made structures. Tasseled Cap Band 3 data which indicates wetness was thus combined with lost cropland areas to visually determine whether or not these phenomena can be observed.

Changes in land use are very likely related to changes in population. As BICC (2013, pp.30-32) reports, the number of inhabitants in major towns of the AOI is growing. This can be attributed to factors like the return of formerly displaced people or the so called pull-factor of the oil industry. The latter describes the fact that people are attracted by the prospect of jobs in the oil fields. In order to examine population growth, LandScan data was examined. Table 20 shows available LandScan population data. Unfortunately datasets for all years concerned were not available. The 2010 dataset was used for the year of 2011 since those year's images were acquired in early January of 2011. Population data from the previous year was therefore considered feasible to use.

5 Results and Discussion

This chapter presents and discusses the results of the study in detail.

5.1 Mapping

The results of this study were visualized in 19 maps in A3 format. They are shown in the Annex, reduced in size to fit an A4 page. The original size maps can be found on the accompanying CD.

The main reference map differs from the rest as it contains not only features that were outcomes of satellite image analysis but information taken from additional data sources. These features comprise oil field infrastructure like pipelines and the planned refinery near the town of Thiangrial. They were taken from a map provided by Petry (2013e). The information shown therein was collected during field trips in 2013. The majority of the concerned features such as the pipeline connecting Adar and Paloich were not visible on Landsat imagery.

The main reference map also contains settlements that were taken from a variety of sources such as GeoNames (2013), United Nations Sudan Information Working Group (UN Sudan IMWG) (2011), United Nations Logistics Cluster Transport Map of Upper Nile State (2013) and the aforementioned map of Petry. Names of villages found in maps and data sets differ enormously. ECOS (2006, p.9) reported general unreliability of place names found in the majority of available maps, whether of Soviet, UN or Swiss origin. This observation was confirmed after consultation of a number of data sets such as the Swiss CDE maps, UN sources like UN IMWG or GeoNames. The United Nations Logistics Cluster Transport Map of Upper Nile State and the Petry map were considered to be the most accurate data sources since Petry checked the majority of settlements during his field work.

Differences in names stem from the fact that for each place, names in Dinka, English, Arabic or even more languages exist. Different translations between names contributed to differences in spelling, too. Sudan's history is being reflected in this. During the times of northern dominance, Arab names were often used while after independence, re-naming set in (BICC, 2013, p.31). To give one example, spellings of the name of the town of Paloich include Palogue (Arabic), Paloch, Palouch, Palough, Falouj, Paloic (ECOS, 2006, p.9). The GeoNames dataset uses Paloich as well as Baloish.

Since the main reference map contains a high number of data sources, they were not listed on the map itself.

5.2 Land cover classification: 2009

The pixel-based land cover classification shows a high level of overall accuracy with a value of 85% (Table 5). The same applies for Kappa. Water and Wetland area classification was of high quality with only a little misclassification between those classes. Misclassified pixels were usually situated on the border between the White Nile and its river banks where some pixels showed characteristics of both classes which were otherwise easy to separate. The producer's accuracy for Burned Area is slightly lower than the ones for Water and Wetland but still above the threshold of 80%. Compared to the high user's accuracy of the Burned Area class, this means that not enough areas were classified as Burned Area. Those areas were misclassified as Savanna-Sparse due to their very similar appearance in some places. Generally speaking, the classification of areas as Savanna of either type – Dense and Sparse – was much more challenging and less accurate compared with the other classes. This is being reflected by relatively low accuracy values with the exception of producer's accuracy for Savanna-Sparse. Misclassifications occurred between the two types of Savanna. The reason has already been mentioned in chapter 4.2.3: No natural or distinctive break between those classes exists with regard to vegetation cover. Instead, a continuous, uninterrupted range of infrared values indicates vegetation in the image. Decisions made concerning training site selection were not being reproduced in every case during the accuracy assessment. Low accuracy values testify this.

2009: Pixel-based land cover classification						
	Water	**Wetland**	**Burned A**	**Savanna-D**	**Savanna-S**	Total
Water	**50**	0	0	0	0	50
Wetland	7	**46**	0	0	1	54
Burned A	0	0	**109**	1	3	113
Savanna-D	0	2	1	**56**	12	71
Savanna-S	0	0	24	24	**164**	212
Total	57	48	134	81	180	500
Producer's Accuracy	87.71%	95.83%	81.34%	69.14%	91.11%	Overall Accuracy: **85.00%**
User's Accuracy	100%	85.19%	96.46%	78.87%	77.36%	
Kappa	1	0.8361	0.9516	0.7479	0.6462	Overall Kappa: **0.7978**

Table 5: Results of accuracy assessment (2009 – Pixel)

The object-based classification of the same mosaic showed similar results for the Water, Wetland and Burned Area classes and better results for the Savanna classes (Table 6). Overall

accuracy and overall Kappa were improved as well. Between the Water and Wetland classes minor misclassifications occurred. The number of Wetland areas that were misclassified as Savanna-Dense rose in comparison to the pixel-based classification which resulted in a lower producer's accuracy. The above mentioned problems to separate Burned Area from Savanna-Sparse areas occurred less often but were still present. The most important finding of the object-based classification is the fact that the separation between the two types of Savanna seems to succeed slightly better with an object-based approach. User's accuracy values were lifted above the 80% threshold for both types with Kappa rising from 0.7479 to 0.8025 for densely vegetated Savanna. Nevertheless, the problem of class separation still persisted. MSAVI values were used for class assignment in the rule set. Since the human eye cannot visualize MSAVI values, an accuracy assessment using the satellite image the classification was based on and band combinations of 4-3-2 did necessarily reveal the weaknesses of the classification.

2009: Object-based land cover classification						
	Water	**Wetland**	**Burned A**	**Savanna-D**	**Savanna-S**	Total
Water	**45**	4	0	0	1	50
Wetland	2	**51**	0	0	0	53
Burned A	0	0	**105**	1	10	116
Savanna-D	0	5	0	**55**	6	66
Savanna-S	0	1	17	22	**175**	215
Total	47	61	122	78	192	500
Producer's Accuracy	95.74%	83.61%	86.07%	70.51%	91.15%	Overall Accuracy: **86.20%**
User's Accuracy	90.00%	96.23%	90.52%	83.33%	81.40%	
Kappa	0.8896	0.9570	0.8746	0.8025	0.6980	Overall Kappa: **0.8123**

Table 6: Results of accuracy assessment (2009 – Object)

5.3 Land cover classification: 2002

Most of the results from the accuracy assessments for the 2009 scene applies to the 2002 image as well (Table 7, Table 8) and need no further explanation. These are the superiority of the object-based classification in general, the reliable classification of Burned Area, Water and Wetland areas and the problem of separation between the two types of savanna. Even the overall accuracy and overall kappa values are very similar for each type of classification. What differs though, are the exact classification results for the two savanna classes. The separation between those classes was even more complex in comparison with the 2009 scene. This is due

to the change in resolution of the image from 30 m to 15 m which leads to an increase in spectral information and detail. A more defensive approach was employed which consisted of assigning areas to Savanna-Sparse when in doubt. User's and producer's accuracy for this class show a high level of reliability with the object-based classification's kappa value being much higher than the pixel-based one. The results for Savanna-Dense are worse compared to the 2009 classification. While the object-based classification boosted the producer's accuracy from 78.95% to a very satisfying 93.33%, the user's accuracy changed for the worse from the pixel- to the object-based approach. A value of little more than 50% means that only half the pixels in the Savanna-Dense class belong to this class in reality. The overwhelming majority of the other half should have been classified as Savanna-Sparse. As mentioned above, MSAVI and NDVI thresholds were not being visually recognized in a satisfactory manner during the accuracy assessment.

2002: Pixel-based land cover classification						
	Water	**Wetland**	**Burned A**	**Savanna-D**	**Savanna-S**	Total
Water	**43**	3	1	1	2	50
Wetland	5	**46**	0	3	0	54
Burned A	0	0	**87**	0	14	101
Savanna-D	0	2	6	**45**	21	74
Savanna-S	0	0	11	8	**202**	221
Total	48	51	105	57	239	500
Producer's Accuracy	89.58%	90.20%	82.86%	78.95%	84.52%	Overall Accuracy: **84.60%**
User's Accuracy	86.00%	85.19%	86.14%	60.81%	91.40%	
Kappa	0.8451	0.8350	0.8245	0.5577	0.8353	Overall Kappa: **0.7827**

Table 7: Results of accuracy assessment (2002 – Pixel)

2002: Object-based land cover classification						
	Water	**Wetland**	**Burned A**	**Savanna-D**	**Savanna-S**	Total
Water	**47**	2	0	0	1	50
Wetland	0	**51**	0	1	1	53
Burned A	0	0	**86**	2	8	96
Savanna-D	0	4	1	**42**	34	81
Savanna-S	0	0	14	0	**206**	220
Total	47	57	101	45	250	500
Producer's Accuracy	100.00%	89.47%	85.15%	93.33%	82.40%	Overall Accuracy: **86.40%**
User's Accuracy	94.00%	96.23%	89.58%	51.85%	93.64%	
Kappa	0.9338	0.9574	0.8695	0.4709	0.8727	Overall Kappa: **0.8071**

Table 8: Results of accuracy assessment (2002 – Object)

The resulting maps (Chapter 8.2) show a very different picture for the two points in time concerning land cover. The appearance of the area of interest changes for every date of observation. This is caused by many factors, mainly fires which create what has been classified as Burned Area. Different levels of rainfall and overall weather conditions contribute by accounting for the state of vegetation. To perform change detection on the 2002 and 2009 images was found to be useless. It would have resulted in an overall change except for the Water and Wetland areas. No meaningful information would have been extracted from it. Change detection would have made sense if much more detailed land cover classes like settlements or cropland had been classified. The reason why this had not been the case is given in chapter 4.2.1. Nevertheless, the rule set for the object-based land cover classification was used as a valuable base for cropland classification.

A second useful outcome was the finding of object-based classification performing slightly better than pixel-based approaches. This is true for the overall accuracy and kappa accuracy. For individual classes, the picture is a more complex one with some pixel-based classified land cover classes showing the same or even a higher level of accuracy than the object-based derived ones. Even though Landsat imagery is usually seen as data to be used with pixel-based approaches, the data used in this study showed that OBIA methods can lead to good results and may even outperform traditional pixel-based practices.

Accuracy would have reached a very high level if the separation between the two savanna classes with regard to vegetation density had not been implemented at all.

5.4 Cropland classification

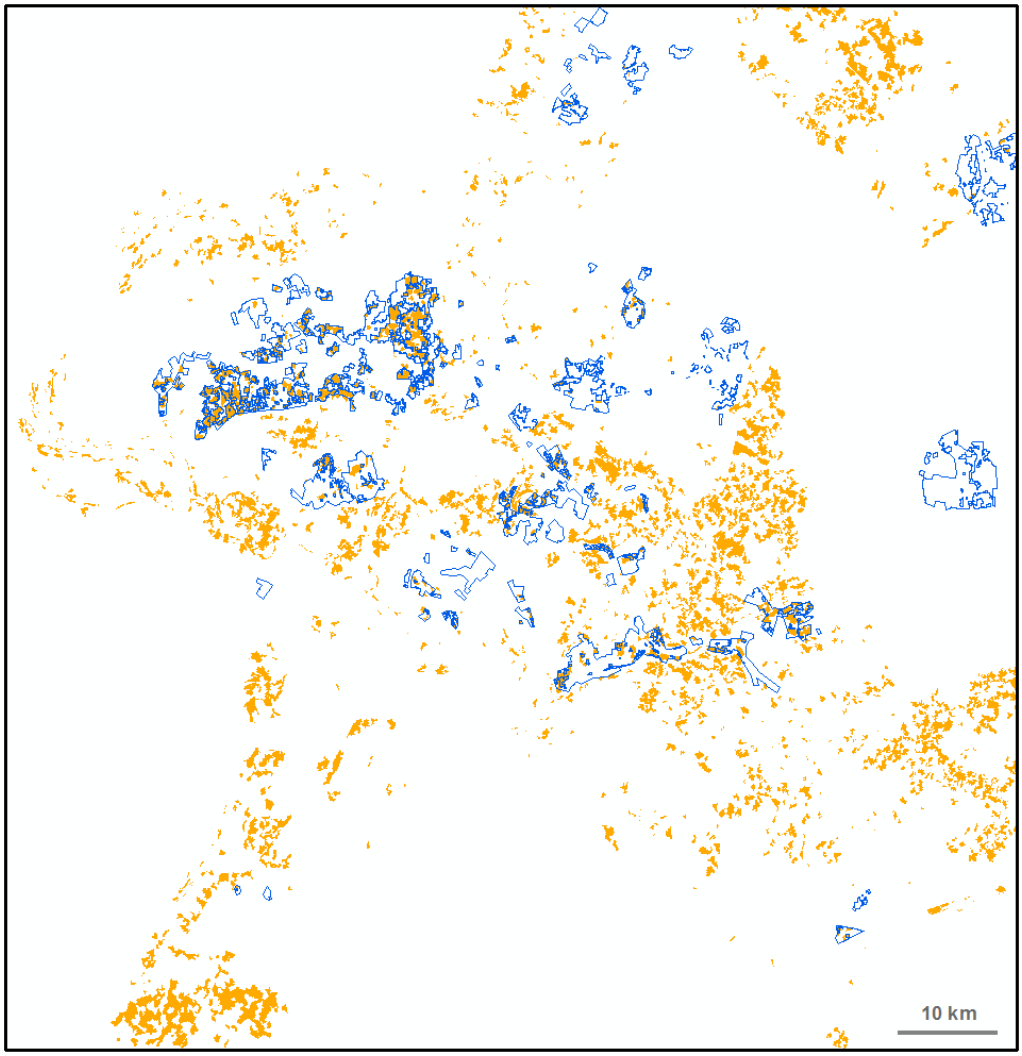

Figure 14: Object-based classification of cropland
Blue: Reference cropland areas, derived by digitization; Orange: Classified cropland areas

The results of the cropland classification as described in chapter 4.3 were considered unfeasible for further use. Figure 14 clearly shows the mismatch between the classified and digitized cropland areas. The reason for the poor results was the fact that the majority of cropland areas was impossible to address directly via spectral or geometrical characteristics. These characteristics, even though they are a reality, apply to too many non-cropland areas as well. The similarity between cropland and similar-looking non-cropland areas was found to be too high. This is illustrated by the huge number of orange colored areas in Figure 14 that are not cropland. At the same time, some of the blue framed objects shown in the figure above do not contain a single orange polygon. The idea to extract cropland from the entire AOI using a single rule set was discarded. In order to test whether the object-based approach would yield better results on a subset of the satellite image, two areas of interest were chosen and two

subsets created. Figure 10 shows their positions. The results of the subset based cropland classification are shown in Figure 15 and Figure 16.

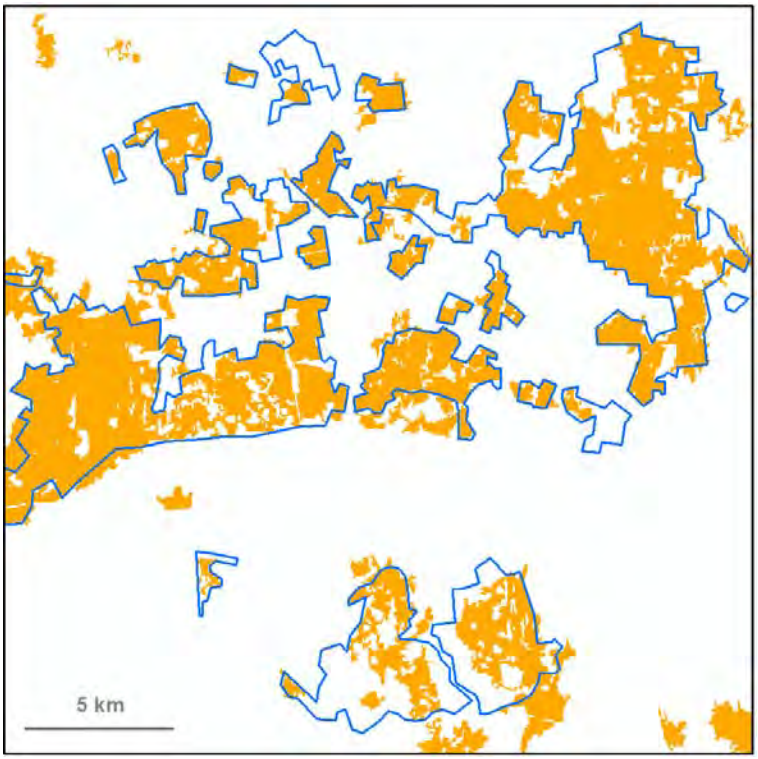

Figure 15: Cropland classification - Subset A
Blue: Reference cropland areas, derived by digitization; Orange: Classified cropland areas

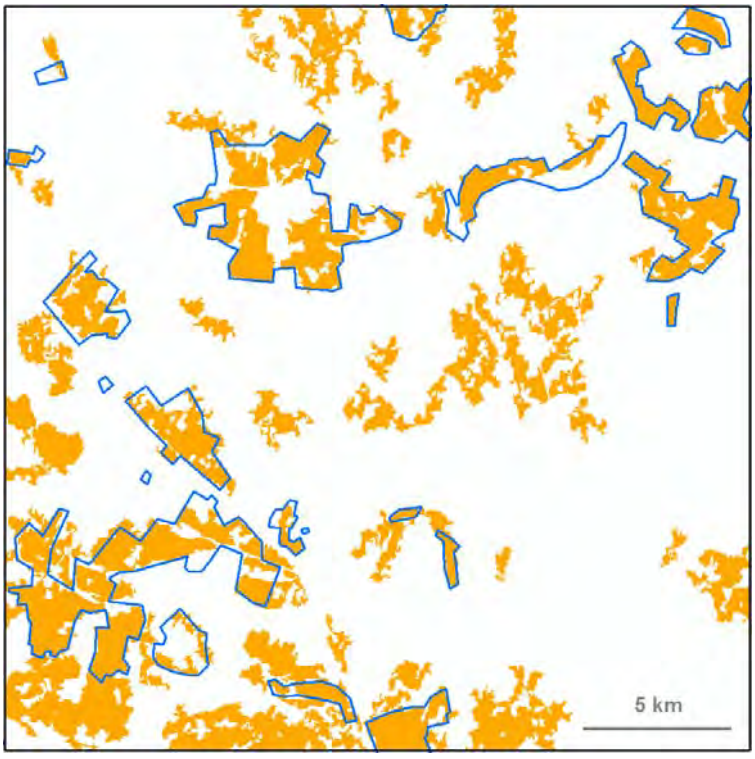

Figure 16: Cropland classification – Subset B
Blue: Reference cropland areas, derived by digitization; Orange: Classified cropland areas

Object-based cropland classification – Accuracy assessment					
Subset	**Digitized Area (Blue)**	**Classified Area (Orange)**	**Area that has been correctly classified (Orange within Blue)**	**Percentage of digitized area which was correctly classified (Producer's accuracy)**	**Percentage of classified area that is actually cropland in reality (User's accuracy)**
A	164.01 km²	134.83 km²	111.94 km²	68.25%	83.02%
B	82.16 km²	129.16 km²	56.70 km²	69.01%	43.90%

Table 9: Accuracy assessment for object-based cropland classification

A superficial glance at the statistics (Table 9) seems to give the impression that the results for both subsets are very similar with 68.25% and 69.01% of the reference cropland areas correctly classified (this corresponds to the producer's accuracy). However, the last column of the table shows the differences when it comes to the area classified as cropland that is actually cropland in reality (this corresponds to the user's accuracy). The classification for subset A features a much higher accuracy than the one for subset B. Figure 15 and Figure 16 emphasize this. A closer look reveals what types of areas were correctly classified and what types were misclassified. Figure 17 shows on the left a well classified detail view of the image. The areas correctly classified as cropland distinguish themselves from their surroundings because of high values in the infrared band. At the same time, some cropland areas as identified by visual image interpretation did appear very pale and greyish looking as shown in the red box. These areas were not classified as cropland because they resembled too much non-cropland and savanna-areas. Even their distinctive geometry did not enable reliable classification.

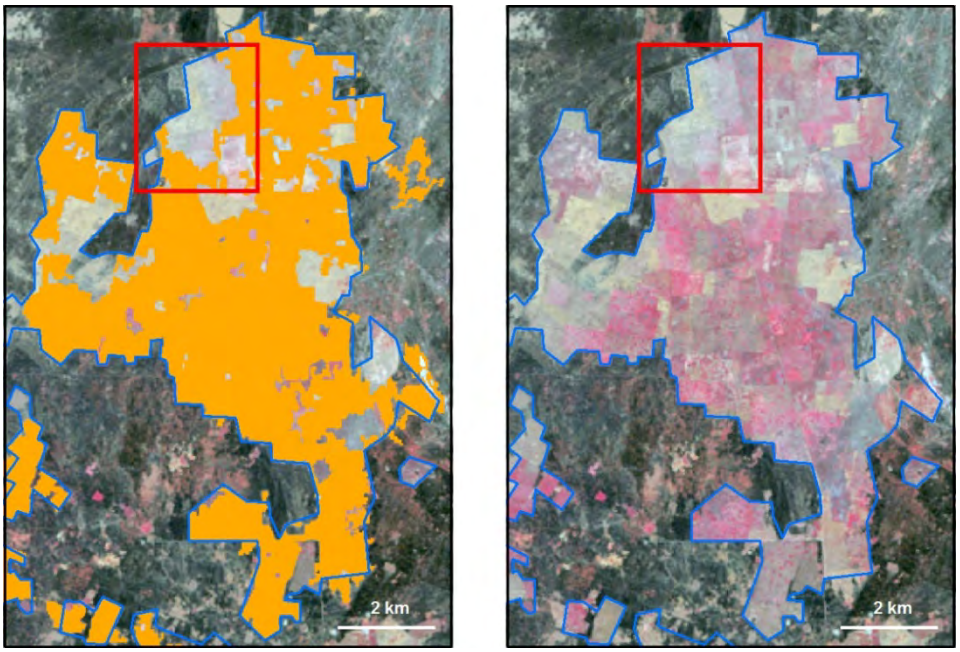

Figure 17: Subset A – Detail
Blue: Reference cropland areas, derived by digitization; Orange: Classified cropland areas

As mentioned already above, subset B included a lot of areas that appeared too similar to non-cropland in color, shape, and texture in order to successfully separate them. Figure 18 shows what some of the misclassified areas looked like. The visually identified cropland appears almost identical to burned areas or savanna which led to poor classification results.

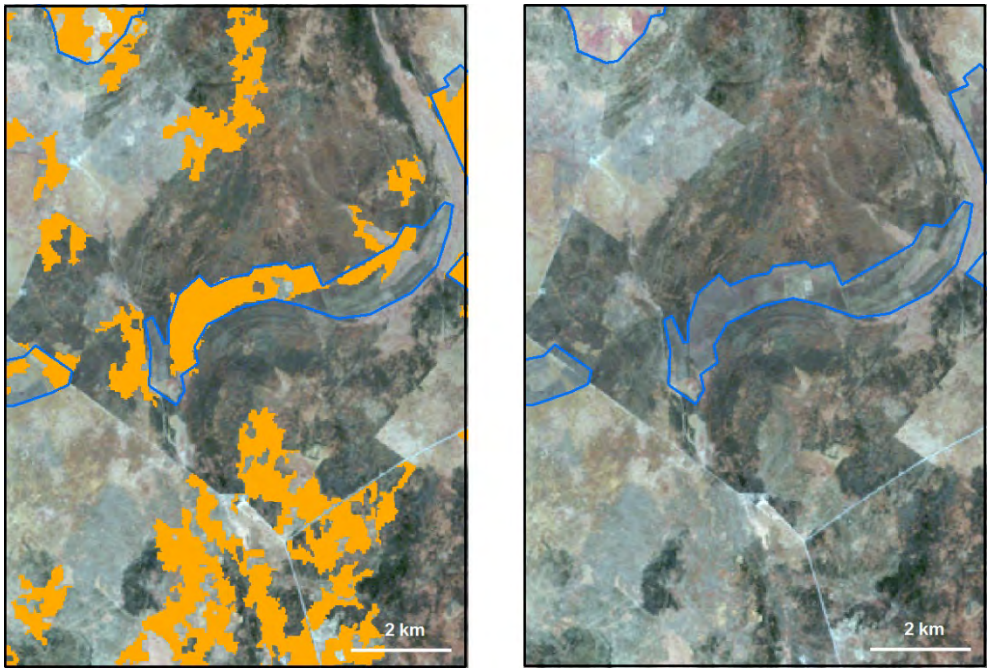

Figure 18: Subset B – Detail
Blue: Reference cropland areas, derived by digitization; Orange: Classified cropland areas

As a result, subset-based cropland classification using an OBIA approach yielded much better results on the given data than classification of the entire scene. Good results can be achieved locally. However, some areas consist of features closely resembling each other regarding their geometrical and spectral characteristics. The limits of object-based image analysis on 30 m-resolution data were obvious. This is not in contrast to the statement made in chapter 5.3 about the applicability of OBIA for Landsat. The statement made above is true for the classification of features that lack detail such as the land cover classes used in this study. Sophisticated features with less obvious spectral differences and geometrical characteristics that are similar to those of neighboring object ones are much more difficult to extract with OBIA methods at the given scale of 30 m and even 15 m. Very high resolution is needed to accomplish those tasks.

5.5 Oil well pad classification

As with the cropland classification, the oil well pad classification did not yield satisfying results for the entire scene. Too many bright looking objects of approximately the same size populate the scene for the oil well pads to be identifiable in every case. Even though locally the rule set

led to accurate results (Figure 19), the overall picture is one of too many misclassifications as can be seen in Table 10. Good use could be made of the rule set when used simply to identify areas where oil well pads cluster. In a second step, such areas could then be examined with very high resolution data. Selg (2013) investigated this in detail. A different approach could start by dividing the whole AOI into subsets that would then be classified with the use of distinct rule sets. Hese and Schmulius (2009) performed OBIA to extract oil well pads on Landsat-5 data for Russia. They used a subset of approx. 16.5 km x 16.5 km but even then did not fully succeed. Only parts of the oil well pads under investigation were correctly classified. Splitting the AOI into small subsets like the ones used by Hese and Schmulius would result in 36 subsets, of which supposedly 33% - 50% would contain oil well pads. Working this way would establish the need to modify a very high number of rule sets which is not easily feasible; at least not for more than one point in time.

Oil well pad classification - Accuracy assessment			
Number of digitized oil well pads	**Number of classified oil well pads**	**Percentage of digitized pads which were correctly classified (Producer's accuracy)**	**Percentage of classified oil well pads that are actually oil well pads in reality (User's accuracy)**
487	763	54.62%	34.86%

Table 10: Accuracy assessment for object-based oil well pad classification

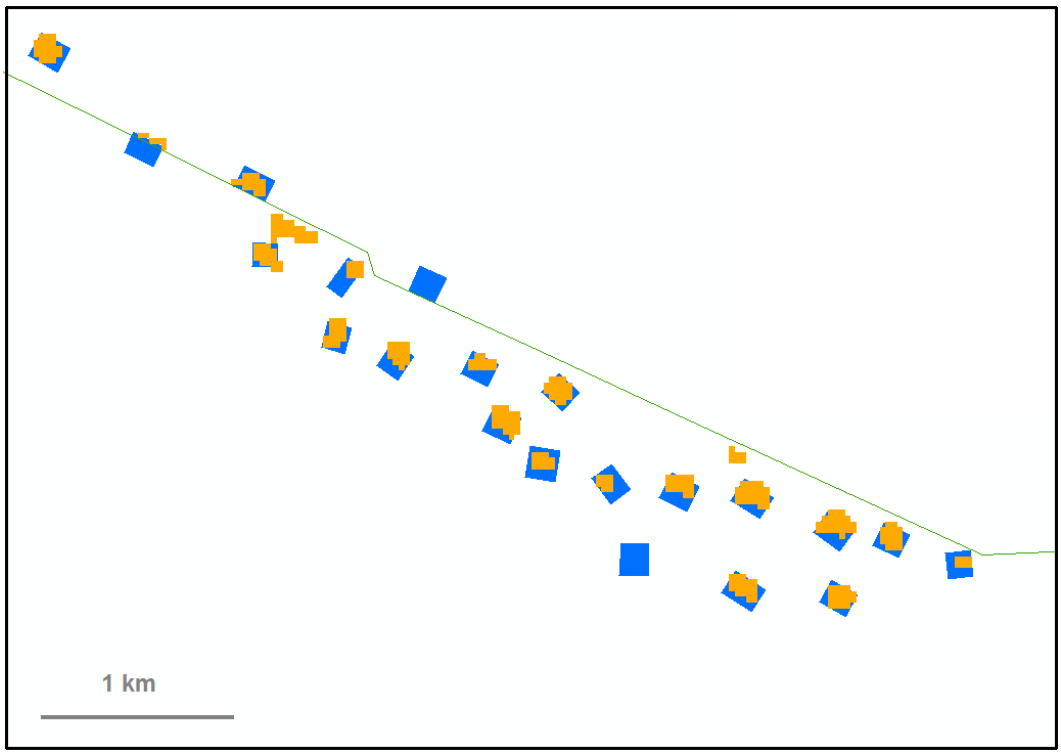

Figure 19: Oil well pad classification – Detail view
Blue: Reference oil well pads, derived by digitization; Orange: Classified oil well pads

As a consequence of the poor classification results for oil well pads and cropland areas, the initial plan of using those results for further GIS analysis was abandoned. Instead, the vector data, derived by visual interpretation and manual digitization, was used.

5.6 GIS-Analysis

5.6.1 Cropland change analysis

The amount of cropland as identified on the imagery was calculated. The results are shown below as well as in Figure 52 – Figure 57. Table 11 gives an overview over the size of the areas covered with cropland, changes in cropland as well as the percentage of cropland areas to the total area. With regard to cropland, the term total area refers to the part of the AOI that lies on the right of the White Nile. It comprises an area of 8,838.81 km². On the left hand side of the White Nile no cropland observation was performed. Please note that Table 11, Figure 20, Figure 21 and Figure 22 present results for the entire AOI while Table 12 shows the results for Melut County only.

Cropland statistics - Entire AOI (Right of White Nile river)			
Year	**Cropland in km²**	**Changes in cropland areas**	**Percentage of cropland to total area**
1999	167.71		1.90%
2002	37.92	-77.39%	0.43%
2004	112.05	195.49%	1.27%
2006	171.89	53.40%	1.94%
2009	433.67	152.30%	4.91%
2011	592.86	36.71%	6.71%

Table 11: Cropland statistics – Entire area of interest

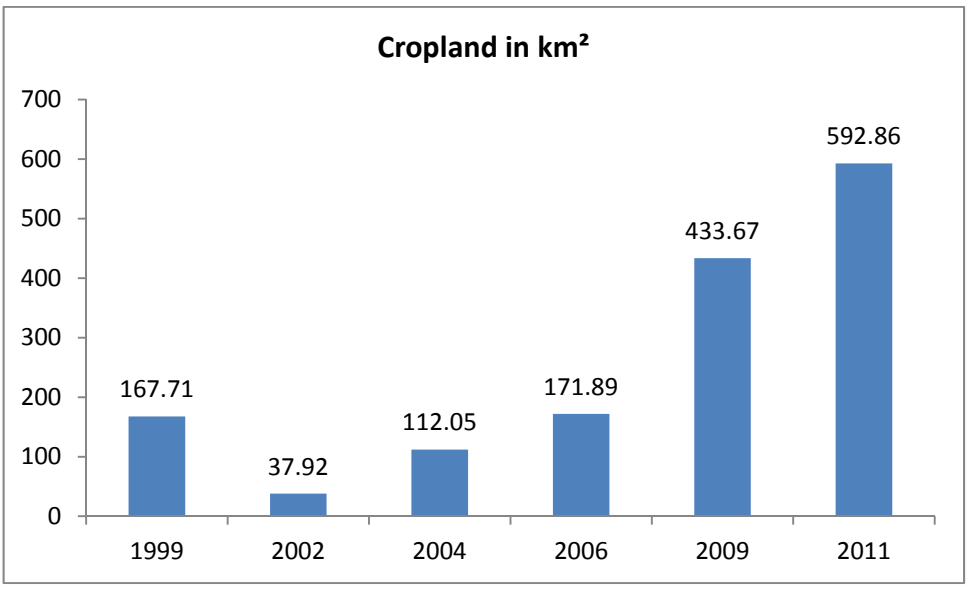

Figure 20: Cropland statistics – Entire area of interest

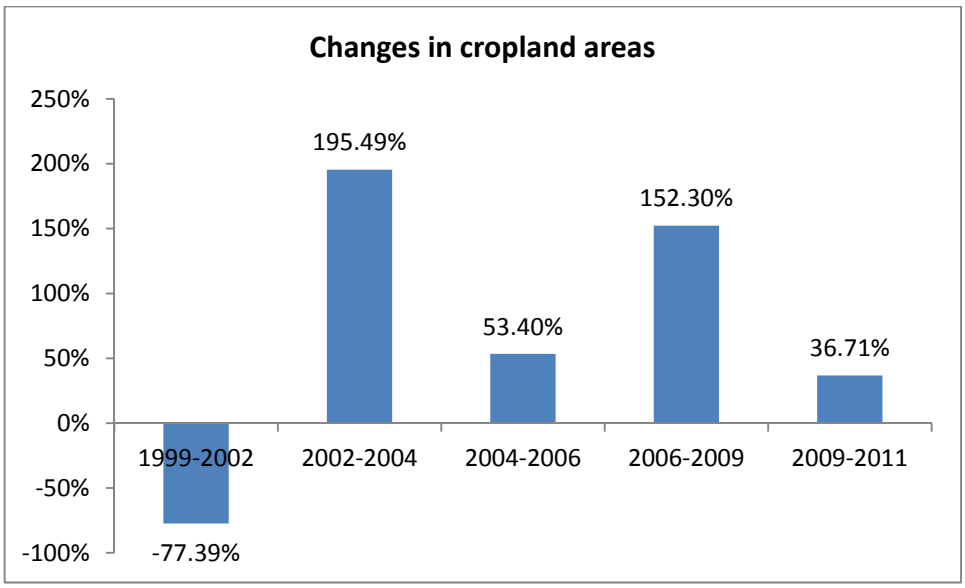

Figure 21: Changes in cropland areas – Overview – Entire AOI

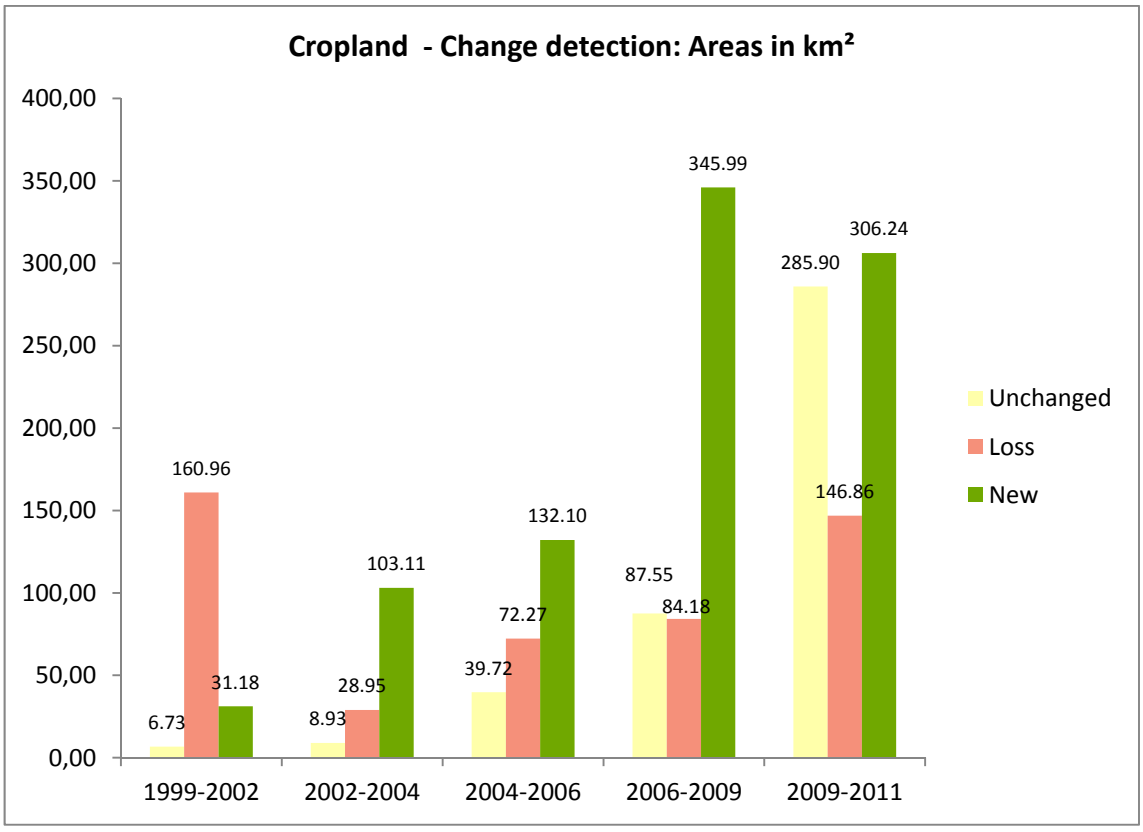

Figure 22: Changes in cropland areas – Detail – Entire AOI

Cropland statistics - Melut County			
Year	**Cropland in km²**	**Changes in cropland areas**	**Percentage of cropland to total area**
1999	157.38		2.27%
2002	35.95	-77.16%	0.52%
2004	112.05	211.68%	1.62%
2006	165.37	47.59%	2.39%
2009	364.5	120.41%	5.27%
2011	463.67	27.21%	6.70%

Table 12: Cropland statistics – Melut County

Five change maps were produced (Figure 58 - Figure 62) to present the locations of the changes in detail. The most important finding is the dramatic decrease of approx. -77% in cropland from 1999 to 2002. Change map no. 1/5 shows that the overwhelming majority of farm lands in the central part of the AOI disappeared. The period between 1999 and 2002 was characterized by the most intense fighting the oil field areas had witnessed. Thousands of people were forcefully displaced and fled their homes (ECOS, 2006, p.19). This seems to be the main reason for the decrease in agricultural lands. The following period (2002-2004) saw a strong recovery even though the cropland size of the year 1999 was not yet reached again. New cropland areas appeared in similar areas where they had been present in 1999. Full recovery was observed in 2006, when the amount of 1999 cropland was surpassed for the first time in both the entire AOI and in Melut County only. Gains in cropland were made in the south-eastern part of the AOI along the road between Paloich and Adar and around the town of Galdora. Losses were detected along the new road running in south-western direction from Galdora. The central areas around Paloich and east of Melut showed a lot of unchanged areas as well as expansion in northern direction. Apart from the losses on the road from Galdora to the south, there is a substantial area south-east of Paloich were cropland disappeared. The second civil war ended in 2004. From then on, formerly displaced persons returned to Melut County in great numbers (BICC, 2013). This could be a major reason for the increase in cropland as observed between 2004 and 2006. The following period (2006-2009) was characterized by major gains in farm lands. The corridor between Paloich and Melut was almost completely covered with cropland which reflects the strong population growth in both towns. South of the connecting road between both settlements appeared a new farming area as well. In the upper north, north-east and east huge areas were turned into cropland. Losses were visible west and north of Paloich but they were outnumbered by gains, especially East and south-east of Paloich. For the first time, the figure for unchanged areas had moved up from the bottom to the medium spot. It stayed there for the final period (2009-2011) but grew enormously in size: From 87.55 km² in 2009 to 285.90 km² in 2011. Gains were made in the southern and eastern parts of the AOI. The majority of centrally located cropland areas between the towns of Paloich and Melut remained unchanged or grew. Losses occurred all

over the AOI in a relatively high number which was almost as big as the one for the 1999-2002 period.

Precipitation data was used to check if the decrease in cropland areas from 1999 to 2002 can be linked to rainfall levels. The Global Precipitation Climatology Project (GPCP) provides global merged rainfall datasets that can be downloaded from NASA Godard Earth Sciences Data and Information Services Center (GPCP, 2013). GPCP combines satellite-based observations with rain gauge station data to calculate monthly rainfall on a 2.5-degree global grid. For a period from January 1999 to December 2010, monthly data for the AOI was summed up. Figure 23 shows that the level of rainfall indeed decreased from 1999 to 2002. Rainfall levels in 2004 were even lower while an increase in cropland area of 195.49% was observed (Figure 21) for that period. Annual rainfall rose steadily to reach its peak in 2007. For the period from 1999 to 2010 the lowest rainfall level was recorded for the year 2009 when 433.67 km² of cropland area were identified compared to 37.92 km² in 2002. While rainfall levels may have played a role in the development of cropland areas, it seems highly unlikely that the sharp decline in cropland areas from 1999 to 2002 can solely be attributed to weather conditions. Mass-displacement and people fleeing from the violence of the civil war seem to be the more important factor at work.

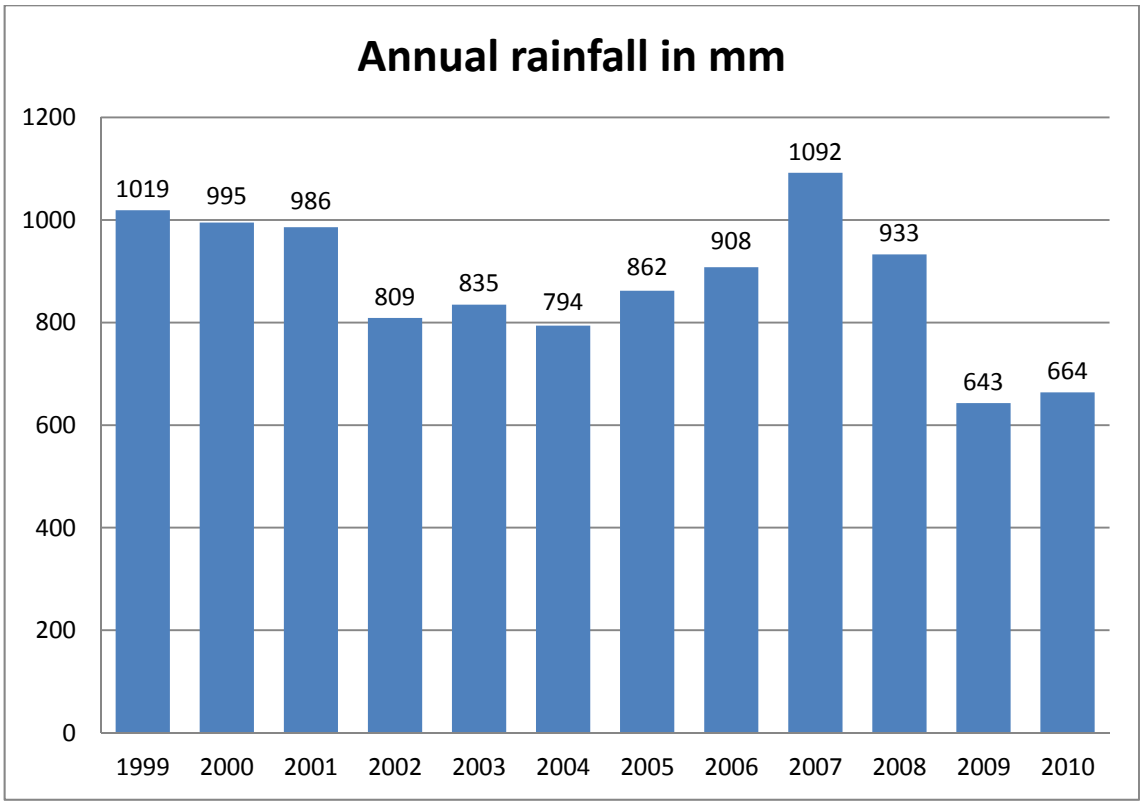

Figure 23: Annual rainfall 1999 - 2010

As a summary it is to be said that the ever increasing areas used for farming reflect the ever increasing number of people living in the area of interest. Thousands of people returned after the events of 2004/2005 and then again after independence when Sudan refused citizenship for South Sudanese (BICC, 2013, p.32). The attraction posed by the oil fields should also be accounted for.

When thinking about the massive growth in cropland areas one must keep in mind that the findings result from visually interpreted Landsat data with a resolution that does not allow for a detailed analysis of the state of the farm lands which were captured. Whether croplands were cultivated, fallow or even given up on could not be established. No reference or ground-truth data was available. Over-capture is a possibility and caution must be advised. This view is supported by the findings of the South Sudan National Bureau for Statistics (2010, p. 93). The statistical yearbook for Southern Sudan presents a number of 5,531 ha of harvested areas in Melut County and 5,072 ha for Maban County. The first would amount to 55.31 km². For the same year, 364.5 km² of cropland areas were identified on Landsat data. Even though the statistical yearbook refers to this number as an estimation only, the gap cannot be explained by this alone. More important seems to be the fact that it only accounts for harvested areas while satellite data analysis included all cropland areas that were visible as such, regardless of their status at the time of observation. Ground-truth data would have been needed for a strict separation between different types of agricultural lands.

5.6.2 Correlation analysis between cropland and road network

The extension of the road network was a steady process. It expanded from approx. 190 km in 1999 to approx. 1085 km in 2011. For the last change period the increase was very small compared to the previous years. Table 13, Figure 24 and Figure 25 present details.

Road network statistics				
Year	Road length in km (Entire AOI)	Road length change (Entire AOI)	Road length in km (Melut County)	Road length change (Melut County)
1999	190.432		185.948	
2002	257.311	35.12%	226.23	21.66%
2004	444.24	72.65%	369.693	63.41%
2006	658.208	48.16%	575.622	55.70%
2009	996.634	51.42%	872.366	51.55%
2011	1085.252	8.89%	960.983	10.16%

Table 13: Road network – statistics

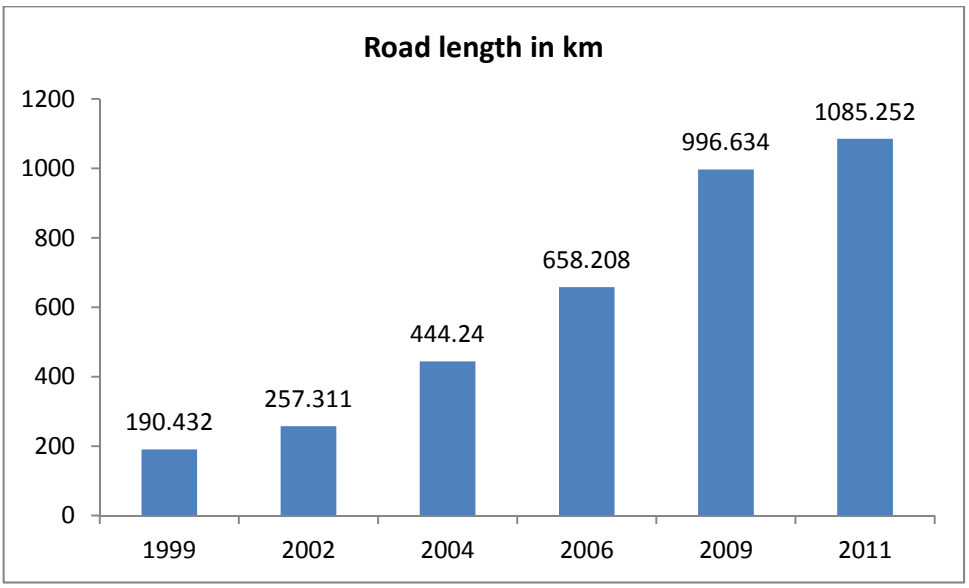

Figure 24: Road length – Entire AOI

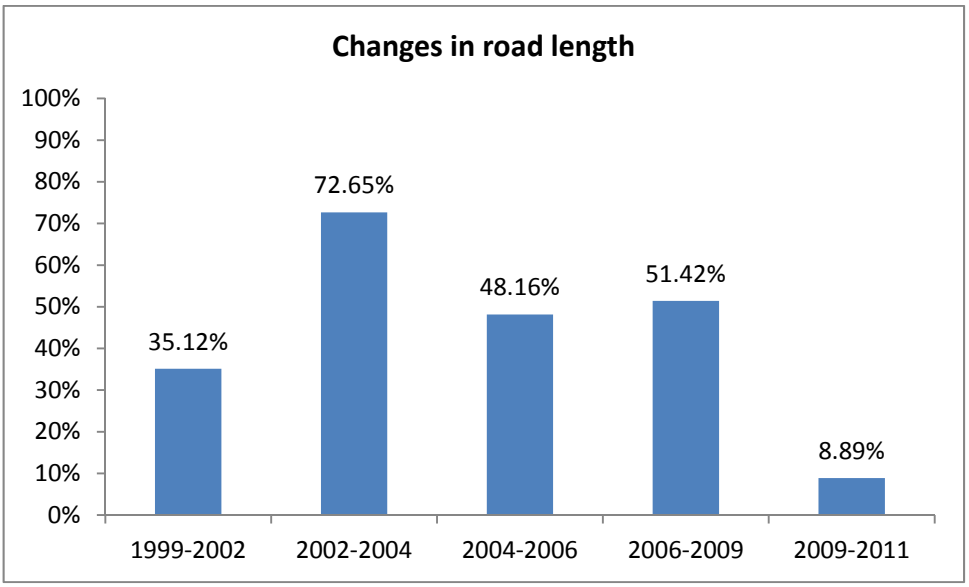

Figure 25: Changes in road length – Entire AOI

The relationship between cropland and road construction was investigated with three questions in mind: What is the distance between cropland areas and the road network for every year? Does the construction of new roads lead to the establishment of new cropland areas? Does the construction of new roads lead to loss of existing cropland? The first question was raised with Tobler's (1970) first law of geography in mind: "Everything is related to everything else, but near things are more related than distant things." Figure 26 is to be read like this: In the year 1999, approx. 25% of all existing cropland was situated within a 2,500 m-buffer to the nearest road. To provide a second example: In the year 2004, approx. 80% of all identified cropland was found to be within a 5,000 m-buffer around the road network.

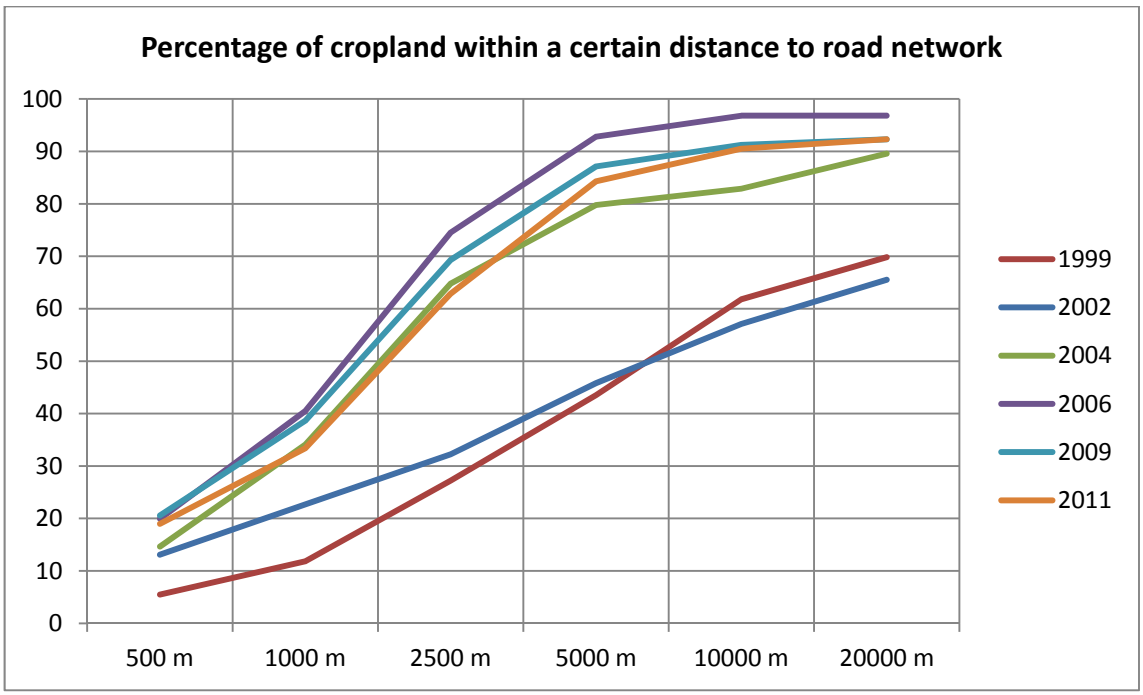

Figure 26: Distance cropland – road network

When all six points in time are considered, the diagram shows that from 2004 on, cropland was situated closer to the road network than before. The year 2006 tops the list. Almost 100% of the 2006 cropland was located within 10,000 m of the road network. For the years 2009 and 2011, only 90% were located within this distance. The main reason for cropland being further away from the roads in the years of 1999 and 2002 was simply the fact that there were little roads at all. This comprises roads that were identified on 15 m Landsat data. Obviously some sort of roads or tracks must have existed. Otherwise people would not have been able to cultivate their lands which they did because cropland has been identified for these years. From this followed the simple observation that with an increase in roads and cropland, the two types of features tended to be located closer to each other. Whether cropland growth was directly caused by transport network development could not be determined from the statistics.

The second question – Does the construction of new roads lead to the establishment of new cropland areas? – asks about positive effects of road development. To answer it, a buffer analysis was performed as well. To avoid confusion, the results are shown in five tables instead of a single one.

2002: Percentage of new cropland located in a certain distance to the road network						
	500 m	1000 m	2500 m	5000 m	10000 m	20000 m
Roads 1999	8.02	12.83	25.79	40.09	50.10	59.88
New roads 2002	3.43	6.96	18.76	26.65	33.39	50.61

Table 14: 2002 – New cropland / new roads

2004: Percentage of new cropland located in a certain distance to the road network						
	500 m	1000 m	2500 m	5000 m	10000 m	20000 m
Roads 2002	9.11	20.10	39.81	53.92	81.37	87.59
New roads 2004	7.57	17.52	45.22	75.67	81.85	90.23

Table 15: 2004 – New cropland / new roads

2006: Percentage of new cropland located in a certain distance to the road network						
	500 m	1000 m	2500 m	5000 m	10000 m	20000 m
Roads 2004	7.94	15.11	43.04	76.18	92.17	-
New roads 2006	11.12	24.49	56.19	84.10	95.14	95.79

Table 16: 2006 – New cropland / new roads

2009: Percentage of new cropland located in a certain distance to the road network						
	500 m	1000 m	2500 m	5000 m	10000 m	20000 m
Roads 2006	11.12	21.61	46.81	68.15	79.83	90.08
New roads 2009	8.76	19.14	48.27	76.97	84.03	90.32

Table 17: 2009 – New cropland / new roads

2011: Percentage of new cropland located in a certain distance to the road network						
	500 m	1000 m	2500 m	5000 m	10000 m	20000 m
Roads 2009	19.28	30.51	54.70	77.98	88.37	92.74
New roads 2011	1.18	2.60	8.45	20.99	48.71	79.88

Table 18: 2011 – New cropland / new roads

For every change period, Table 14 to Table 18 shows the percentage of new cropland located within a certain distance to the road network. The idea was to examine whether new cropland areas were located closer to newly built roads instead of already existing ones. If that was the case, one could argue that road construction might have made former inaccessible areas accessible for farming. The tables are to be read like this: In 2006, 24.49% of new cropland was located within a distance of 1,000 m to newly built roads while only 15.11% of new cropland was located within distance of 1,000 m to previously existing roads, i.e. roads that were

already present in 2004. If the value in the “New roads yyyy”-column is higher than the one in the “Roads yyyy”-column, the new cropland was closer to the new roads than to the previously existing ones. For 2002 this was not the case at all. In the year of 2004, new cropland was closer situated to new roads than “old” ones for distances from 2,500 m on. The same phenomena could be observed for 2006 with new cropland being closer to new roads than existing ones from the smallest buffer distance on. In 2009 the situation resembled the year of 2004. The trend was reversed in 2011 when proximity to previously existing roads was much higher than to new ones. Although important gains in new cropland were made in the concerned change period, only a very small number of new roads were constructed. This examination led to the same results as the observation of the general distances between cropland and roads: Even though in some cases new cropland areas were located in closer proximity to newly built roads and therefore may ultimately have been an outcome or side-effect of road construction, this could not be assessed from satellite imagery and the resulting statistics alone.

The third question, asking about possible negative effects of road construction, could have been answered in the same way as the two previous ones by performing a buffer analysis. Since these did not seem to yield clear results, the approach was not followed. Instead, a purely visual inspection and interpretation of the relationship between cropland loss and road development was undertaken. This way, the results of the distance analyses were reviewed as well. For each change period, the following figures (Figure 27 – Figure 31) show new and lost cropland as well as previously existing and new roads.

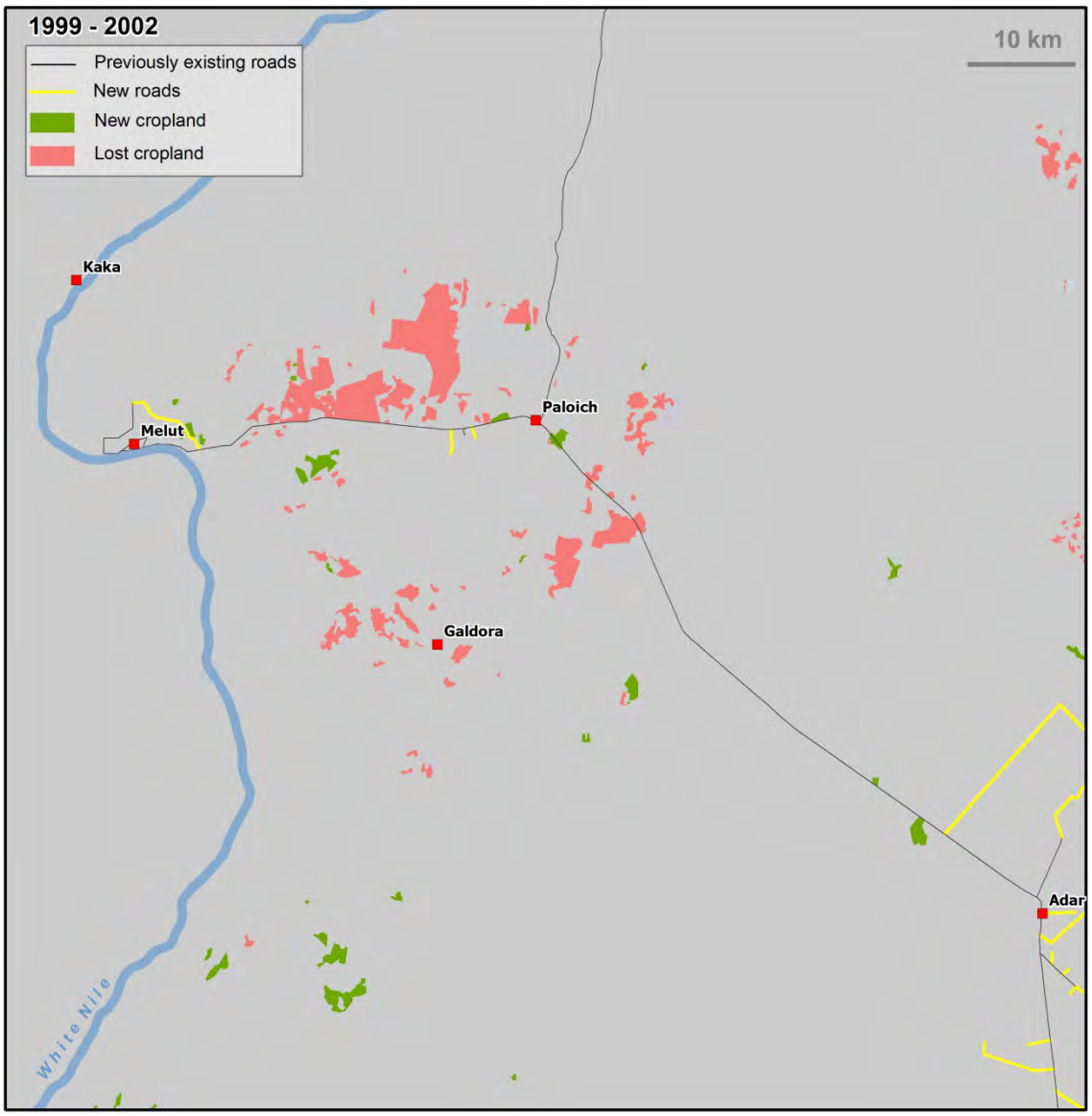

Figure 27: 1999-2002 - Impacts of road construction

For the period of 1999-2002, no negative impacts of road construction are visible. Only little road development can be observed. East of the town of Melut, small new cropland areas were identified which lie next to a new road. Whether the two were connected is unknown as has been discussed above but cannot be ruled out either.

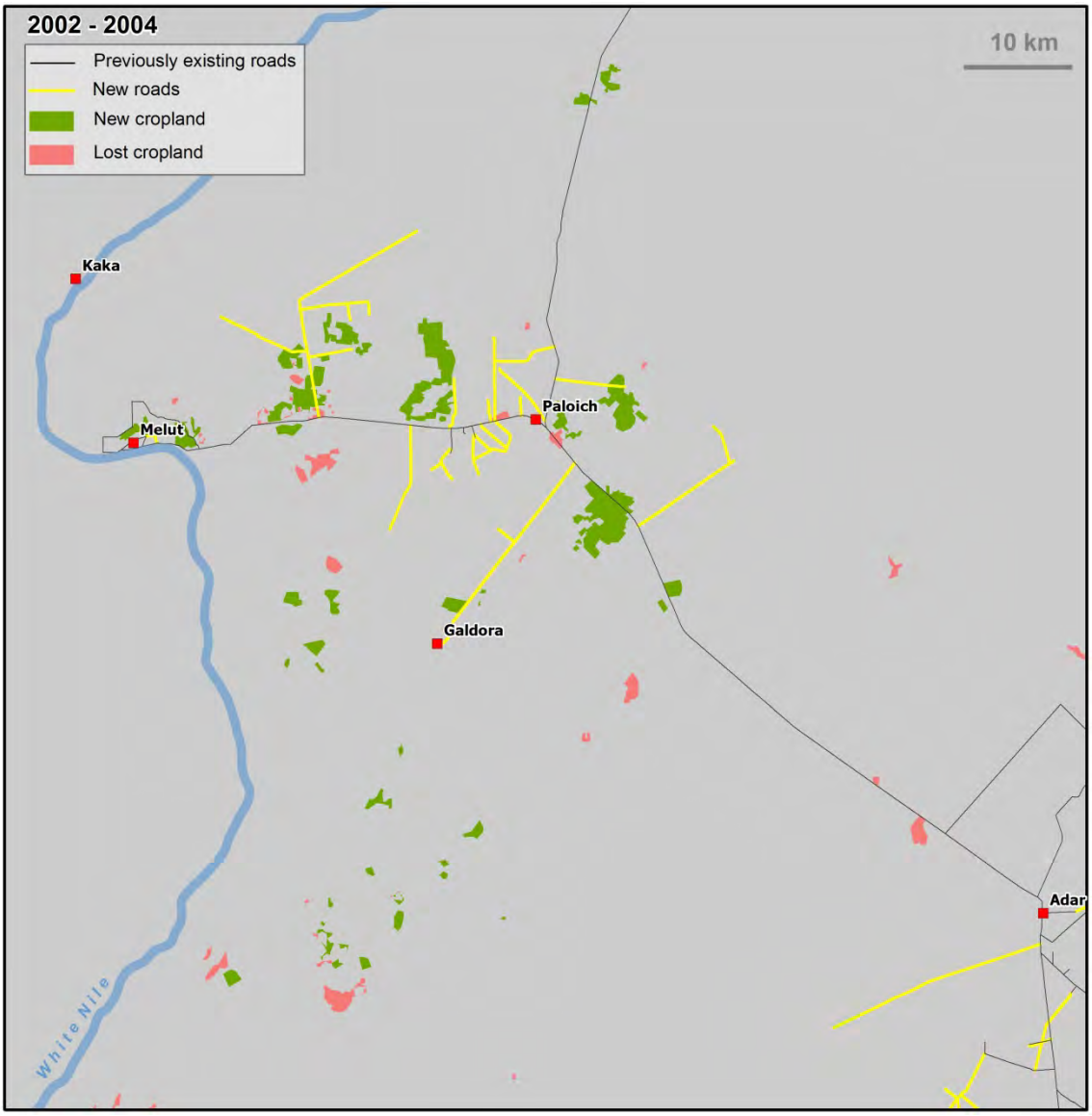

Figure 28: 2002-2004 - Impacts of road construction

Much more cropland was gained than lost from 2002 to 2004. Areas of loss were not located in closer proximity to new roads than to previously existing roads. As stated above, some of the new cropland areas laid closer to new roads than to previously existing roads for this period of observation. This phenomena can be seen east of Paloich and in the corridor between Melut and Paloich.

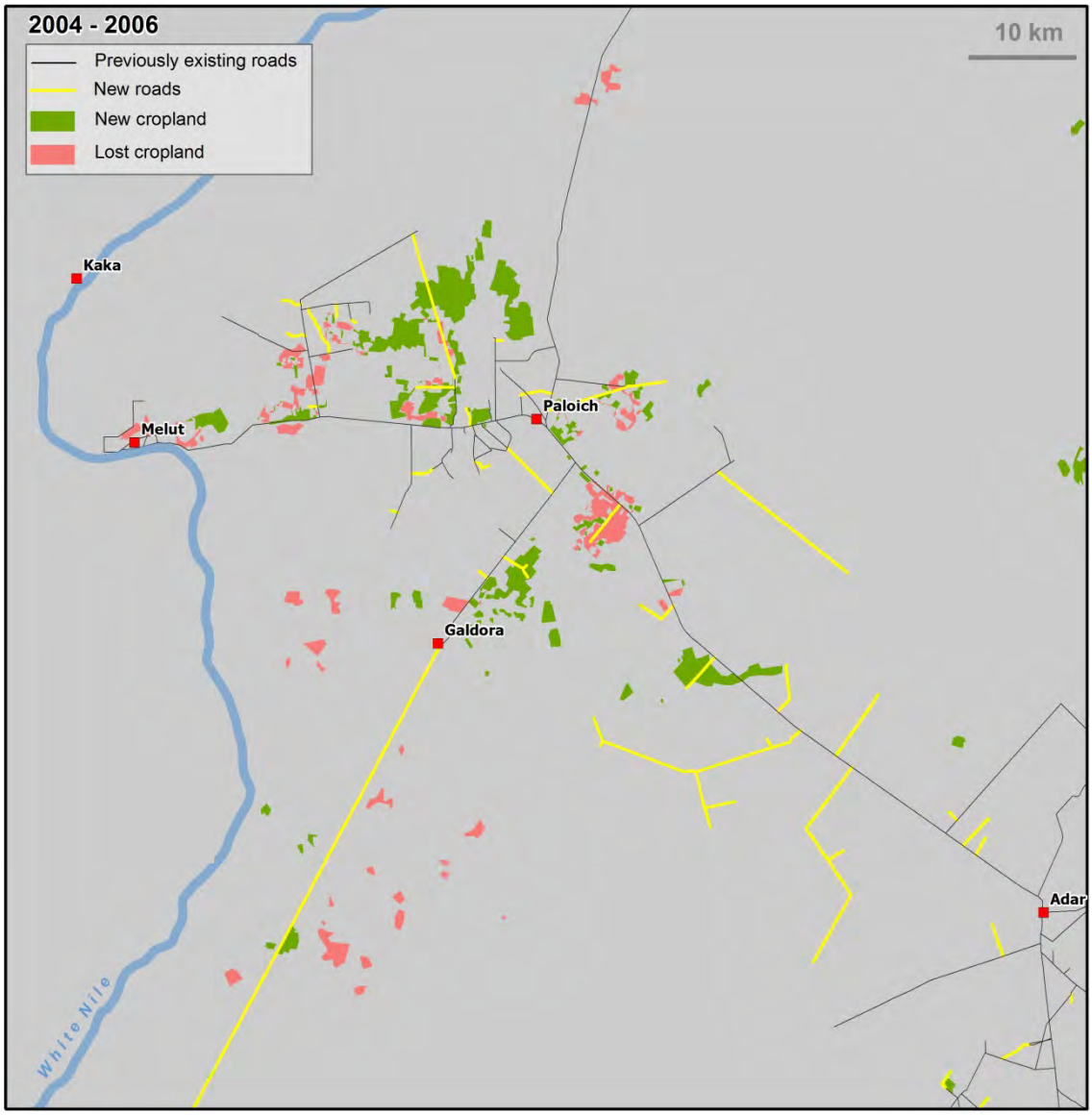

Figure 29: 2004-2006 - Impacts of road construction

There is an area north-east of Galdora where a new road seems to cut through former farming areas. At the same time, small new cropland areas appear around this new road. The same can be said about the new major road from Galdora to the south where new and lost cropland can equally be found. This is also true for areas around a new road east of Paloich where losses and gains in cropland were identified.

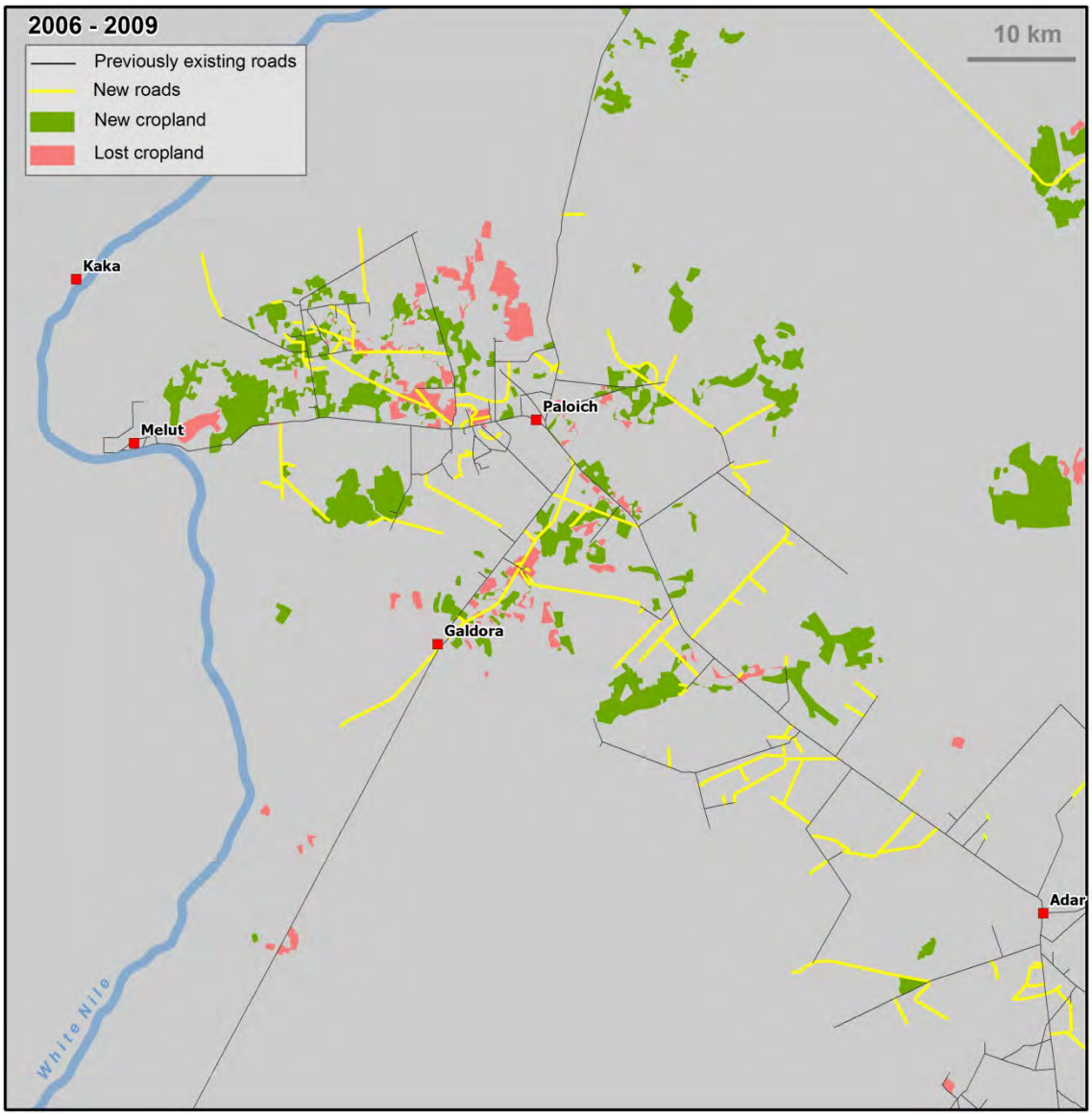

Figure 30: 2006-2009 - Impacts of road construction

More new roads appeared between 2006 and 2009 than during any other period. Figure 30 gives various examples of cropland losses and gains in close proximity to new roads. This is especially the case in the area east of Paloich and in the far north-eastern corner of the map where a causal connection between the new road and new cropland areas seems likely.

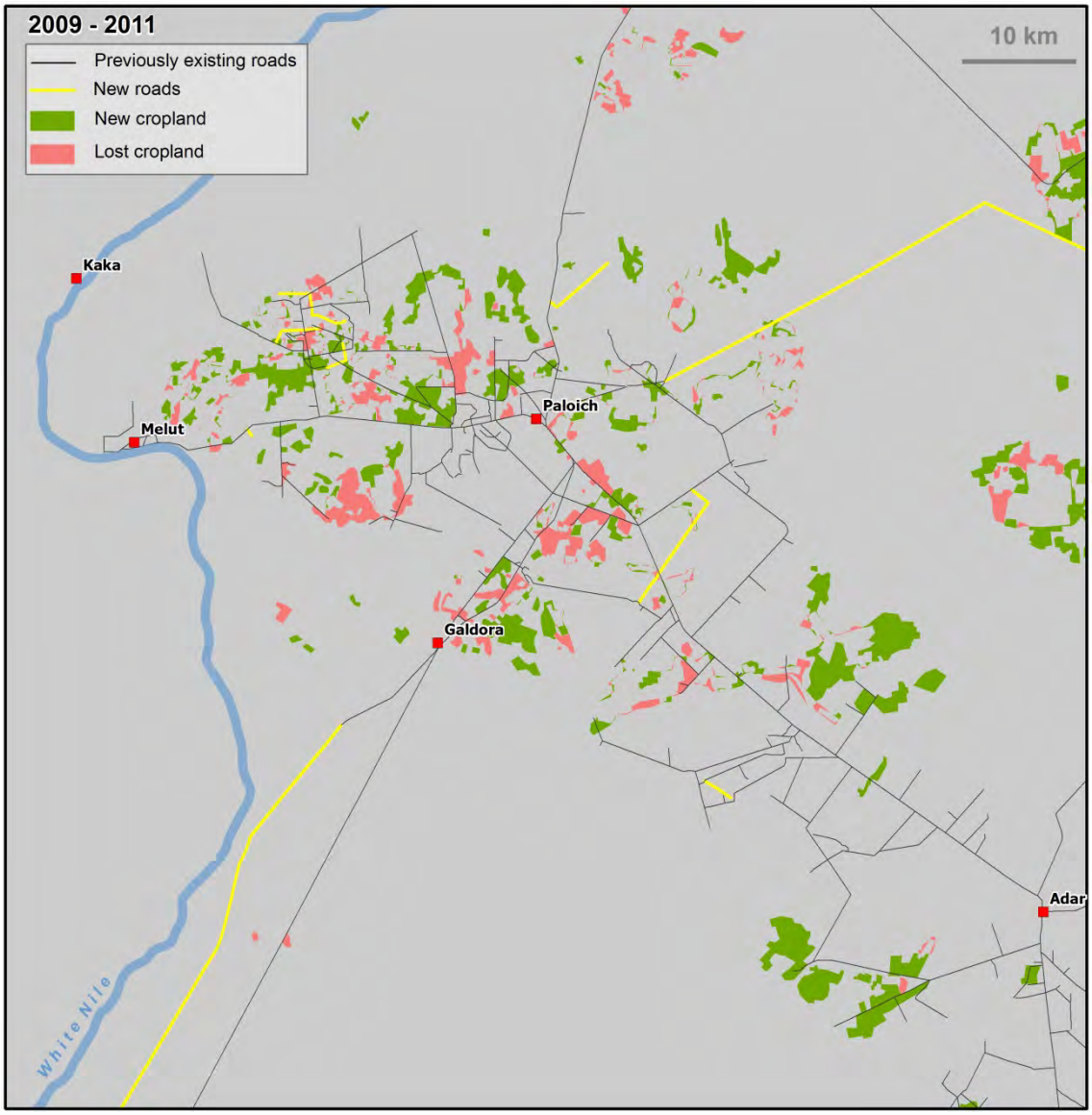

Figure 31: 2009-2011 - Impacts of road construction

While the period from 2009 to 2011 exhibits almost as many lost cropland areas as the first change period (1999-2002), the majority of the concerned areas is not closely located to newly erected transport infrastructure.

As a general outcome of the visual inspection, it can be said that there is no straight answer to the third question regarding the impact of road construction. Many examples for and against the assumption that cropland areas were lost due to road construction were found. The same is true for the more positive assumption of road networks opening up former inaccessible areas. As shown above, some statistics and the GIS-based overlay of cropland areas with the transport network suggest that this was partly the case. From satellite-based image analysis, only a status quo picture can be derived. Even though some of the information gained from image interpretation and statistics indicate a certain likelihood for or against specific conclusions, other means of investigation are necessary to give definite answers. Image

analysis is therefore a tool out of which important questions to ask arise but not a tool to provide easy answers.

5.6.3 Oil field development

In the area of interest, the number of identified oil well pads rose from a single one in 1999 to 555 in 2011. Similar to the expansion of cropland areas and transport infrastructure, the oil field development seemed to have slowed down from 2009 on.

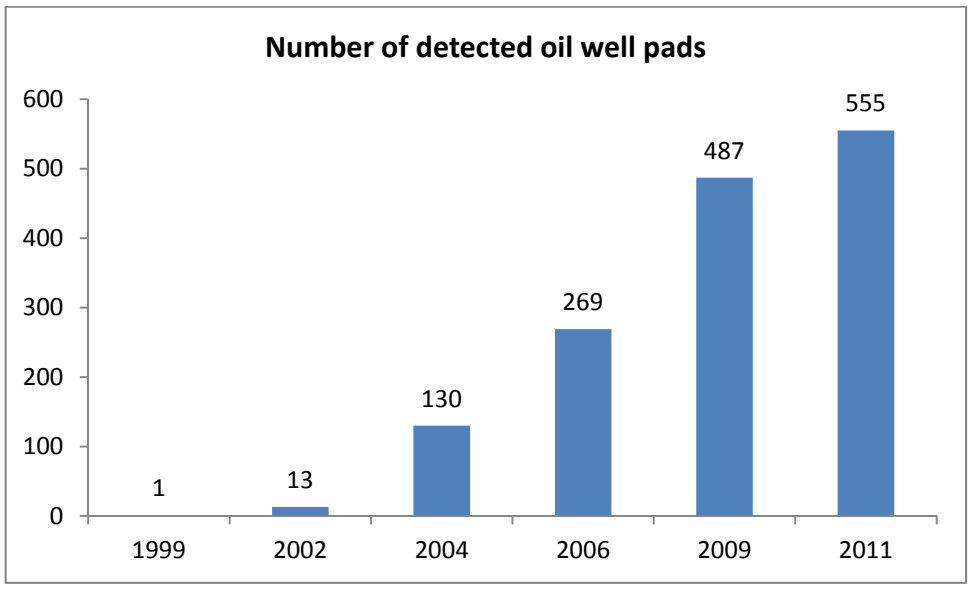

Figure 32: Number of detected oil well pads

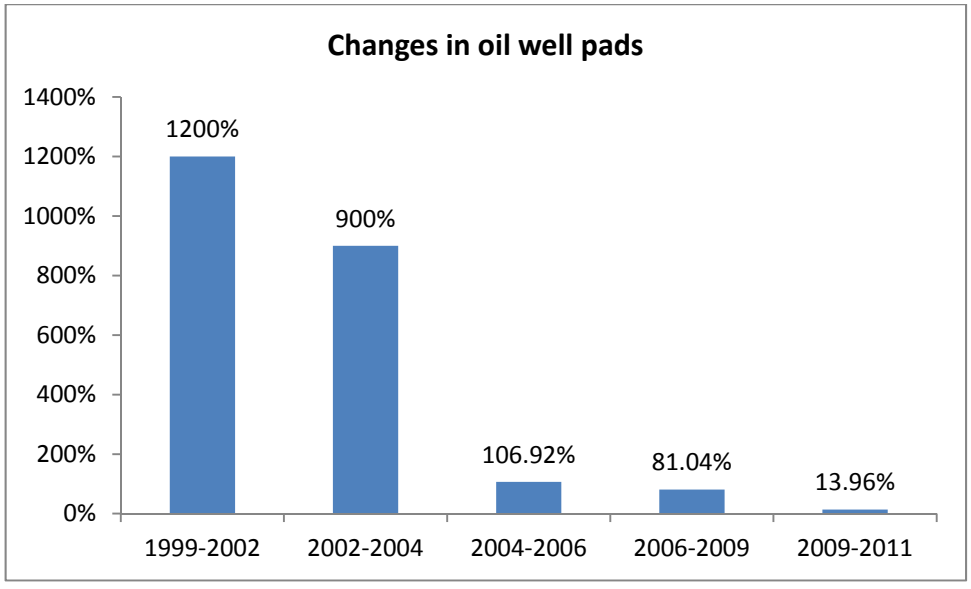

Figure 33: Changes in oil well pads

Oil field development				
Year	Number of oil well pads (Entire AOI)	Changes in oil well pads (Entire AOI)	Number of oil well pads (Melut County)	Changes in oil well pads (Melut County)
1999	1		1	
2002	13	1200%	3	200.00%
2004	130	900%	95	3066.67%
2006	269	106.92%	213	124.21%
2009	487	81.04%	400	87.79%
2011	555	13.96%	458	14.50%

Table 19: Oil field development

Figure 63 visualizes the expansion of the four oil fields. In 1999, only a single well pad in what was to become the Paloich oil field could be seen. Three years later, the Adar Yale field had expanded while the Paloich oil field had also grown in size. The picture changed as observed on the 2004 images with a massive increase of oil well pads in the Paloich field and substantial growth in Adar Yale. The Muleeta oil field north-west of Paloich was active as well. For the following three points in time – 2006, 2009, 2011 – all fields expanded considerably. Another new field, the Gumry oil field located between Adar Yale and Paloich, was identified in the 2006 imagery.

According to a report by the Nile Research Initiative (2013, p.37), the combined number of oil well pads from all four oil fields was 601. Taking into account that parts of the Adar Yale field are located outside the AOI and further expansion of the fields between 2011 and 2013 seems likely, the number of 555 identified oil well pads for 2011 suggests a very high level of accuracy.

Tiede and Lang (2010) suggested the use of 3D globe viewers such as *Google Earth* or *NASA World Wind* for data visualization purposes. By "using the third dimension as an additional, explicit carrier of information" (Tiede, 2010), scientific results can be placed in a spatial context most people are familiar with. User engagement with and understanding of the data would be greatly enhanced by being able to zoom, rotate and explore data on different scales. This way, the limitations of traditional maps, whether analog or digital, can be overcome. To explore these possibilities*, ESRI ArcScene* and *Google Earth* software were used to visualize the development of the oil fields with the height of the grid blocks representing the number of oil well pads. Colors are the same as in Figure 63. Figure 34 shows the Muleeta and Paloich fields in 2009 as well as the bend of the White Nile between the towns of Melut and Kaka. Figure 35 presents a view from the north-east with the Paloich oil field in the foreground and the road to Adar, leading to the fields of Gumry and Adar Yale, closing on the horizon. These two examples show the potential and advantages of putting GIS analysis results in an easy-to-navigate context, especially when compared with the static oil field development map (Figure 63).

For reasons still unknown, visualization in *ESRI ArcScene* worked smoothly while the conversion to *Google Earth* KML-files encountered massive problems. These have not been resolved. Data conversion did only work for the oil field data representing the year 2009 while all the other files did not work. Persistent trouble-shooting did not lead to satisfactory results and was given finally up on. Further research into conversion problems is necessary.

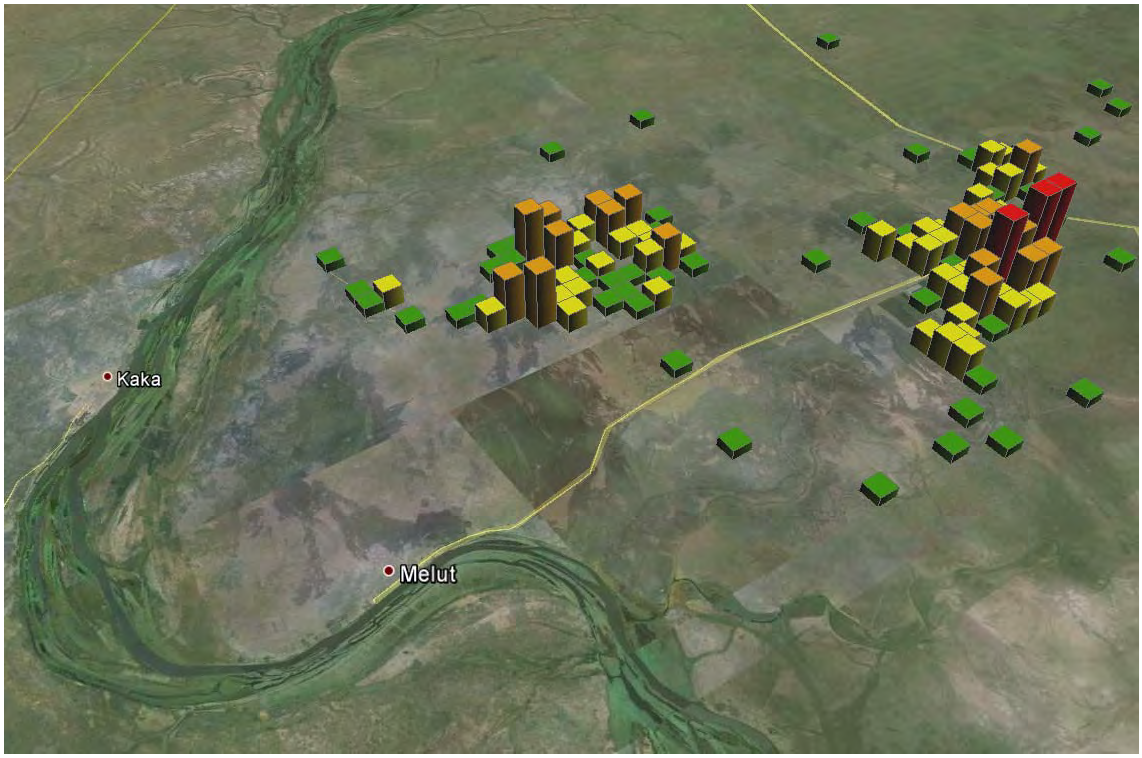

Figure 34: Muleeta and Paloich oil fields

Figure 35: Paloich to Adar

The results of the visual analysis to determine whether or not the expansion of the oil fields led to losses of cropland areas are given below in Figure 36 to Figure 44.

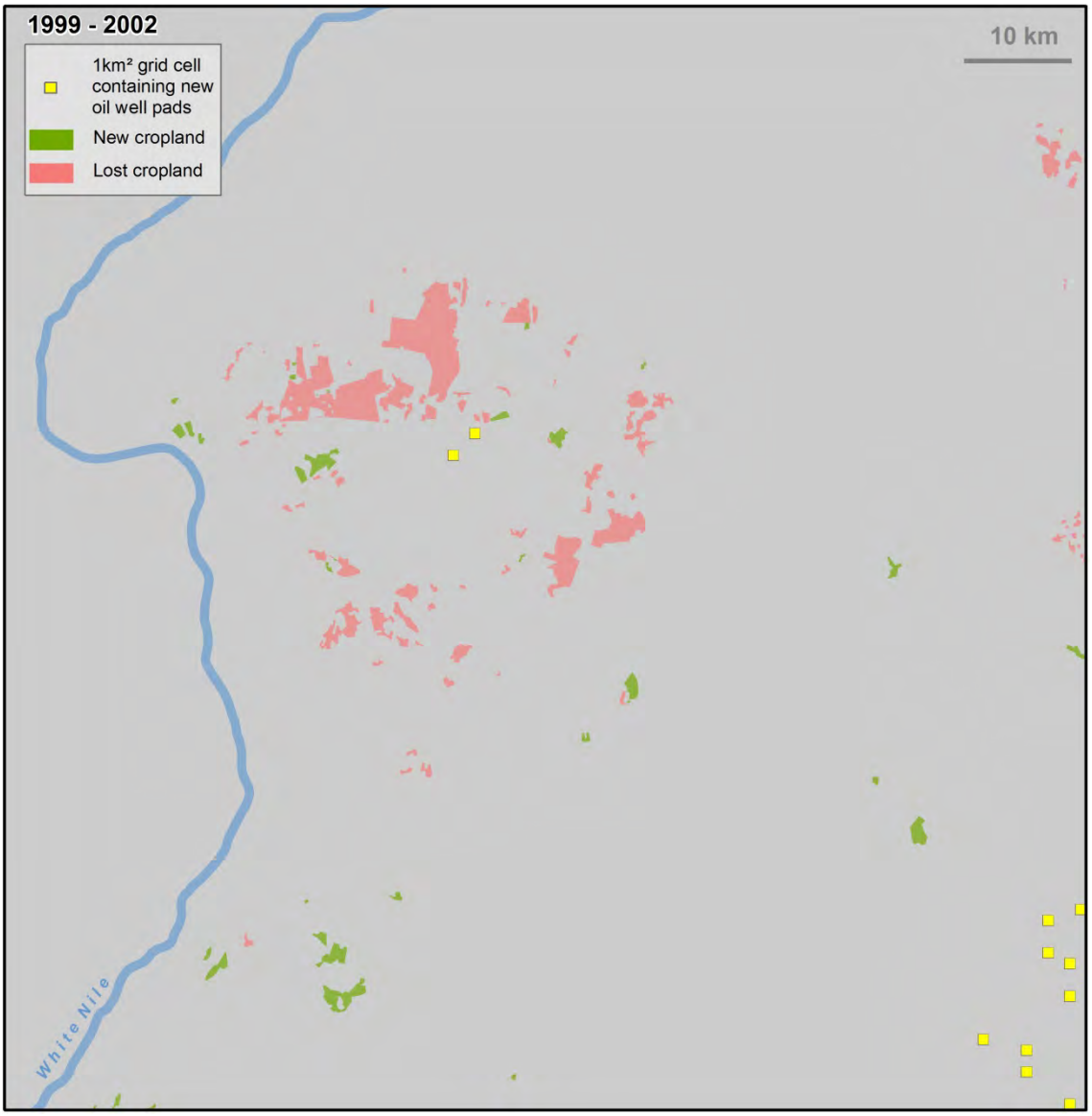

Figure 36: 1999-2002 – Impacts of oil field expansion

No spatial connection was observed between new oil well pads and changes in cropland areas for the period of 1999-2002.

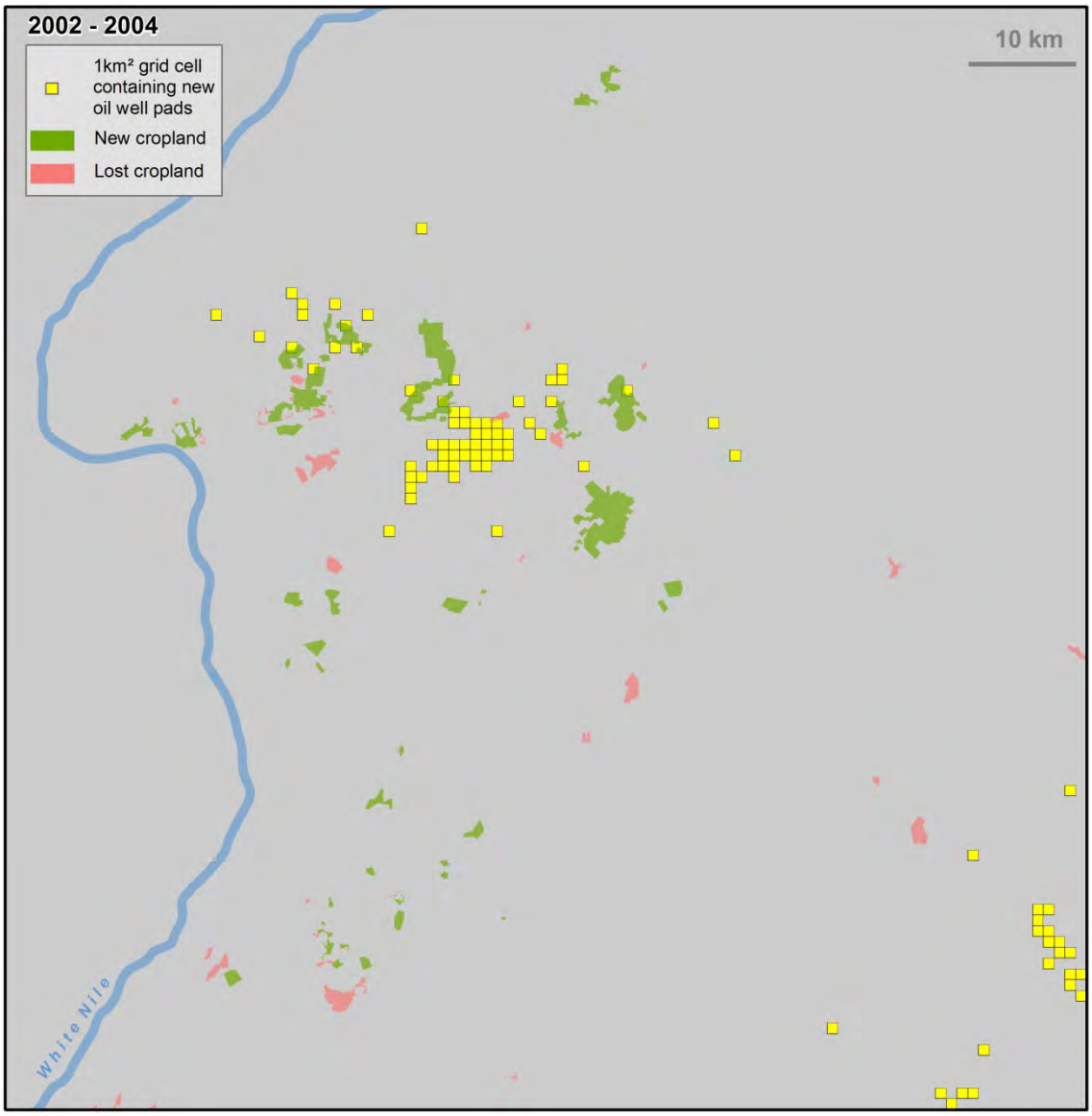

Figure 37: 2002-2004 – Impacts of oil field expansion

Figure 37 shows that lost and gained cropland areas overlap grid cells containing new oil well pads. It was assumed that new oil infrastructure supplants farm lands. Figure 38 shows a more detailed view of the situation with the actual positions of the oil well pads visualized as black dots. An example is given in the right part of Figure 38, supporting the above-mentioned assumption. At the same time, new cropland areas emerged around new oil well pads. In fact, for the change period under consideration, more examples were found for the latter mentioned instance than for the suppression of croplands.

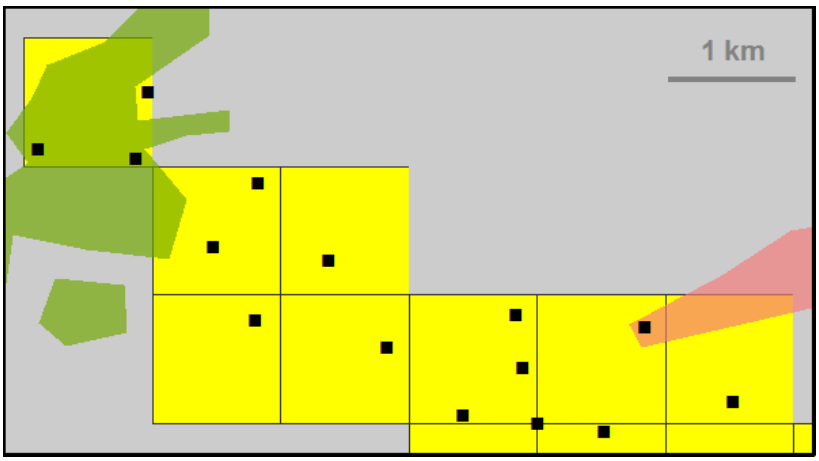

Figure 38: 2002-2004 – Detail view

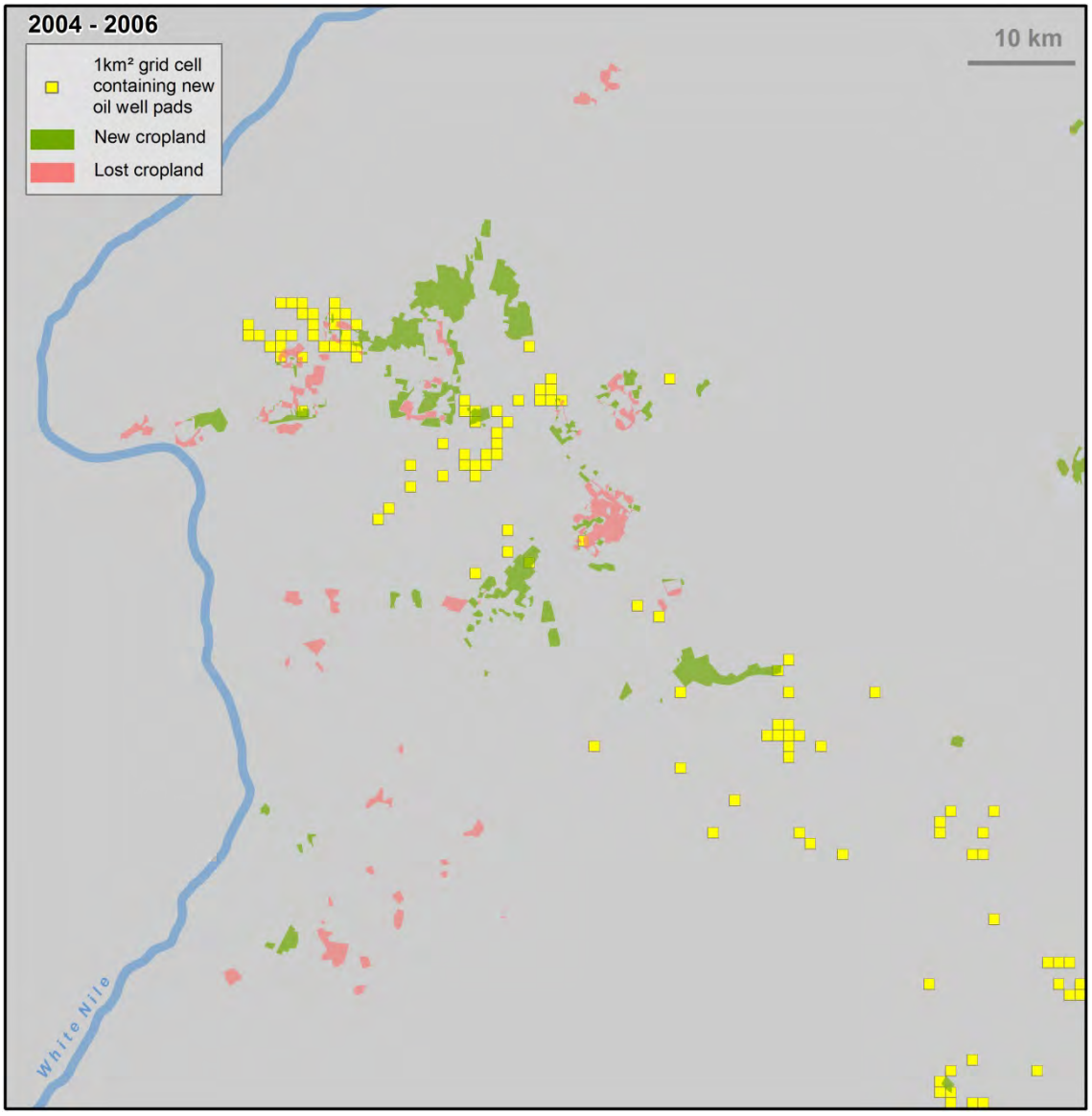

Figure 39: 2004-2006 – Impacts of oil field expansion

Examples for new and lost cropland on top of grid cells containing new oil well pads were found for the change period 2004-2006. In the north-west of the area of interest, suppression seems to have taken place.

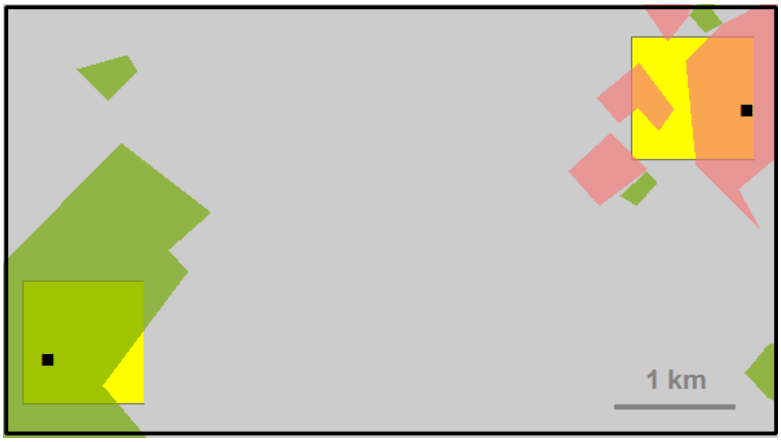

Figure 40: 2004-2006 – Detail view

Figure 41: Cropland close to oil well pad

Figure 41, taken from *Google Earth*, shows farm lands in close proximity to an oil well pad.

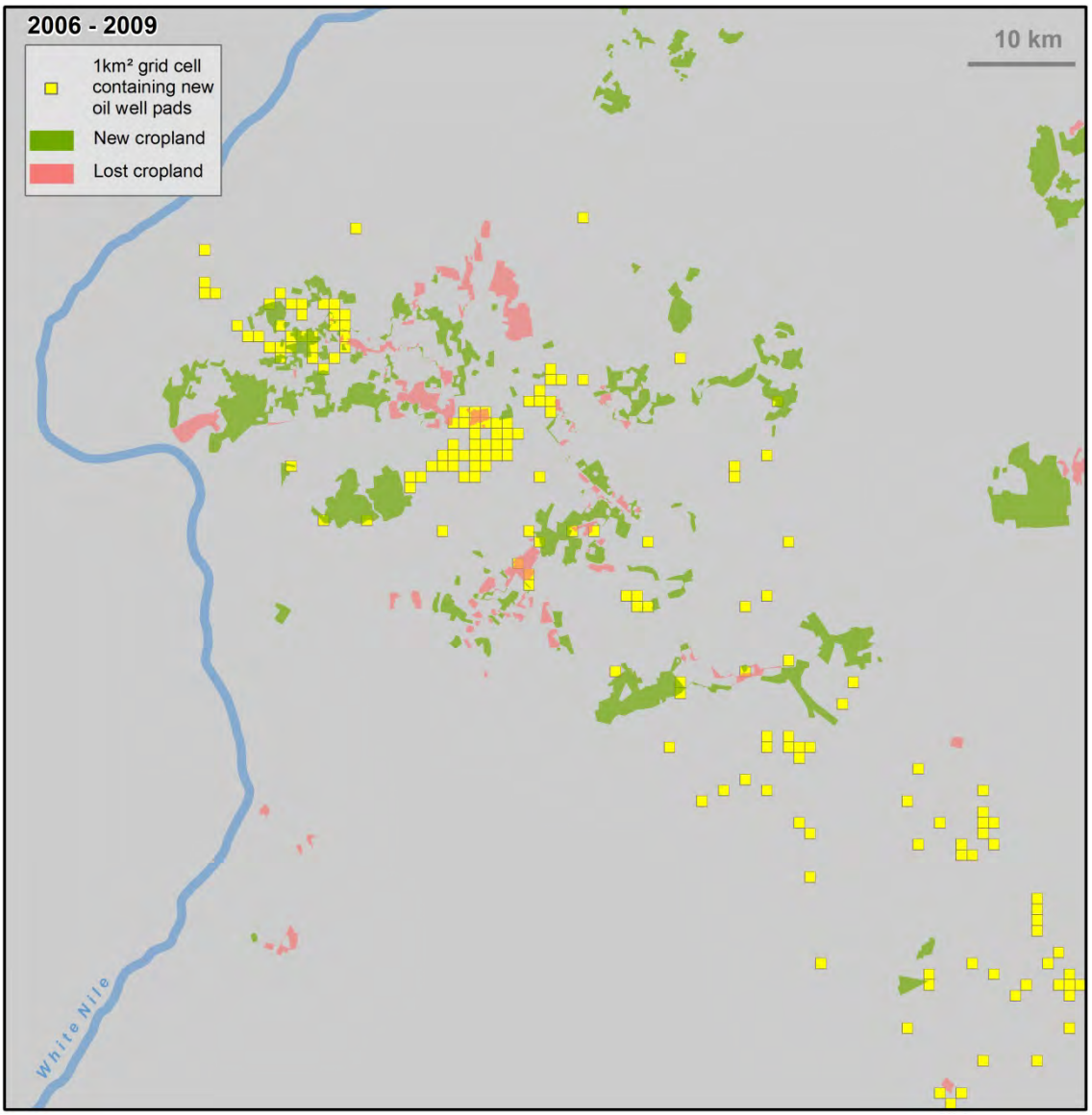

Figure 42: 2006-2009 – Impacts of oil field expansion

Figure 42 and Figure 44 provide more examples for losses and gains of cropland areas that seem to be connected to oil field expansion. Two examples from the period of 2006-2009 are shown below in detail.

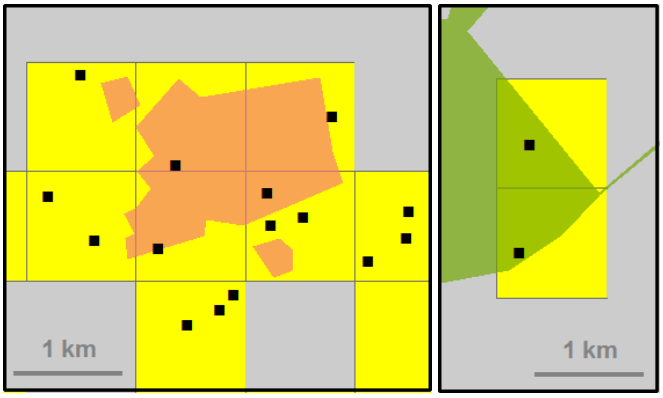

Figure 43: 2006-2009 – Detail view

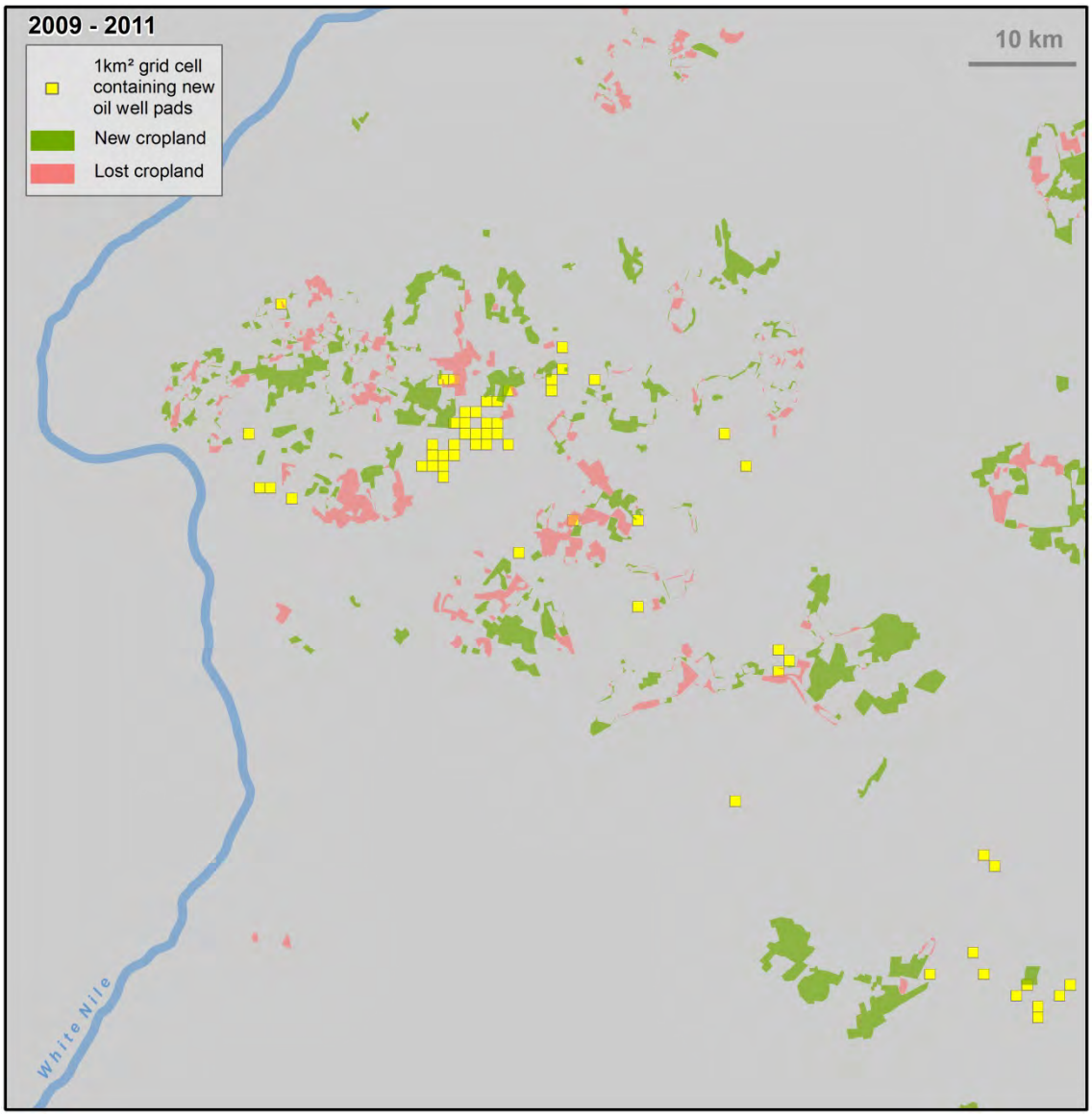

Figure 44: 2009-2011 – Impacts of oil field expansion

The main conclusion from all those examples is the fact that oil field expansion simultaneously accounts for the replacement of existing cropland and the creation of new farm lands. By erecting oil well pads on former agricultural lands, cropland is being lost while at the same time the possibility exists that the expansion of oil well pads and especially the associated infrastructure like roads and tracks opens up new lands for cultivation. To verify this assumption, the development of every single new cropland area and its connection with oil field expansion would have to be examined in detail and on the ground. As has been stated above about the connection between cropland areas and the road network, in this case, remotely-sensed data and its derived products can only provide an “as is”-picture instead of delivering unambiguous answers.

Oil field expansion was also the reason for the disappearance of villages. During field trips in 2013, Petry (2013a), together with locals, tried to find the locations of such villages south and

south-east of the field processing facility in the Paloich oil field. In a small area measuring approx. 40 km², as many as eight villages (Mareng, Lugul, Rodong, Katolok, Wunyongdeng, Wengajok, Ageliu, Adhiau) were replaced by oil infrastructure (Petry, 2013d). The data used for this study is of too coarse a resolution to investigate the fate of small villages which sometimes consist only of a couple of huts. Very high resolution data is needed to document incidents like the disappearance of small settlements.

5.6.4 Miscellaneous

With regard to the hypothesis about the Petrodar pipeline affecting cropland areas, a visual investigation came to the conclusion that this cannot be confirmed for the area of interest by image analysis methods and the given data. This does not mean that these effects did not take place. They have been reported by affected people (Wesselink, 2006, p.3). The analysis simply showed that these effects cannot be confirmed with the data used in this study. Very high resolution imagery needs to be applied.

The same statement can be made about drain blocks. Some potential drain blocks were identified on some of the images but evidence for a connection between drain blocks and cropland was not found. Figure 45 shows what appears to be a drain block, caused by a road (Landsat-5, acquisition date: 09.12.2009). The depicted Tasseled Cap Band 3 image represents levels of wetness. The brighter one pixel appears, the wetter its corresponding piece of land on the ground. Based on this, Figure 45 shows that the area on the right hand side of the road is much dryer than the one on the left.

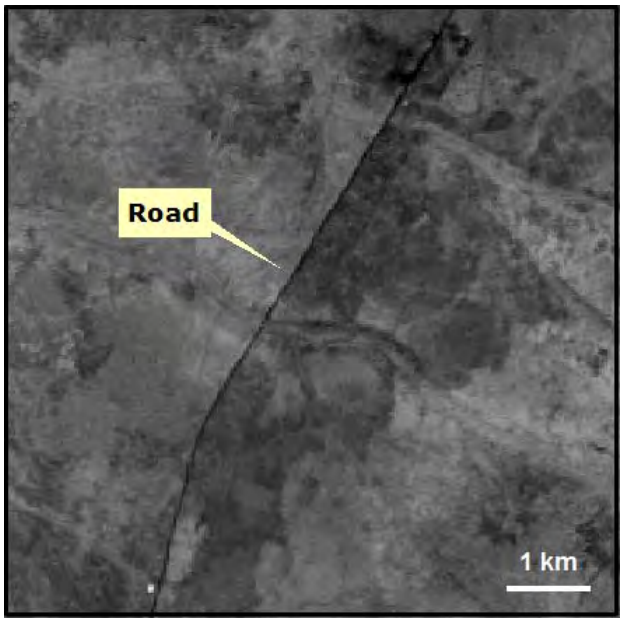

Figure 45: Potential drain block

Analysis of LandScan population data for Melut County led to the results shown in Table 20 together with the corresponding cropland area sizes for Melut County.

Population and cropland areas in Melut County				
Year	**Population**	**Increase in population**	**Cropland area**	**Increase in cropland areas**
2002	28700		35.95 km²	
2004	36435	26.95 %	112.05 km²	211.68 %
2009	40554	11.31 %	364.50 km²	225.30 %
2010	63991	57.79 %	463.67km²	27.21 %

Table 20: Population and cropland areas in Melut County

(Please note that Table 20 deals with the population and cropland areas of Melut County only which is slightly smaller than the entire AOI. The reason is that census population data is based on counties of South Sudan.)

LandScan data for the area of interest seems to be of poor quality. The 2008 census identified 49,242 people living in Melut County. The number seems to underestimate the actual size of the population (BICC, 2013, p.30). LandScan registers only 39,715 inhabitants. A second, more impressive example is the fact that according to BICC (2013, p.31) the town of Paloich was home to 16,215 people in 2008. That year's LandScan data set specifies a number of 319 people for Paloich and its close surroundings. Based on these findings, no further LandScan data analysis was undertaken.

Very high resolution data as described in chapter 3.5.1 was used to investigate population growth in the town of Paloich. This was done by digitizing single buildings (Figure 64). The findings are in line with reports about massive population growth in Paloich. While 1161 buildings were captured on the 2004 image, the number more than doubled for 2012 with 2829 extracted buildings. The digitized features consist of a variety of buildings for residential, commercial and agricultural use, such as houses, huts or sheds.

6 Summary and Conclusion

At the beginning of this study, three questions were asked: What changes can be observed? What spatial connections exist between those observed changes? Can they be explained with existing knowledge concerning events in relation to oil production?

In order to answer those questions, the study was split into two parts: (1) Presentation and discussion of the overall picture of developments in the AOI which was introduced in the first chapter as the aim of the study and (2) final map products based on earth observation data and GIS analysis. The first question can be answered straightforward. For the three features under examination, the following observations were made: A significant decrease in cropland areas occurred as observed on images dating from 1999 and 2002. More than 160 km² of former farm lands were not used as such anymore. From this base, the size of cropland areas rose steadily throughout the years. The level of 1999 was surpassed as identified on the 2006 image. After that, the sum of areas used for agricultural purposes more than trebled to reach 593 km² in 2011, of which 464 km² are located in Melut County. A lot of new cropland areas developed along the road from Adar to Paloich, in the eastern parts of the AOI and in the central part between the towns of Melut and Paloich, where the majority of people live. The changes observed for roads and oil well pads are similar in such a way as a steady increase in both features was assessed. The four oil fields in the AOI grew massively in size to feature 555 oil well pads on the 2011 imagery, compared with a single one in 1999. Since most of the captured roads connect oil infrastructure, it is obvious that enlargement of the road network on a large scale was documented.

To answer the third question before the second one: Yes, the observed changes are in line with what is known to have happened in the area. As stated above, the period between 1999 and 2002 saw vicious fighting with displacement and flight of thousands of people. A sharp drop in agricultural activities reflects these circumstances. As it was the reason for all the bloodshed, the oil field development took huge steps forward during the same period. From the year 2004 on, thousands of refugees returned. These people must have been fed which in turn led to new cropland areas being cultivated all over Melut County. Apart from all the negative effects on people and the environment, the development of the oil fields brought benefits to the area like improved transport possibilities. Former small towns such as Paloich began to exhibit signs of socio-economic change with emerging market integration. The oil industry also attracted people in the hope of jobs. A complex interplay between all those factors exists which leads to the second question.

What spatial connections exist between those observed changes? This question demands a more complex answer compared with the previous ones. While social and political scientists will find it easy to give socio-economic reasons for the mutual reinforcement of oil field development, population growth and increases in farming, it is challenging to find connections purely on spatial grounds. The analyses as documented in chapter 5.6 show only very weak evidence of causal spatial relationships between the development of roads and oil well pads on the one and cropland on the other side. Examples were presented that support the assumption that new roads led to losses in cropland while at the same time as many examples exist that support the opposite assumption. It is beyond dispute that the erection of oil well pads led to the disappearance of croplands and even whole villages. On the other hand, new cropland areas sprung up in very close proximity to new well pads. The distance analysis concerning proximity of new roads to new cropland areas showed that for some years it was likely that new roads enabled new croplands to emerge. As a summary of this discussion, ground-truth data and insight into the local processes that lead to cultivation of one field while other fields are given up on would be very helpful and could possibly provide answers. As an outcome of this study, spatial connections between the observed features were very difficult to establish. Explicit conclusions about the interplay between certain developments could not be made.

The satellite data used for this study was found useful for some purposes while limitations of it were clearly visible. To start with the process of digitization, oil well pads were easy to identify, even on 30 m TM data. The resolution did not allow for a distinction between types of well pads but that was not of importance. Unfortunately, no accuracy assessment could be made with regard to captured croplands. As explained above, the possibility of too much non-cropland being captured exists and must be taken into account when looking at the results of this study. The need for ground-truth data or other reference data was obvious. Features that were reportedly present, such as the exploration patterns in the north-western part of Melut County or the pipeline running from Adar to Paloich, were not visible on Landsat-5 scenes.

One of the most important outcomes was the fact that the object-based land cover classification led to better results compared with the pixel-based one. Even though OBIA was designed with very high resolution data in mind, application for less accurate data is possible and can yield good results. The problems arising from the attempt to distinguish between sub-types of savanna could have been avoided by simply using one class only, which would have boosted accuracy. Since no ground-truth data or very high resolution imagery was available, this would have been justified.

Object-based classification of cropland and oil well pads was partly successful with Landsat-5 data but with small subsets only. In general, in many areas the imagery exhibited too little distinction between pixels in terms of spectral characteristics and between objects in terms of spatial characteristics. While OBIA seems to be applicable to 30 m data for the extraction of rather coarse features such as land cover classes, it is less suitable when more subtle features need to be classified.

The study showed that GI-Science offers valuable tools to document changes and to support the work of conflict research institutions. While it does not provide definite answers, it surely helps redefining important questions. Due to its unique point of view from space, remote sensing puts apparently isolated incidents into a larger context, which in turn can change perspectives on the ground.

7 References

Action Against Hunger Southern Sudan, 2008. *Nutritional anthropometric survey children under five years of age*. [pdf]Available at http://www.actionagainsthunger.org/sites/default/files/publications/ACF-NUT-South-Sudan-Upper-Nile-State-Melut-2008-11-EN.pdf [Accessed 21 July 2013].

Aksyonov, D.E., 2006. *Cumulative Environmental Impact Assessment of Oil Production Using Space Imagery Products*. [pdf] Available at http://www.scanex.ru/en/publications/pdf/publication15.pdf [Accessed 14 July 2013].

Albertz, J., 2007. *Einführung in die Fernerkundung*. 3rd ed. Darmstadt: Wissenschaftliche Buchgesellschaft.

Azizi, Z., A. Najafi and H. Sohrabi, 2008. Forest canopy density estimating, using satellite images. *The International Archives of the Photogrammetry, Remote Sensing and Spatial Information Sciences*, Vol. XXXVII, Part B8, pp.1127-1130.

Baatz, M. and A. Schäpe, 2000. Multiresolution Segmentation: an optimization approach for high quality multi-scale image segmentation. In: Strobl, J., T. Blaschke, G. Griesebner (Hrsg.): *Angewandte Geographische Informationsverarbeitung* XII. Heidelberg: Wichmann, pp.12-23.

Baret, F. and G. Guyot, 1991. Potentials and Limits of Vegetation Indices for LAI and APAR Assessment. *Remote Sensing of Environment*, Vol. 35, pp.161-173.

Blaschke, T., 2010. Object based image analysis for remote sensing. *ISPRS Journal of Photogrammetry and Remote Sensing*, Vol. 65, pp.2-16.

Blaschke, T. and J. Strobl, 2001. What's wrong with pixels? Some recent developments interfacing remote sensing and GIS. *GIS Zeitschrift für Geoinformationssystems*, Vol. 6, pp.12-17.

Bloomberg, 2013. *Sudan Threatens to Shut South Sudan Oil Over Rebel Support*. [online] Available at http://www.bloomberg.com/news/2013-06-09/sudan-threatens-to-shut-down-south-sudan-oil-over-rebel-support.html [Accessed 02 August 2013].

Bonn International Center for Conversion (BICC), 2013. Oil Investment and Conflict in Upper Nile State, South Sudan. *BICC Brief 48*. Bonn.

Centre for Environment and Development (CDE), 2008. *Southern Sudan Topographic Base Map Series*. University of Bern [online] Available at http://www.cde.unibe.ch/MapShop/ [Accessed 22 July 2013].

Chicago Tribune, 2013. *South Sudan resumes oil exports through Sudan*. [online] Available at http://articles.chicagotribune.com/2013-05-07/news/sns-rt-us-sudan-oilbre9460oh-20130507_1_south-sudan-cross-border-oil-flows-oil-shutdown [Accessed 02 August 2013].

Chuvieco, E., M.P. Martin and A. Palacios, 2002. Assessment of different spectral indices in the red-near-infrared spectral domain for burned land discrimination. *International Journal of Remote Sensing*, Vol. 23, No. 23, pp.5103-5110.

Congalton, R.G., 1991. A review of assessing the accuracy of classifications of remotely sensed data. *Remote Sensing of the Environment*, Vol. 37(1), pp.35-46.

Crist, E.P. and R.J. Kauth, 1986. The Tasselled Cap De-Mystified. *Photogrammetric Engineering and Remote Sensing*, Vol. 52, No. 1, pp.81-86.

Definiens, 2009. *eCognition Developer 8*. Reference Book. München.

DigitalGlobe, 2013. *Datasheet on QuickBird-2 satellite*. [pdf] Available at http://www.digitalglobe.com/downloads/QuickBird-DS-QB-Web.pdf [Accessed 19 July 2013].

Dorren, L.K.A., B. Maier and A.C. Seijmonsbergen, 2003. Improved Landsat-based forest mapping in steep mountainous terrain using object-based classification. *Forest Ecology and Management* Vol. 183, pp.31-46.

Economist, 2013. A new country rises from the ruins. *The Economist*, Vol. 407, Number 8834, pp.33-34.

ERDAS, 2010. *ERDAS Field Guide*. ERDAS, Inc. Norcross, USA.

Environmental Systems Research Institute (ESRI), 2013. *ArcGIS Help 10.1.* [online]Available at http://resources.arcgis.com/en/help/main/10.1/index.html [Accessed 22 July 2013].

European Coalition on Oil in Sudan (ECOS), 2006. *Oil development in Northern Upper Nile, Sudan*. [pdf] Available at http://www.ecosonline.org/reports/2006/melut.pdf [Accessed 01 August 2013].

European Coalition on Oil in Sudan (ECOS), 2007. *ECOS Oil Map*. [pdf] Available at http://www.ecosonline.org/oilmap/resources/Soedan%20A5%20kleur.pdf [Accessed 01 August 2013].

European Coalition on Oil in Sudan (ECOS), 2009. *Sudan, Whose oil? Facts and Analysis.* [pdf] Available at http://www.ecosonline.org/reports/2008/dossier%20final%20groot%20web.pdf [Accessed 01 August 2013].

European Coalition on Oil in Sudan (ECOS), 2011. *Sudan's Oil Industry after the Referendum*. Conference Report. [pdf] Available at http://www.ecosonline.org/reports/2011/Oil_conference_report_Dec2010.pdf [Accessed 01 August 2013].

European Space Agency (ESA), 2008. *Land cover of Sudan*. [online]Available at http://www.fao.org/geonetwork/srv/en/main.home?uuid=fbd183b4-88dd-4b26-bb7d-5624c97e16e9 [Accessed 22 July 2013].

European Space Agency (ESA), 2013. *GMES Space Component Data Access Portfolio: Data Warehouse 2011-2014*. [pdf] Available at http://gmesdata.esa.int/web/gsc/dap_document [Accessed 02 August 2013].

Food and Agricultural Organisation (FAO), 2002. *World Land Use – Land Cover*. [online] Available at http://www.fao.org/geonetwork/srv/en/metadata.show?id=12749&currTab=simple [Accessed 22 July 2013].

Food and Agricultural Organisation (FAO), 2003. *Multipurpose Landcover Database for Sudan – AFRICOVER*. [online]Available at http://www.fao.org/geonetwork/srv/en/metadata.show?id=38102&currTab=simple [Accessed 22 July 2013].

Frohn, R.C., B.C. Autrey, C.R.Lane and M.Reif, 2009. Segmentation and object-oriented classification of wetlands in a karst Florida landscape using multi-season Landsat-7 ETM+ imagery. *International Journal of Remote Sensing*, Vol. 32, No. 5, pp.1471-1489.

GeoNames, 2013. *Dataset for South Sudan*. [online] Available at http://www.geonames.org/search.html?q=&country=SS [Accessed 22 July 2013].

Global Precipitation Climatology Project (GPCP), 2013. *Rainfall data.* [online] Available at http://gdata1.sci.gsfc.nasa.gov/daac-bin/G3/gui.cgi?instance_id=GPCP_Monthly [Accessed 21 July 2013].

Graewert, E., 2012. *Information on burned areas*. [e-mail] (Personal communication, 23 October 2012).

Harrison M. N. and J. K. Jackson, 1958. *Ecological classification of the vegetation of the Sudan*. Khartoum: Agriculture publications committee.

Hese, S. and C. Schmullius, 2009. High spatial resolution image object classification for terrestrial oil spill contamination mapping in West Siberia. *International Journal of Applied Earth Observation and Geoinformation*, 11, pp.130-141.

Joint Research Center (JRC), 2004. *Global Land Cover 2000*. [online] Available at http://bioval.jrc.ec.europa.eu/products/glc2000/products.php [Accessed 22 July 2013].

Kauth, R.J. and G.S. Thomas, 1976. The Tasseled Cap – A Graphic Description of the Spectral-Temporal Development of Agricultural Crops as Seen by LANDSAT. *Proceedings of the Symposium on Machine Processing of Remotely Sensed Data*, Purdue University of West Lafayette, Indiana, pp. 4B-41 - 4B-51.

Lillesand, T. M., R. W. Kiefer and J. W. Chipman, 2008. *Remote sensing and image interpretation*. 6th ed, Chichester: John Wiley & Sons Ltd.

de Magalhaes, T.L., M.B. Schimalski, A. Mantovani and R.L.C. Bortoluzzi (2012): Image classification using Landsat TM images to mapping wetlands vegetation (banhados) of the Catarinense plateau, Southern Brazil. *Proceedings of the 4th GEOBIA*, 2012, Rio de Janeiro, Brazil, pp.292-297.

Nile Research Initiative, 2013. *Research on oil business in Melut County in Upper Nile State*. Study report, Catholic Diocese of Malakal, Justice and Peace Department.

Petry, M., 2013a. *Information on disappeared villages*. [phone call] (Personal communication, 11 July 2013).

Petry, M., 2013b. *Information on seismic lines*. [e-mail] (Personal communication, 16 July 2013).

Petry, M., 2013c. *Information on Payams*. [e-mail] (Personal communication, 19 July 2013).

Petry, M., 2013d. *Oil production in Fadiet.* Unpublished map. CORDAID. Axel Müller.

Petry, M., 2013e. *Oil production in Melut County*. Unpublished map. CORDAID. Axel Müller.

Prins, E., 2010. *Satellite Mapping of Land Cover and Use in relation to Oil Exploitation in Concession Block 5A in Southern Sudan 1987 – 2006*. [pdf] Available at http://www.ecosonline.org/reports/2010/Satellite_mapping_Block5a_small.pdf [Accessed 01 August 2013].

Qi, J., A. Chehbouni, A.R. Huete, Y.H. Kerr and S. Sorooshian, 1994. A Modified Soil Adjusted Vegetation Index. *Remote Sensing of Environment*, Vol. 48, pp.119-126.

Richards, J.A. and X. Jia, 1999. *Remote Sensing Digital Image Analysis*. 3rd ed, Berlin; Heidelberg; New York: Springer.

Rouse Jr., J.W., R.H. Haas, J.A. Schell and D.W. Deering, 1974. Monitoring vegetation systems in the Great Plains with ERTS. *Goddard Space Flight Center 3d ERTS-1 Symp*, Vol. 1, Sect. A, p. 309-317.

Satellite Imaging Corporation, 2013. *WorldView-2*. [online] Available at http://www.satimagingcorp.com/satellite-sensors/worldview-2.html [Accessed 19 July 2013].

Selg, F., 2013. *Monitoring spatial impacts of oil exploitation through object-based image analysis of VHR satellite imagery – Great Palogue Field, South Sudan*. Diploma thesis. University of Cologne.

Sergey, M. and T. Oganes, 2009. Landscape Impact Assessment of the Oil and Gas Industry in the Russia using space images interpretation*. Anais XIV Simpósio Brasileiro de Sensoriamento Remoto*, Natal, Brasil, 25-30 April 2009, INPE, pp.6711-6717.

Shankleman, J., 2011. Oil and State Building in South Sudan. *Special Report* 282, United States Institute of Peace, Washington DC.

Singh, A., 1989. Digital change detection techniques using remotely-sensed data. *International Journal of Remote Sensing*, Vol. 10, pp.989-1003.

Song, C., C.E. Woodcock, K.C. Seto, M.P. Lenney and S.A. Macomber, 2001. Classification and change detection using Landsat TM data: When and How to Correct Atmospheric Effects? *Remote Sensing of Environment*, Vol. 75, pp.230-244.

South Sudan National Bureau for Statistics (SSNBS), 2010. *Statistical Yearbook for Southern Sudan 2010*. [pdf] Available at http://ssnbs.org/storage/stats-year-books/Statistical%20Year%20Book%20For%20Southern%20Sudan%202010%20Final.pdf [Accessed 21 July 2013].

Spröhnle, K., 2010. *Earth observation for Environmental Impact Assessment in the Surroundings of Refugee Camps in Darfur*. Magister thesis. University of Bamberg.

Tiede, D. and S. Lang, 2010. Analytical 3D views and virtual globes – scientific results in a familiar spatial context. *ISPRS Journal of Photogrammetry and Remote Sensing*, Vol. 65, pp.300-307.

Tobler, W., 1970. A computer movie simulating urban growth in the Detroit region. *Economic Geography*, 46(2), pp.234-240.

United Nations Environment Programme (UNEP), 2007. *Sudan Post-Conflict Environmental Assessment*. [pdf] Available at http://postconflict.unep.ch/publications/UNEP_Sudan.pdf [Accessed 01 August 2013].

United Nations Information Management Working Group (UNIMWG), 2011. *Geospatial Data for Sudan*. [online] Available at http://www.unitar.org/unosat/sudan [Accessed 22 July 2013].

United Nations Logistics Cluster, 2013. *South Sudan Upper Nile State – Detailed Transport Map, January 2013*. [online]Available at http://reliefweb.int/map/south-sudan-republic/south-sudan-upper-nile-state-detailed-transport-map-17-jan-2013 [Accessed 22 July 2013].

United States Geological Survey (USGS), 2003a. *Land Use – Land Cover of Africa*. [online] Available at http://www.fao.org/geonetwork/srv/en/metadata.show?id=12755&currTab=simple [Accessed 22 July 2013].

United States Geological Survey (USGS), 2013b. *Landsat.* [online] Available at http://landsat.usgs.gov/index.php [Accessed 18 July 2013].

United States Geological Survey (USGS), 2013c. *Filling the Gaps to use in Scientific Analysis*. [online] Available at http://landsat.usgs.gov/sci_an.php [Accessed 20 July 2013].

Wesselink, E. and E. Weller, 2006. Oil and Violence in Sudan. Drilling, Poverty and Death in Upper Nile State. *Multinational Monitor*, Vol. 27, No. 3.

World Factbook, 2013. *South Sudan*. Central Intelligence Agency. [online] Available at https://www.cia.gov/library/publications/the-world-factbook/geos/od.html [Accessed 11 July 2013].

8 Annex

8.1 Definiens eCognition rule sets

R1 - Rule set for 2009 land cover classification

Classes:
Burned Area
Savanna_Dense_Veg
Savanna_Sparse_Veg
Water
Wetland

Customized Features:
Burned Area Index: 1/(((0.1-[Mean Red])*(0.1-[Mean Red]))+((0.06-[Mean NIR])*(0.06-[Mean NIR])))
MSAVI: (2*[Mean NIR]+1-(((2*[Mean NIR]+1)^2)-8*([Mean NIR]-[Mean Red]))^0.5)/2
NDVI: ([Mean NIR]-[Mean Red])/([Mean NIR]+[Mean Red])

Process: Main:
Segmentation
multiresolution segmentation: 10 [shape:0.1 compct.:0.5] creating 'Level 1'
Classification
assign class: with Max. diff. >= 1.5 at Level 1: Water
assign class: unclassified with NDVI >= 0.35 at Level 1: Wetland
assign class: unclassified with Mean Green <= 34 and NDVI <= 0.075 at Level 1: Burned Area
New Segmentation
multiresolution segmentation: unclassified at Level 1: 5 [shape:0.1 compct.:0.5] creating 'Level 2'
Classification
assign class: with Existence of super objects Water (1) = 1 at Level 2: Water
assign class: with Existence of super objects Wetland (1) = 1 at Level 2: Wetland
assign class: with Existence of super objects Burned Area (1) = 1 at Level 2: Burned Area
assign class: unclassified with Burned Area Index >= 0.00035 at Level 2: Burned Area
assign class: unclassified with MSAVI >= 0.265 and Brightness < 80 at Level 2: Savanna_Dense_Veg
assign class: unclassified at Level 2: Savanna_Sparse_Veg
[export thematic raster files: Burned Area, Savanna_Dense_Veg, Savanna_Sparse_Veg, Water, Wetland at Level 2: export classification to ExportObjects001]

R2 - Rule set for 2002 (15 m) land cover classification

Classes:
Burned Area
Savanna_Dense_Veg
Savanna_Sparse_Veg
Water
Wetland

Customized Features:
Bare Soil Index: (([Mean NIR]+[Mean Green])-[Mean Red])/(([Mean NIR]+[Mean Green])+[Mean Red])
Burned Area Index: 1/(((0.1-[Mean Red])*(0.1-[Mean Red]))+((0.06-[Mean NIR])*(0.06-[Mean NIR])))
MSAVI: (2*[Mean NIR]+1-(((2*[Mean NIR]+1)^2)-8*([Mean NIR]-[Mean Red]))^0.5)/2
NDVI: ([Mean NIR]-[Mean Red])/([Mean NIR]+[Mean Red])

Process: Main:
Segmentation
multiresolution segmentation: 10 [shape:0.1 compct.:0.5] creating 'Level 1'
Classification
assign class: with Mean SWIR2 <= 28.6 at Level 1: Water
assign class: unclassified with NDVI >= 0 at Level 1: Wetland
assign class: unclassified with Bare Soil Index >= 0.29 at Level 1: Wetland
merge region: Wetland at Level 1: merge region
assign class: Wetland with Border to Water = 0 Pxl at Level 1: unclassified
assign class: Wetland with Number of pixels = 32869 at Level 1: unclassified
assign class: unclassified with Mean Green <= 58 and NDVI <= -0.25 at Level 1: Burned Area
New Segmentation
multiresolution segmentation: unclassified at Level 1: 5 [shape:0.1 compct.:0.5] creating 'Level 2'
Classification
assign class: with Existence of super objects Water (1) = 1 at Level 2: Water
assign class: with Existence of super objects Wetland (1) = 1 at Level 2: Wetland
assign class: with Existence of super objects Burned Area (1) = 1 at Level 2: Burned Area
assign class: unclassified with Burned Area Index >= 0.00019 and NDVI <= -0.215 at Level 2: Burned Area
assign class: unclassified with MSAVI <= -0.835 at Level 2: Burned Area
assign class: unclassified with MSAVI >= -0.43 at Level 2: Savanna_Dense_Veg
assign class: unclassified with NDVI >= -0.16 at Level 2: Savanna_Dense_Veg
assign class: unclassified with Brightness <= 74 and Burned Area Index >= 0.000166 at Level 2: Burned Area
assign class: unclassified with Mean SWIR1 < 90 and Mean SWIR2 >= 70 at Level 2: Burned Area
assign class: unclassified at Level 2: Savanna_Sparse_Veg
export thematic raster files: Burned Area, Savanna_Dense_Veg, Savanna_Sparse_Veg, Water, Wetland at Level 2: export classification to ExportObjects001

R3 – Rule set for cropland classification – Entire scene

Classes:
- Burned Area
- Cropland
- Non-Cropland
- Road
- Water
- Wetland

Customized Features:
- Bare Soil Index: (([Mean NIR]+[Mean Green])-[Mean Red])/(([Mean NIR]+[Mean Green])+[Mean Red])
- Burned Area Index: 1/(((0.1-[Mean Red])*(0.1-[Mean Red]))+((0.06-[Mean NIR])*(0.06-[Mean NIR])))
- NDVI: ([Mean NIR]-[Mean Red])/([Mean NIR]+[Mean Red])

Process: Main:
- Segmentation 1
  - multiresolution segmentation: 10 [shape:0.1 compct.:0.5] creating 'Level 1'
  - Classification
    - assign class: unclassified with OBJECTID: Thematic Layer 1 = 1 at Level 1: Road
    - assign class: unclassified with Max. diff. >= 1.5 at Level 1: Water
    - assign class: unclassified with NDVI >= 0.35 at Level 1: Wetland
    - assign class: unclassified with Mean Green <= 34 and NDVI <= 0.075 at Level 1: Burned Area
- Segmentation 2
  - multiresolution segmentation: unclassified at Level 1: 5 [shape:0.1 compct.:0.5] creating 'Level 2'
  - Classification
    - assign class: with Existence of super objects Water (1) = 1 at Level 2: Water
    - assign class: with Existence of super objects Wetland (1) = 1 at Level 2: Wetland
    - assign class: with Existence of super objects Burned Area (1) = 1 at Level 2: Burned Area
    - assign class: with Existence of super objects Road (1) = 1 at Level 2: Road
    - assign class: unclassified with Burned Area Index >= 0.00035 at Level 2: Burned Area
- Segmentation 3
  - multiresolution segmentation: unclassified at Level 2: 25 [shape:0.6 compct.:0.2] creating 'Level 3'
  - Classification
    - assign class: with Existence of super objects Water (1) = 1 at Level 3: Water
    - assign class: with Existence of super objects Wetland (1) = 1 at Level 3: Wetland
    - assign class: with Existence of super objects Burned Area (1) = 1 at Level 3: Burned Area
    - assign class: with Existence of super objects Road (1) = 1 at Level 3: Road
    - assign class: unclassified with Bare Soil Index < 0.31 at Level 3: Non-Cropland
    - assign class: unclassified with Brightness > 68 at Level 3: Non-Cropland
    - assign class: unclassified with Mean diff. to Red, unclassified <= 0 at Level 3: Cropland
    - assign class: Cropland with Shape index > 2.1 at Level 3: Non-Cropland
    - assign class: Cropland with Bare Soil Index < 0.35 at Level 3: Non-Cropland
    - assign class: Cropland with Distance to Road > 250 Pxl at Level 3: Non-Cropland
    - export thematic raster files: Cropland at Level 3: export classification to ExportObjects001

R4 – Rule set for cropland classification – Subset A

Classes:
  Cropland
  Non-Cropland

Customized Features:
  Burned Area Index: 1/(((0.1-[Mean Red])*(0.1-[Mean Red]))+((0.06-[Mean NIR])*(0.06-[Mean NIR])))
  MSAVI: (2*[Mean NIR]+1-(((2*[Mean NIR]+1)^2)-8*([Mean NIR]-[Mean Red]))^0.5)/2
  NDVI: ([Mean NIR]-[Mean Red])/([Mean NIR]+[Mean Red])

Process: Main:
  Segmentation 1
    multiresolution segmentation: 10 [shape:0.1 compct.:0.5] creating 'Level 1'
    Classification
      assign class: unclassified with Mean Green <= 34 and NDVI <= 0.075 at Level 1: Non-Cropland
      assign class: unclassified with Brightness >= 71 at Level 1: Non-Cropland
      assign class: unclassified with NDVI < 0.06 at Level 1: Non-Cropland
  Segmentation 2
    multiresolution segmentation: unclassified at Level 1: 5 [shape:0.1 compct.:0.5] creating 'Level 2'
    Classification
      assign class: with Existence of super objects Non-Cropland (1) = 1 at Level 2: Non-Cropland
      assign class: unclassified with Brightness >= 65 at Level 2: Non-Cropland
      assign class: unclassified with Burned Area Index >= 0.0002565 and NDVI < 0.15 at Level 2: Non-Cropland
      assign class: unclassified with MSAVI > 0.3395 and Roundness < 0.0847 at Level 2: Non-Cropland
      assign class: unclassified with MSAVI > 0.3 and Shape index > 2 at Level 2: Non-Cropland
      merge region: unclassified at Level 2: merge region
      assign class: unclassified with Area <= 290 Pxl at Level 2: Non-Cropland
      assign class: unclassified at Level 2: Cropland
      assign class: Cropland with Asymmetry > 0.75 and Shape index > 5 at Level 2: Non-Cropland
      assign class: Cropland with Roundness > 2.088 at Level 2: Non-Cropland
      assign class: Cropland with Roundness > 1.8 and MSAVI > 0.3 at Level 2: Non-Cropland
      assign class: Cropland with Length\Width > 2.53 at Level 2: Non-Cropland
      assign class: Cropland with Length\Width < 1.1 and MSAVI > 0.25 at Level 2: Non-Cropland
      assign class: Cropland with Mean SWIR1 < 89 at Level 2: Non-Cropland
      export thematic raster files: Cropland at Level 2: export classification to ExportObjects001

R5 – Rule set for cropland classification – Subset B

Classes:
- Cropland
- Non-Cropland

Customized Features:
- Bare Soil Index: (([Mean NIR]+[Mean Green])-[Mean Red])/(([Mean NIR]+[Mean Green])+[Mean Red])
- NDVI: ([Mean NIR]-[Mean Red])/([Mean NIR]+[Mean Red])

Process: Main:
- Segmentation 1
  - multiresolution segmentation: 10 [shape:0.1 compct.:0.5] creating 'Level 1'
  - Classification
    - assign class: unclassified with Mean Green <= 29.55 and NDVI <= 0.075 at Level 1: Non-Cropland
    - assign class: unclassified with Brightness > 65 at Level 1: Non-Cropland
- Segmentation 2
  - multiresolution segmentation: unclassified at Level 1: 5 [shape:0.1 compct.:0.5] creating 'Level 2'
  - Classification
    - assign class: with Existence of super objects Non-Cropland (1) = 1 at Level 2: Non-Cropland
    - assign class: unclassified with Max. diff. >= 1.077 at Level 2: Non-Cropland
    - assign class: unclassified with Bare Soil Index < 0.306 at Level 2: Non-Cropland
    - assign class: unclassified with Mean Blue < 66 at Level 2: Non-Cropland
    - merge region: unclassified at Level 2: merge region
- Segmentation 3
  - multiresolution segmentation: unclassified at Level 2: 25 [shape:0.6 compct.:0.2] creating 'Level 3'
  - Classification
    - assign class: with Existence of super objects Non-Cropland (1) = 1 at Level 3: Non-Cropland
    - assign class: unclassified with Compactness > 3 at Level 3: Non-Cropland
    - assign class: unclassified with Length\Width > 3.5 at Level 3: Non-Cropland
    - assign class: unclassified at Level 3: Cropland
    - merge region: Cropland at Level 3: merge region
    - assign class: Cropland with Area < 342 Pxl at Level 3: Non-Cropland
    - assign class: Cropland with Compactness > 3.3 at Level 3: Non-Cropland
    - assign class: Cropland with Rectangular Fit < 0.55 and Compactness < 3 at Level 3: Non-Cropland
    - export thematic raster files: Cropland at Level 3: export classification to ExportObjects001

R6 – Rule set for oil well pad classification

Classes:
  Oil Well
  Road

Customized Features:
  Bare Soil Index: (([Mean NIR]+[Mean Green])-[Mean Red])/(([Mean NIR]+[Mean Green])+[Mean Red])
  NDVI: ([Mean NIR]-[Mean Red])/([Mean NIR]+[Mean Red])

Process: Main:
  Segmentation
    multiresolution segmentation: 5 [shape:0.4 compct.:0.6] creating 'Level 1'
    Classification
      assign class: unclassified with OBJECTID: Thematic Layer 1 = 1 at Level 1: Road
      assign class: unclassified with Brightness >= 68 and Area <= 40 Pxl at Level 1: Oil Well
      assign class: unclassified with Bare Soil Index >= 0.3 at Level 1: unclassified
      assign class: Oil Well with Length\Width > 2 at Level 1: unclassified
      assign class: Oil Well with Rectangular Fit < 0.75 at Level 1: unclassified
      assign class: Oil Well with NDVI >= 0.07 at Level 1: unclassified
      merge region: Oil Well at Level 1: merge region
      assign class: Oil Well with Area >= 45 Pxl at Level 1: unclassified
      assign class: Oil Well with Distance to Road > 25 Pxl at Level 1: unclassified
      export thematic raster files: Oil Well at Level 1: export classification to ExportObjects

8.2 Maps

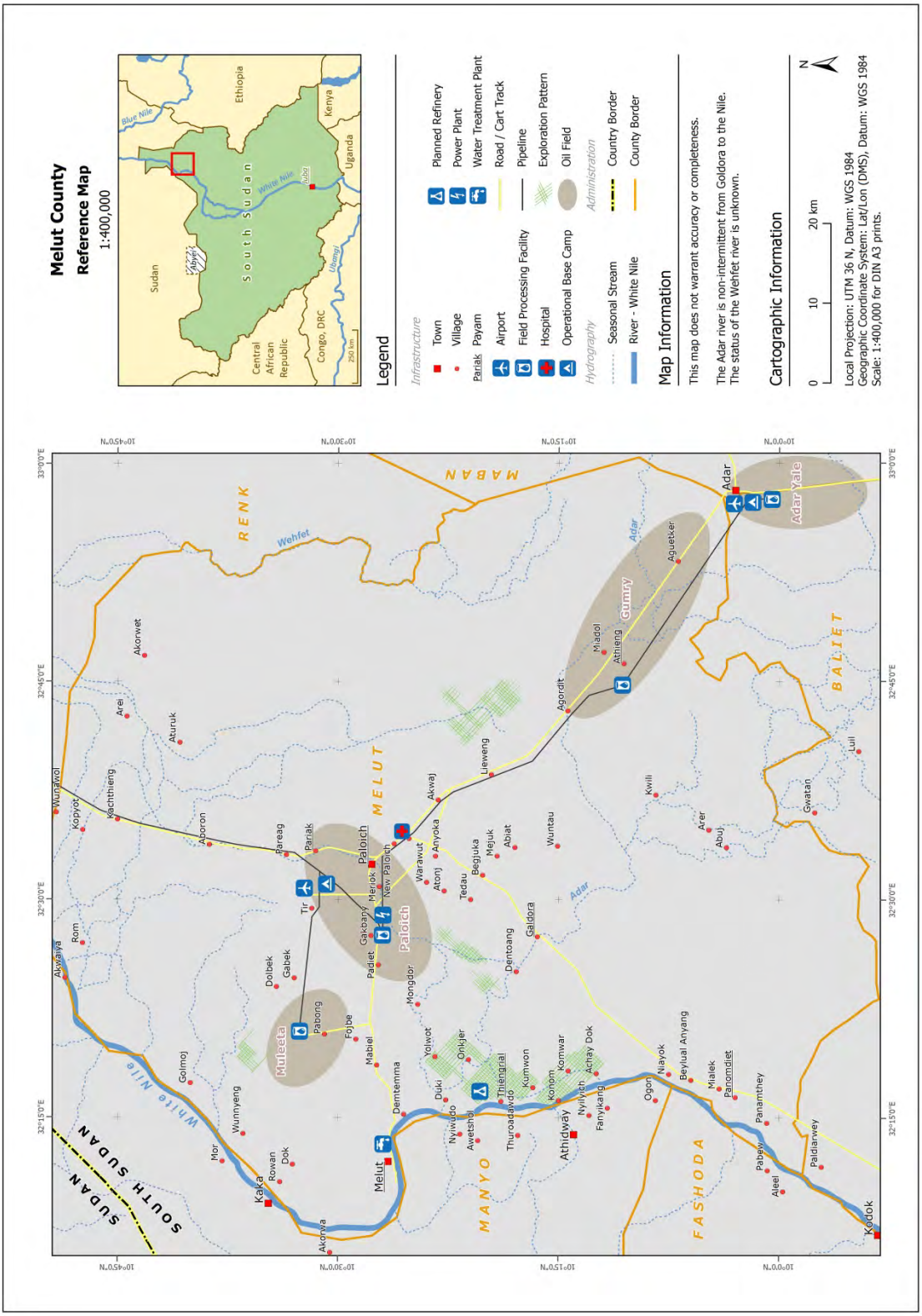

Figure 46: Reference Map

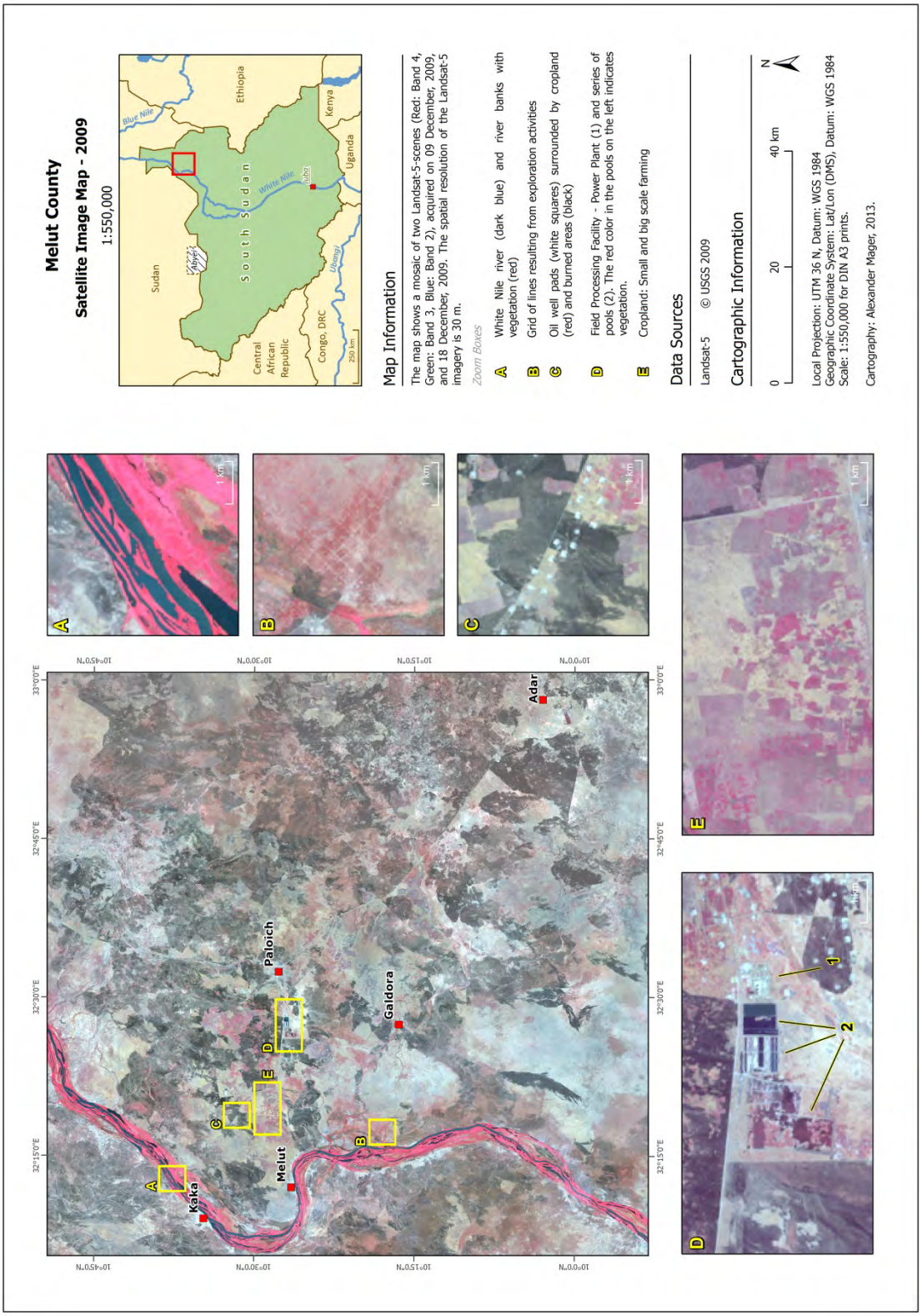

Figure 47: Satellite Image Map - 2009

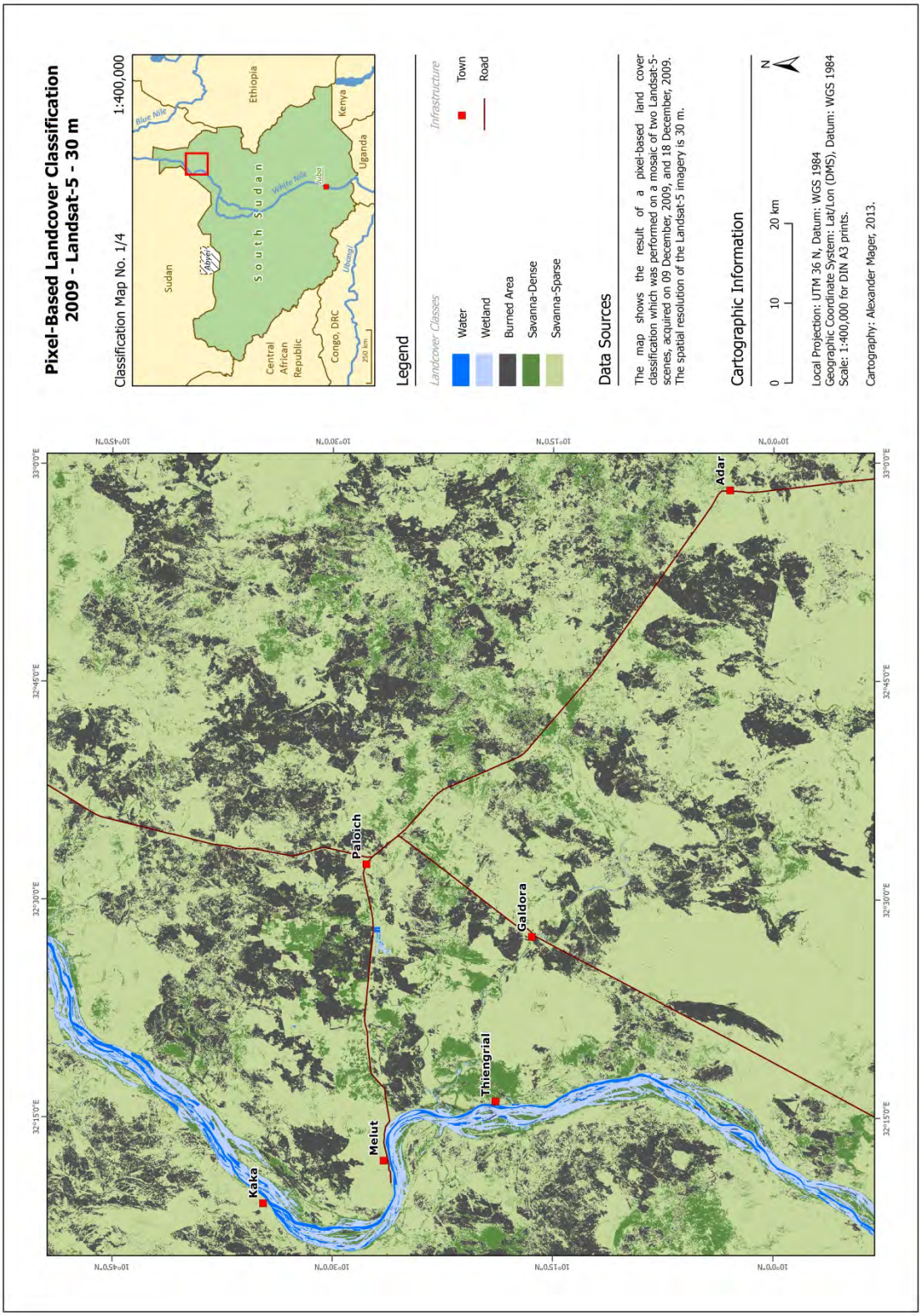

Figure 48: Classification Map No. 1/4 (Pixel 2009)

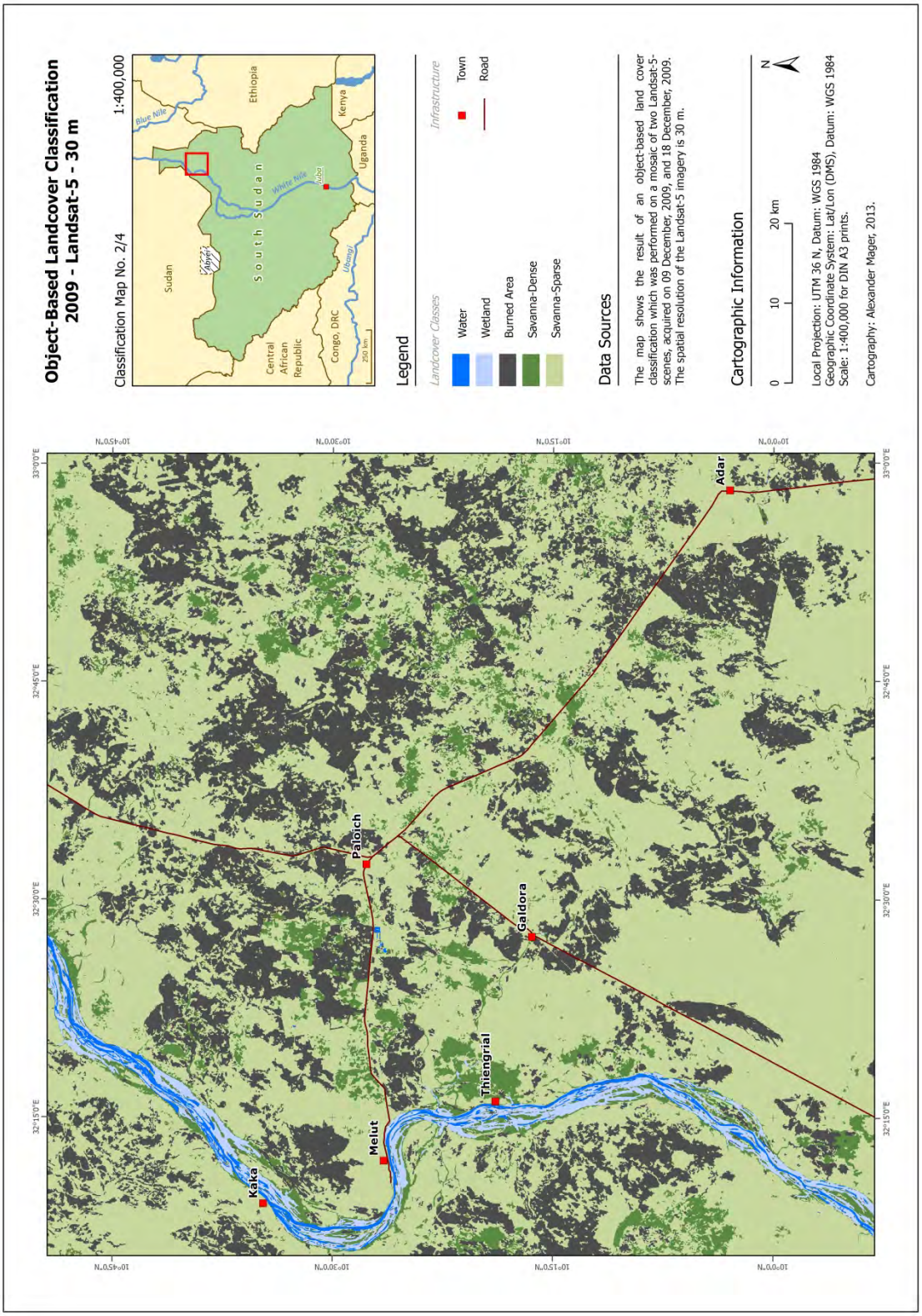

Figure 49: Classification Map No. 2/4 (Object – 2009)

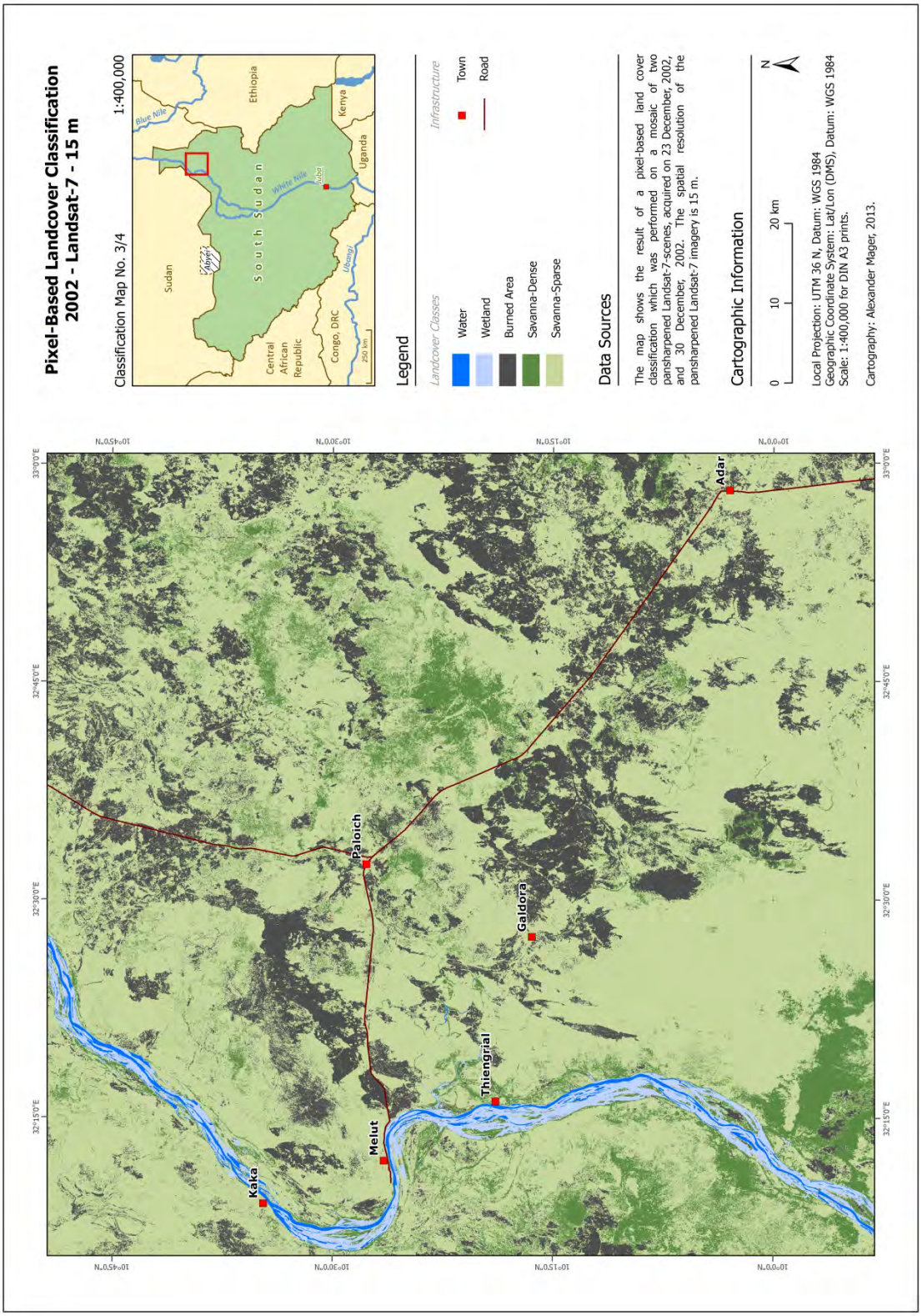

Figure 50: Classification Map No. 3/4 (Pixel – 2002)

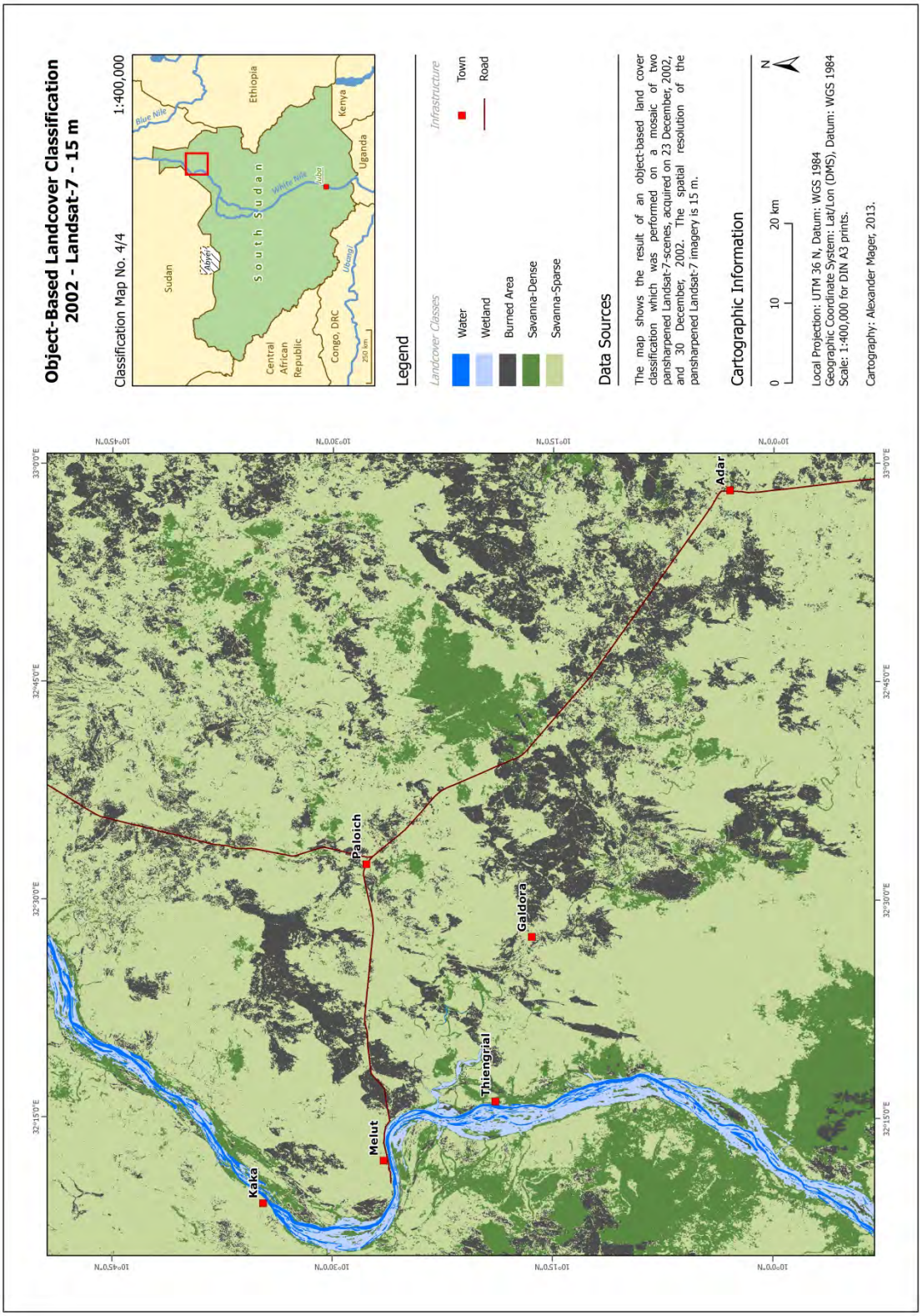

Figure 51: Classification Map No. 4/4 (Object – 2002)

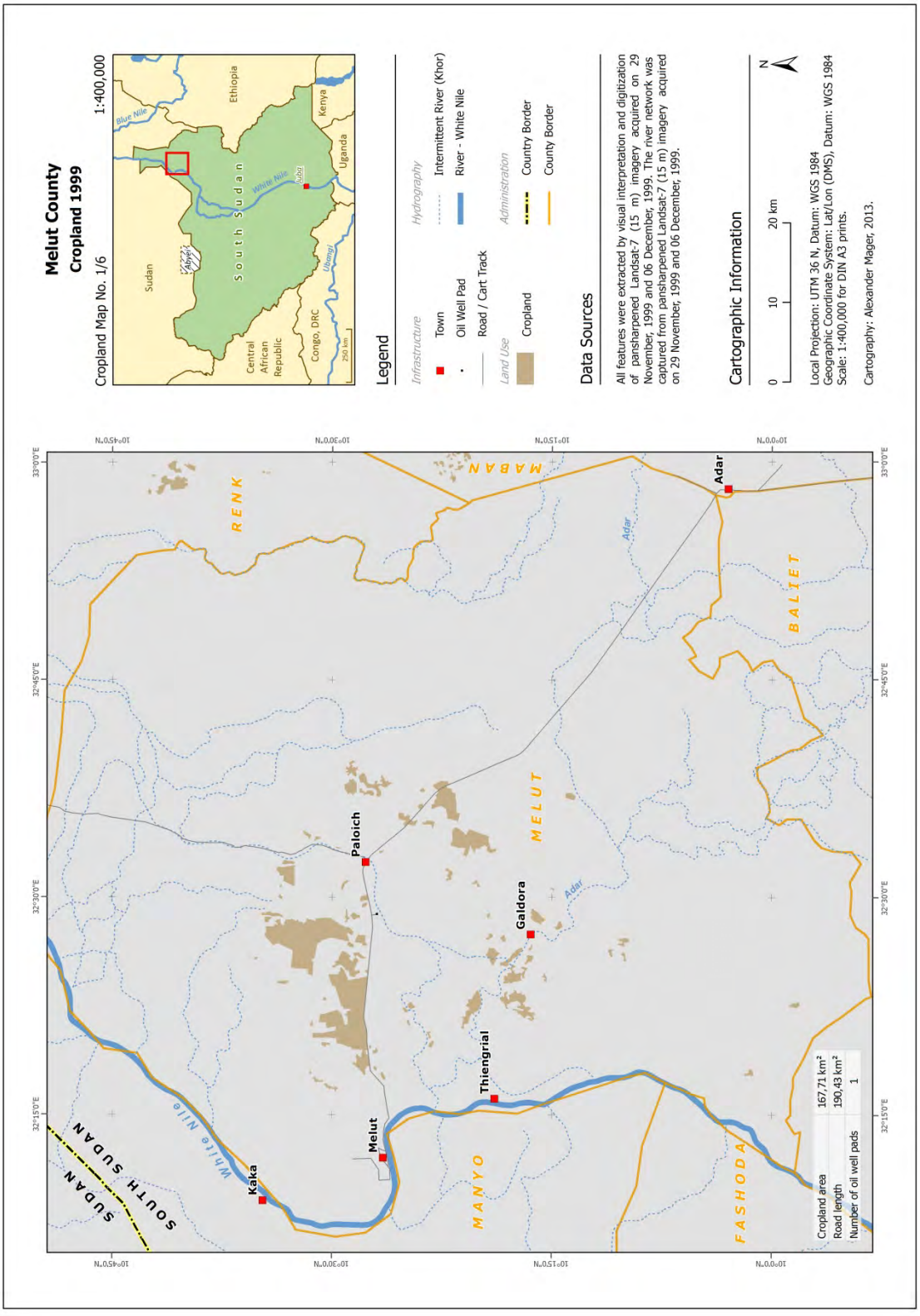

Figure 52: Cropland Map No. 1/6 (1999)

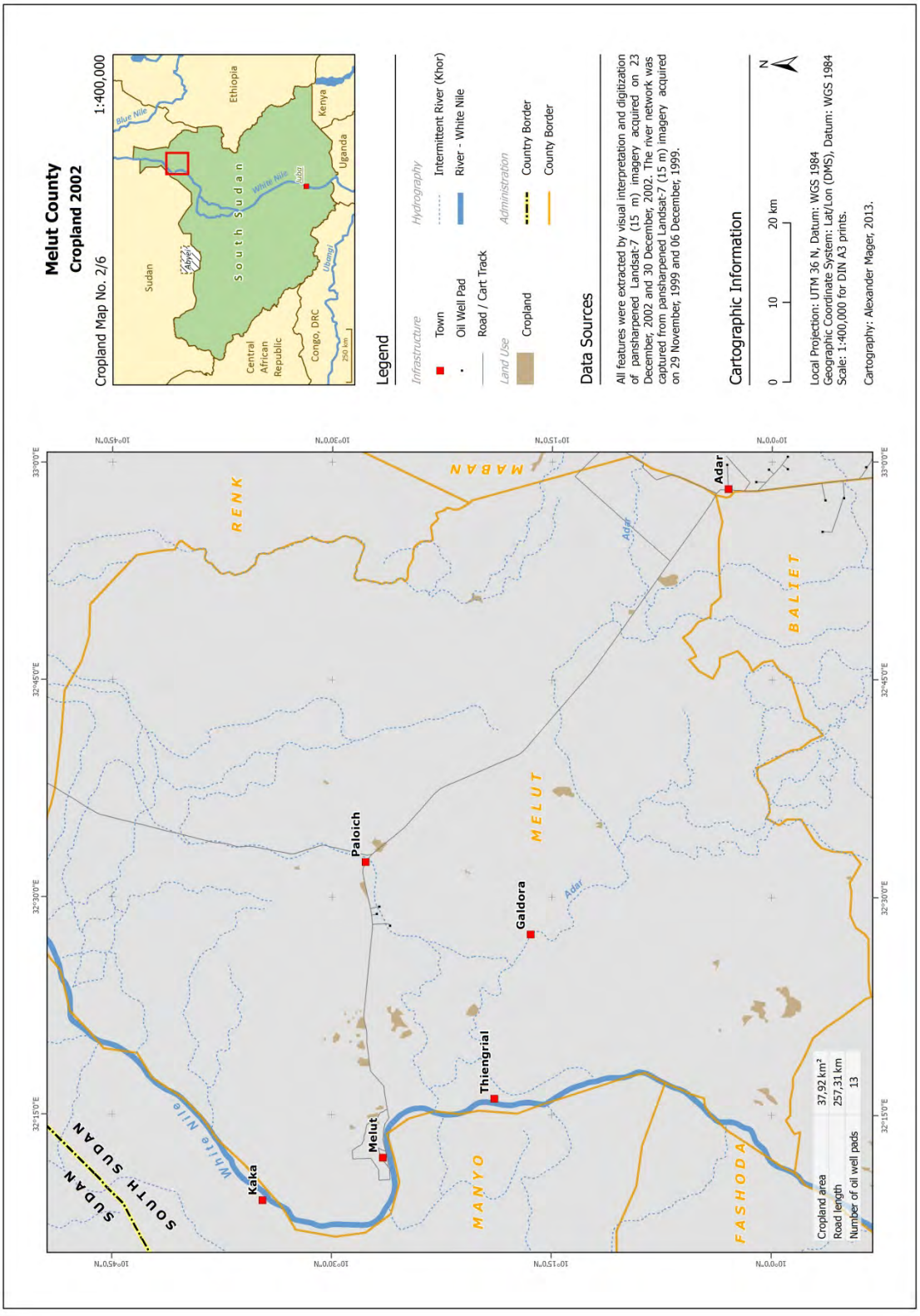

Figure 53: Cropland Map No. 2/6 (2002)

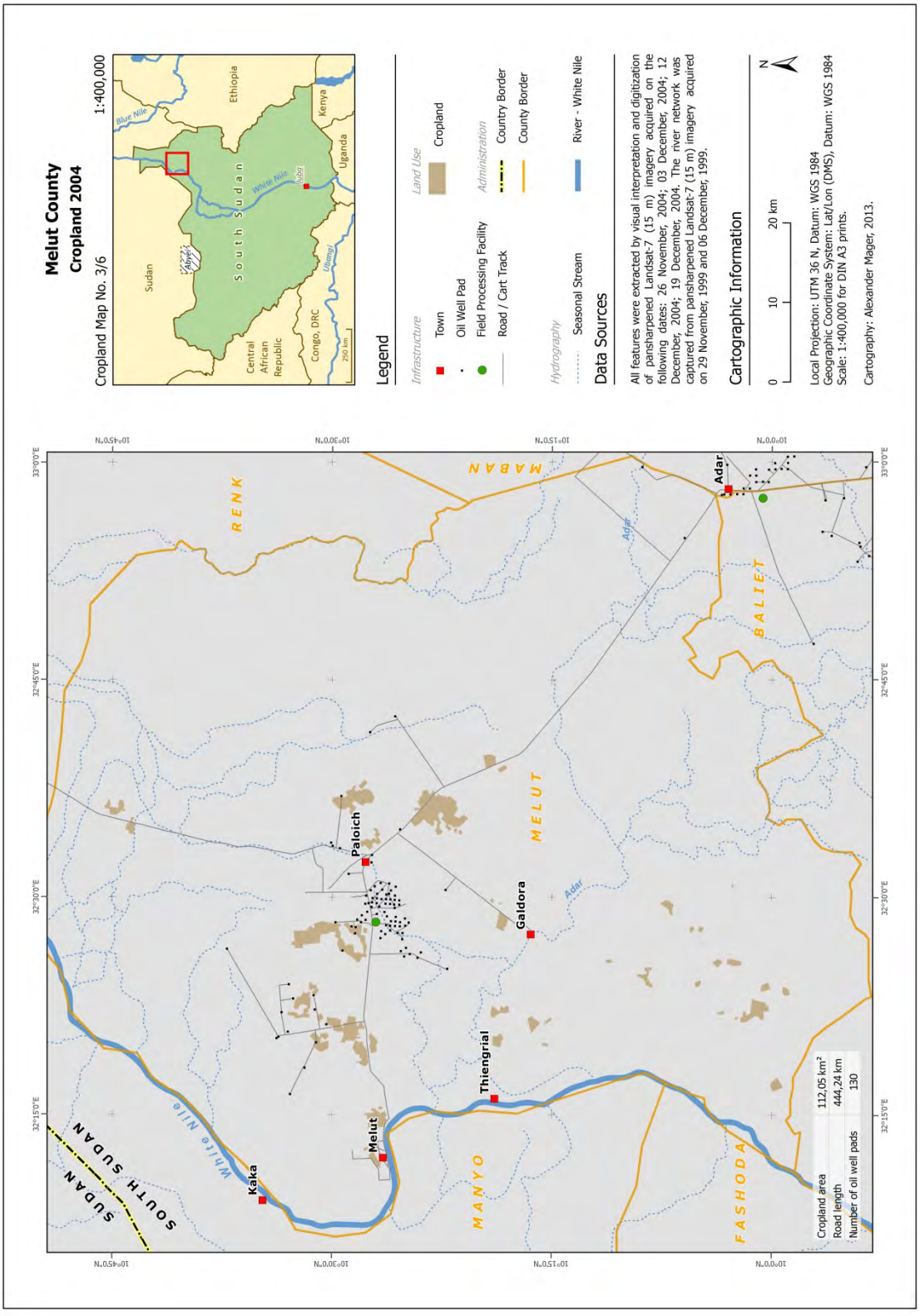

Figure 54: Cropland Map No. 3/6 (2004)

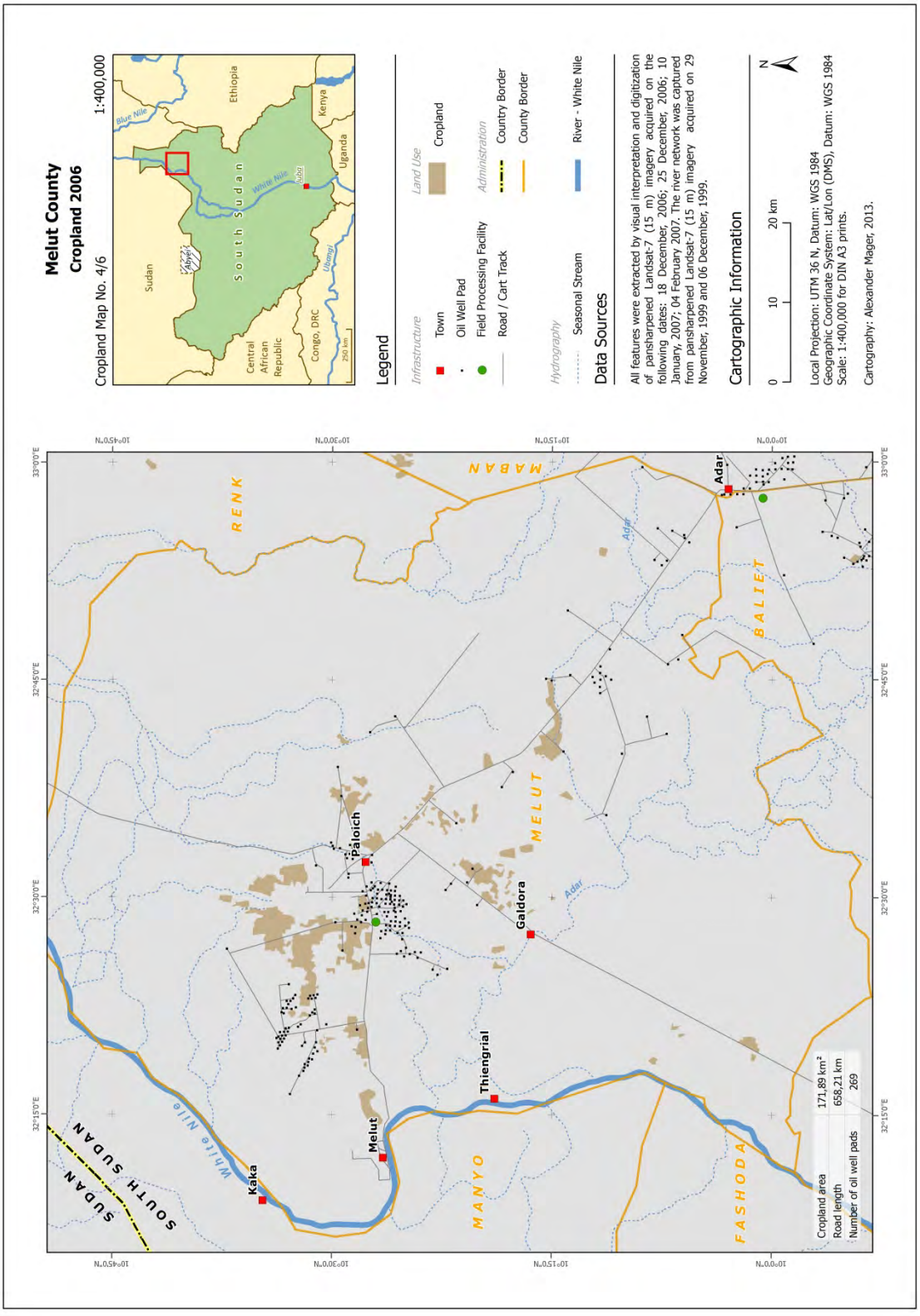

Figure 55: Cropland Map No. 4/6 (2006)

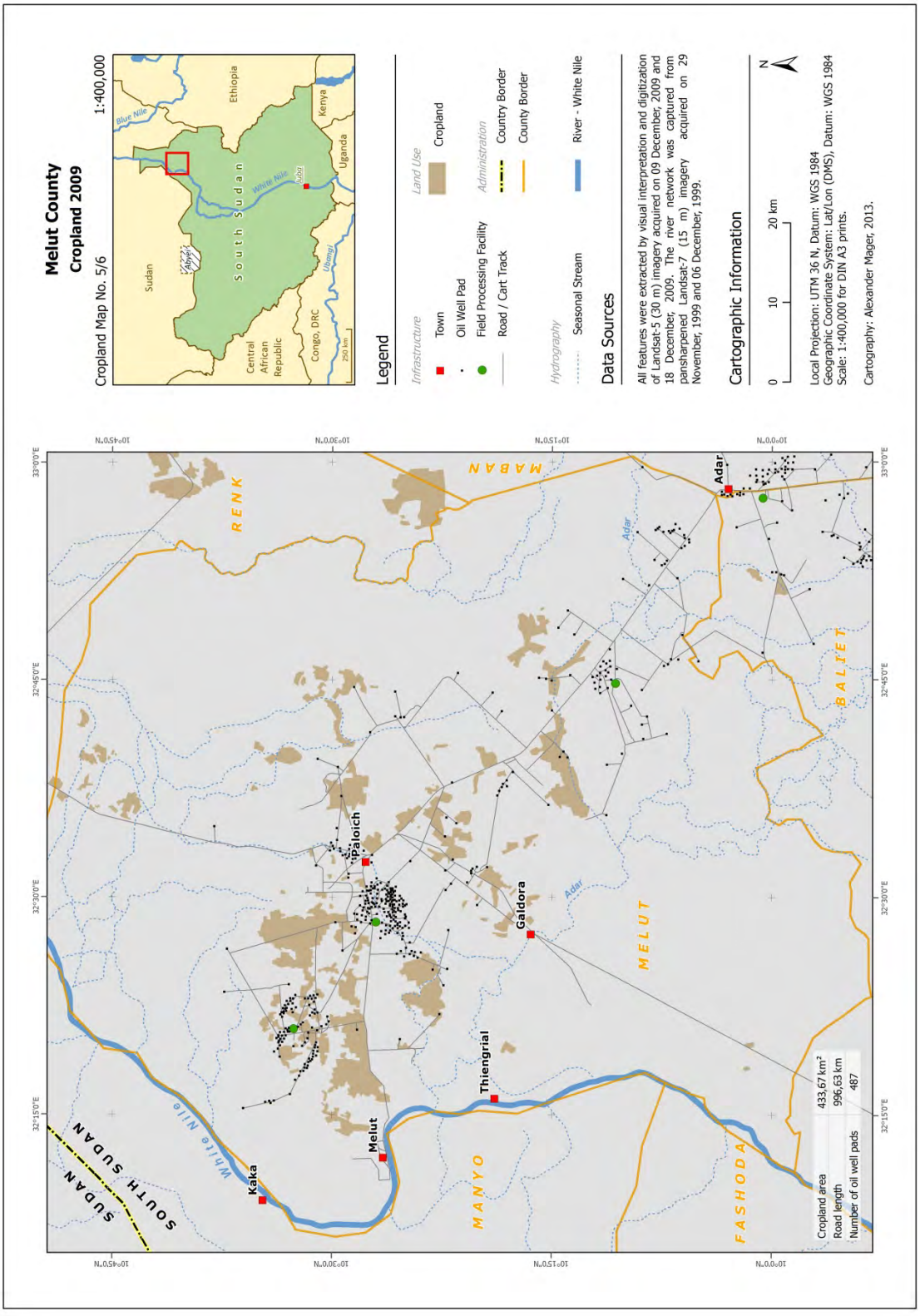

Figure 56: Cropland Map No. 5/6 (2009)

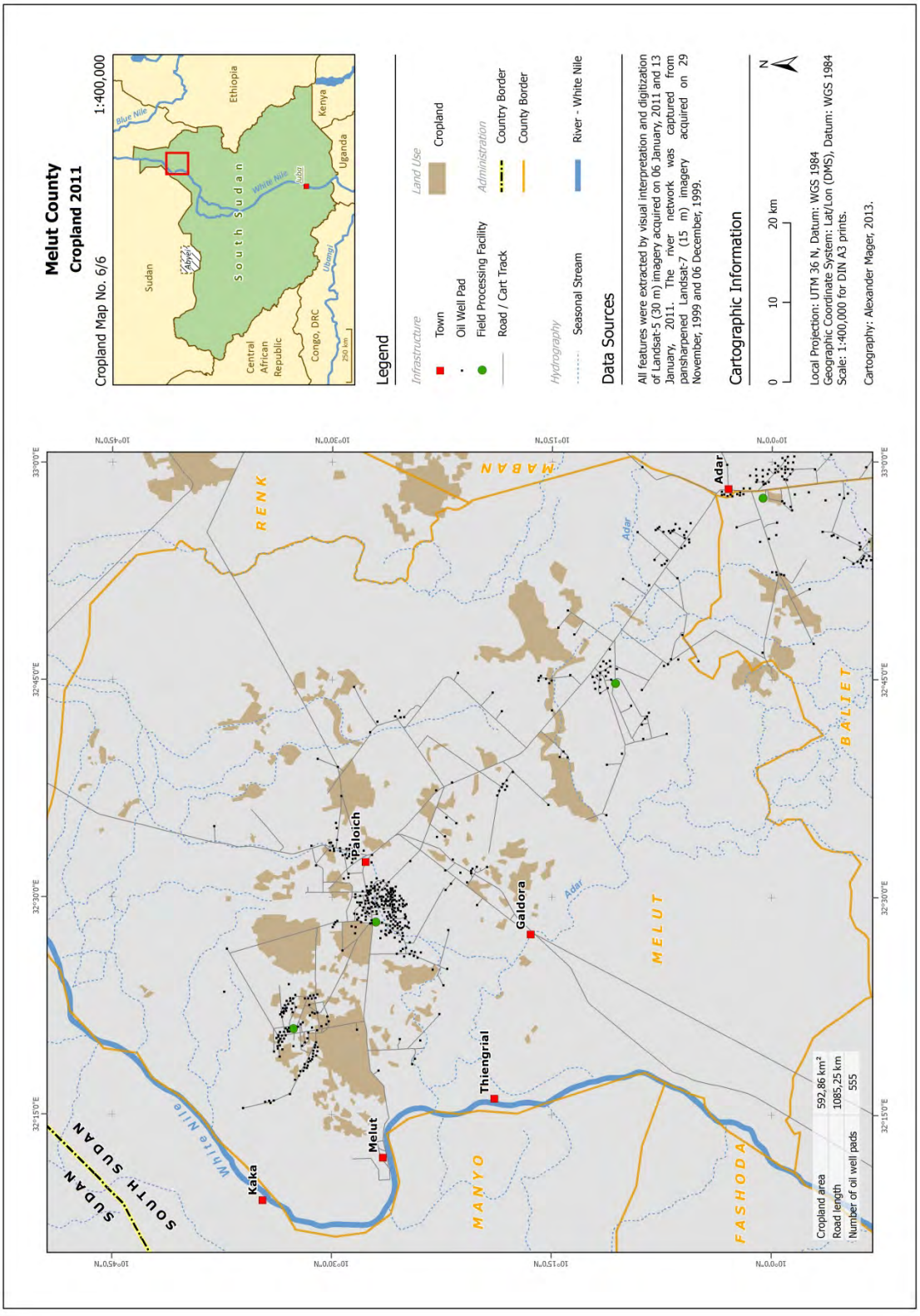

Figure 57: Cropland Map No. 6/6 (2011)

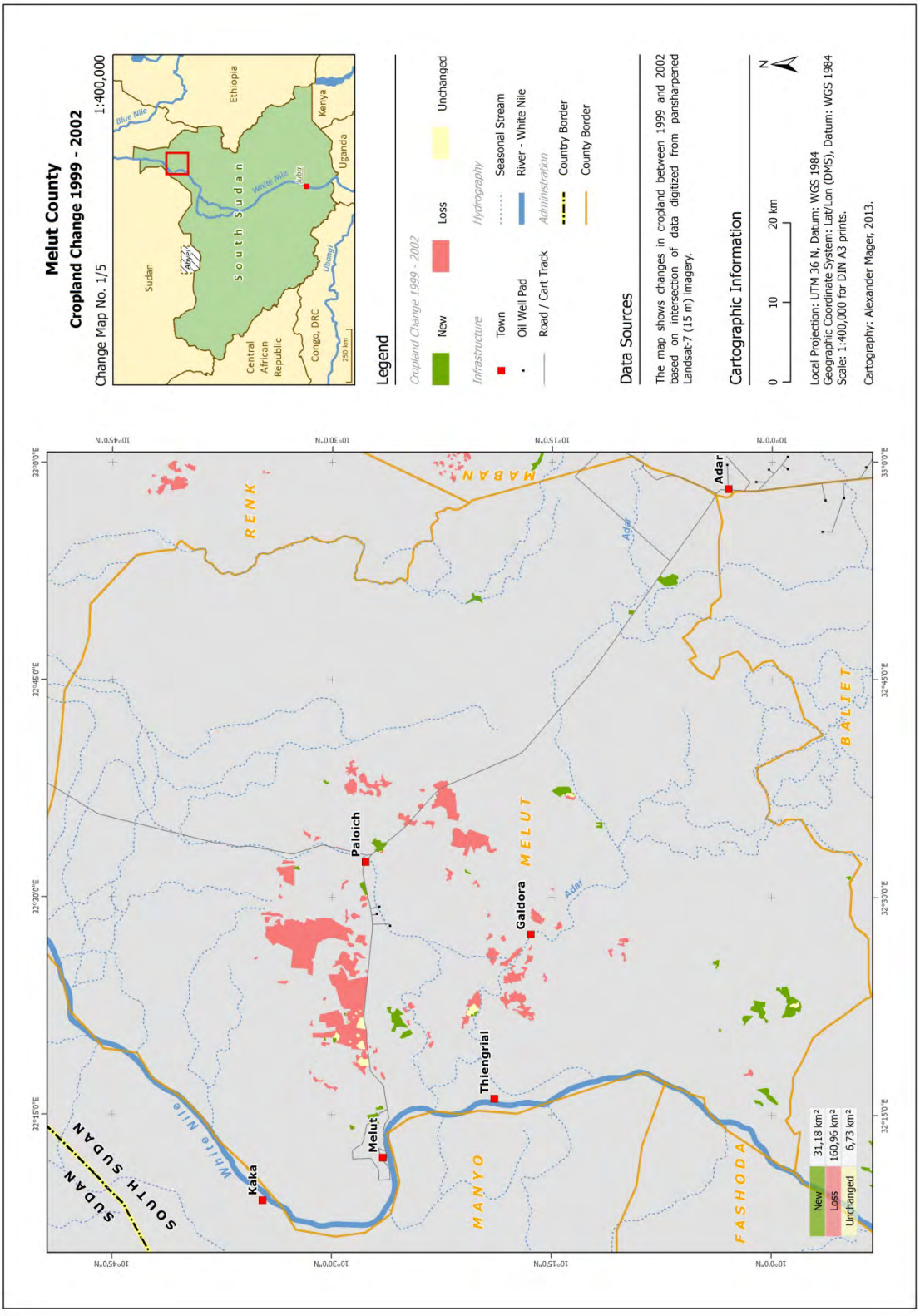

Figure 58: Change Map No. 1/5 (1999-2002)

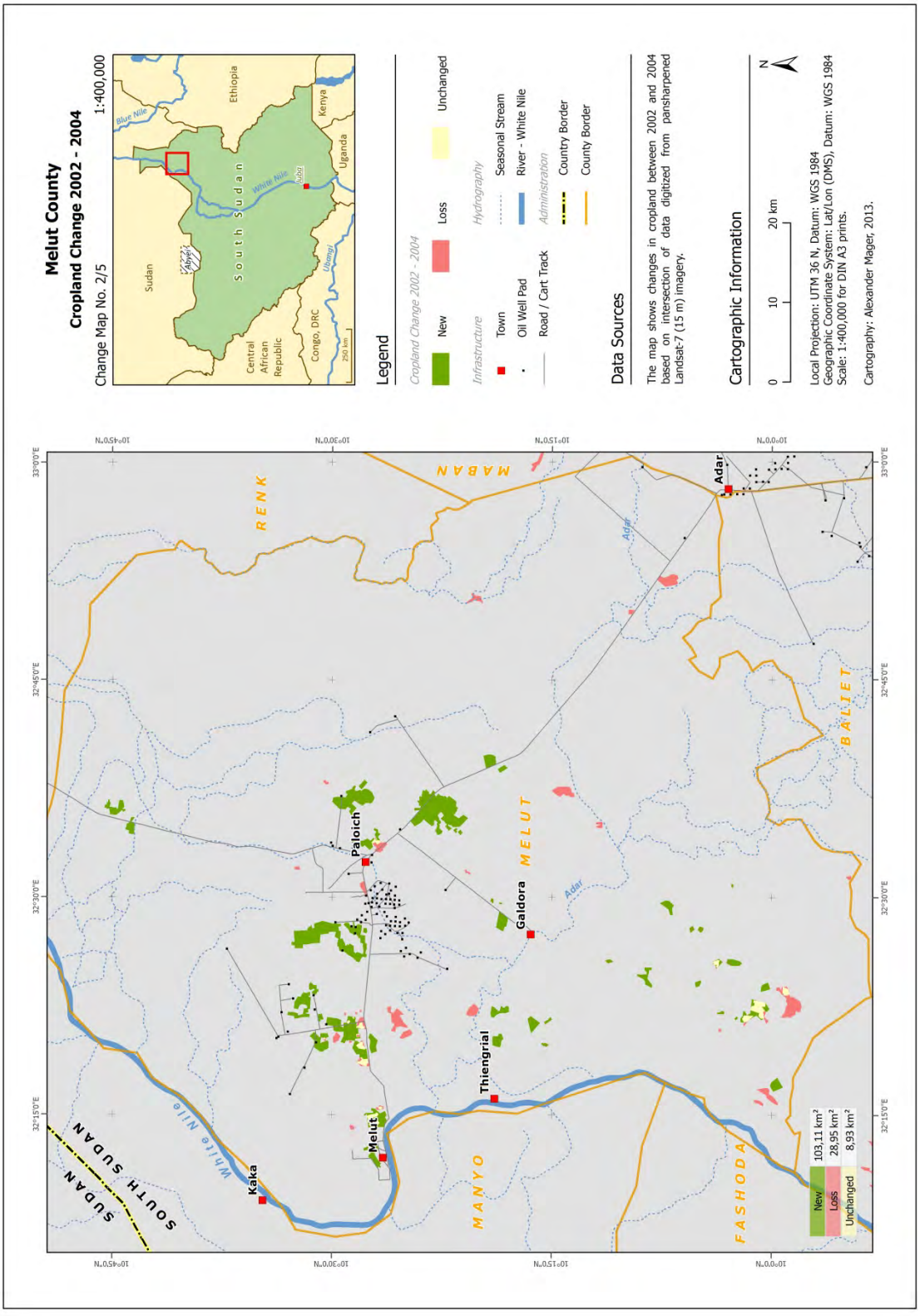

Figure 59: Change Map No. 2/5 (2002-2004)

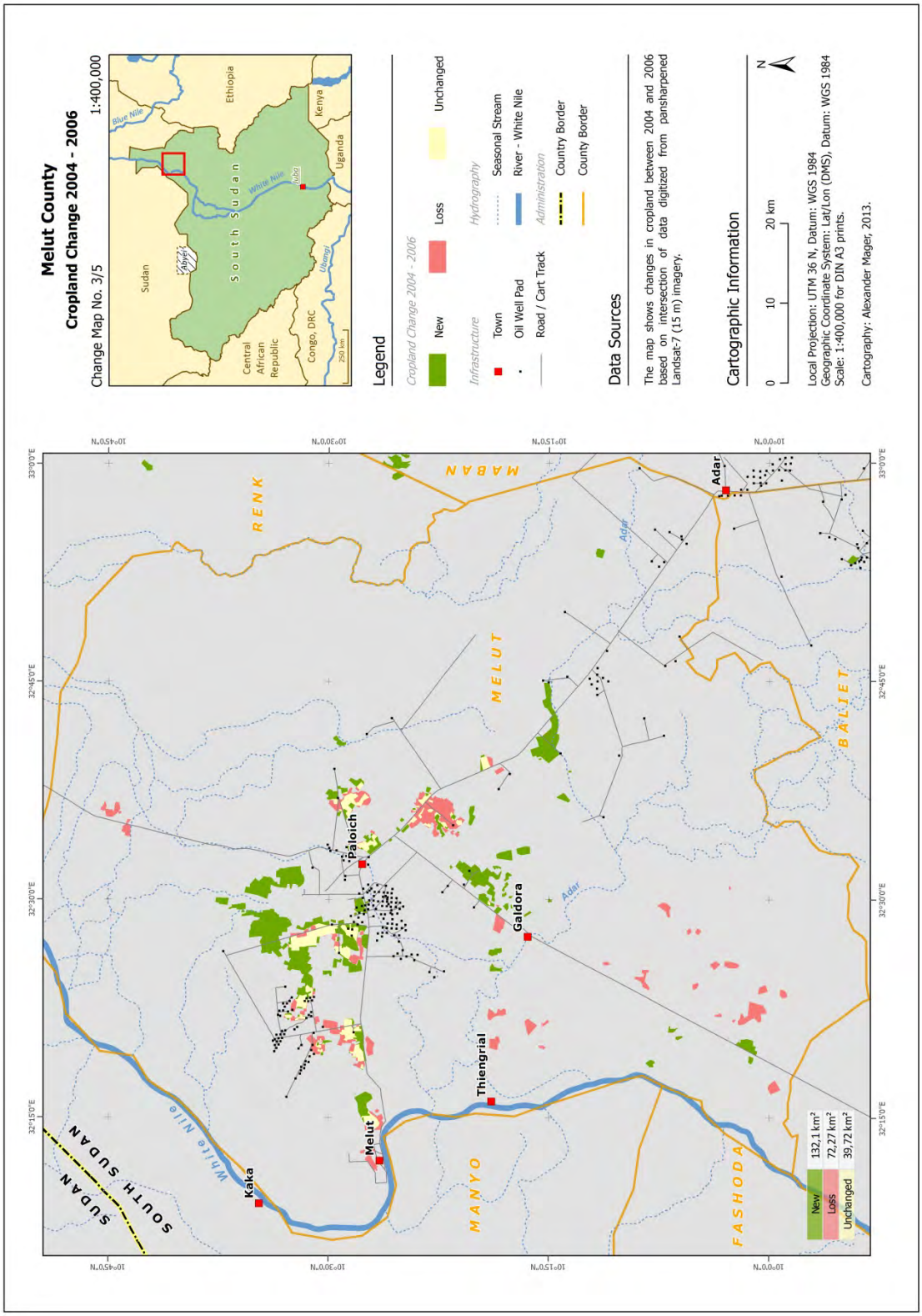

Figure 60: Change Map No. 3/5 (2004-2006)

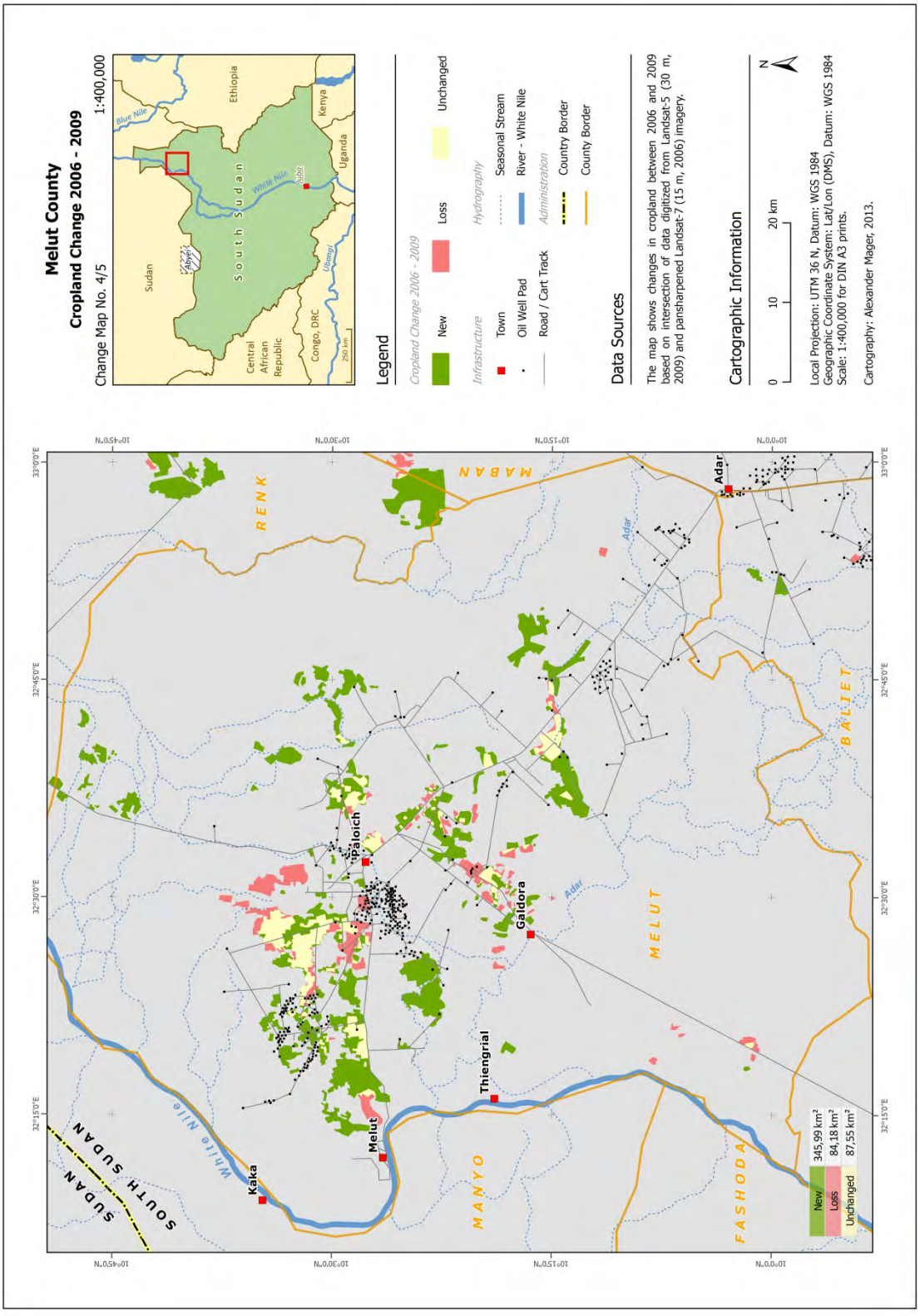

Figure 61: Change Map No. 4/5 (2006-2009)

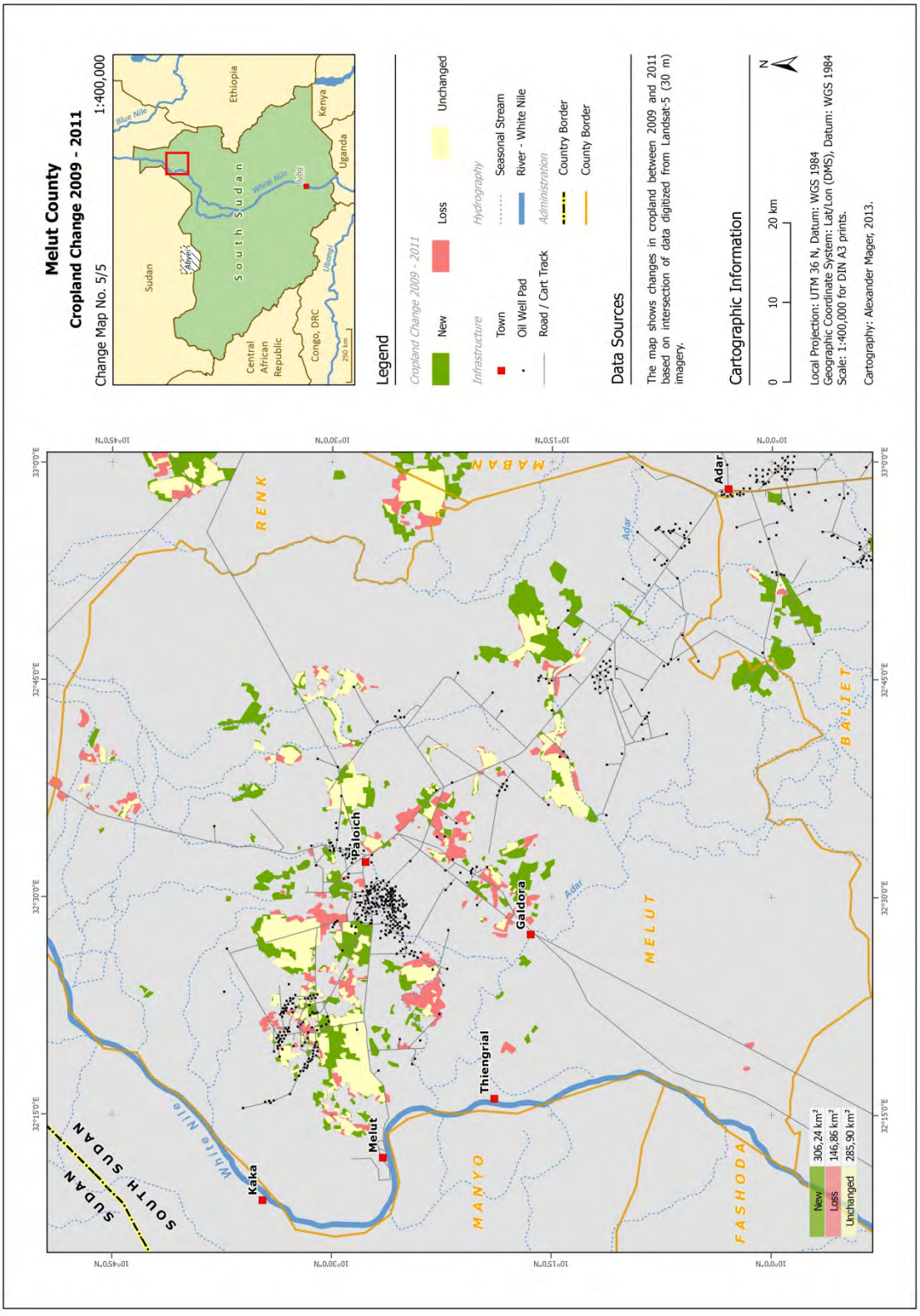

Figure 62: Change Map No. 5/5 (2009-2011)

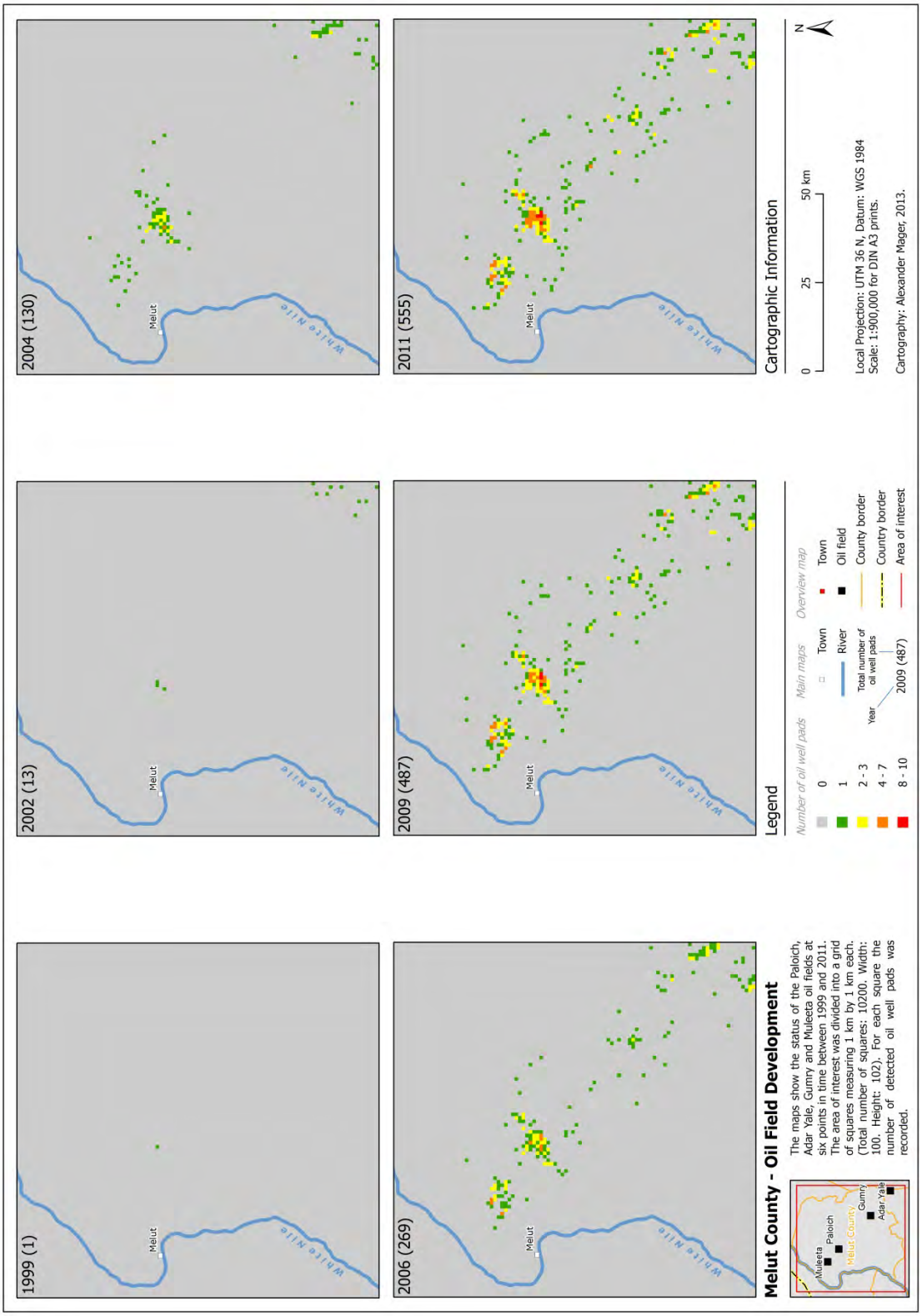

Figure 63: Oil field development

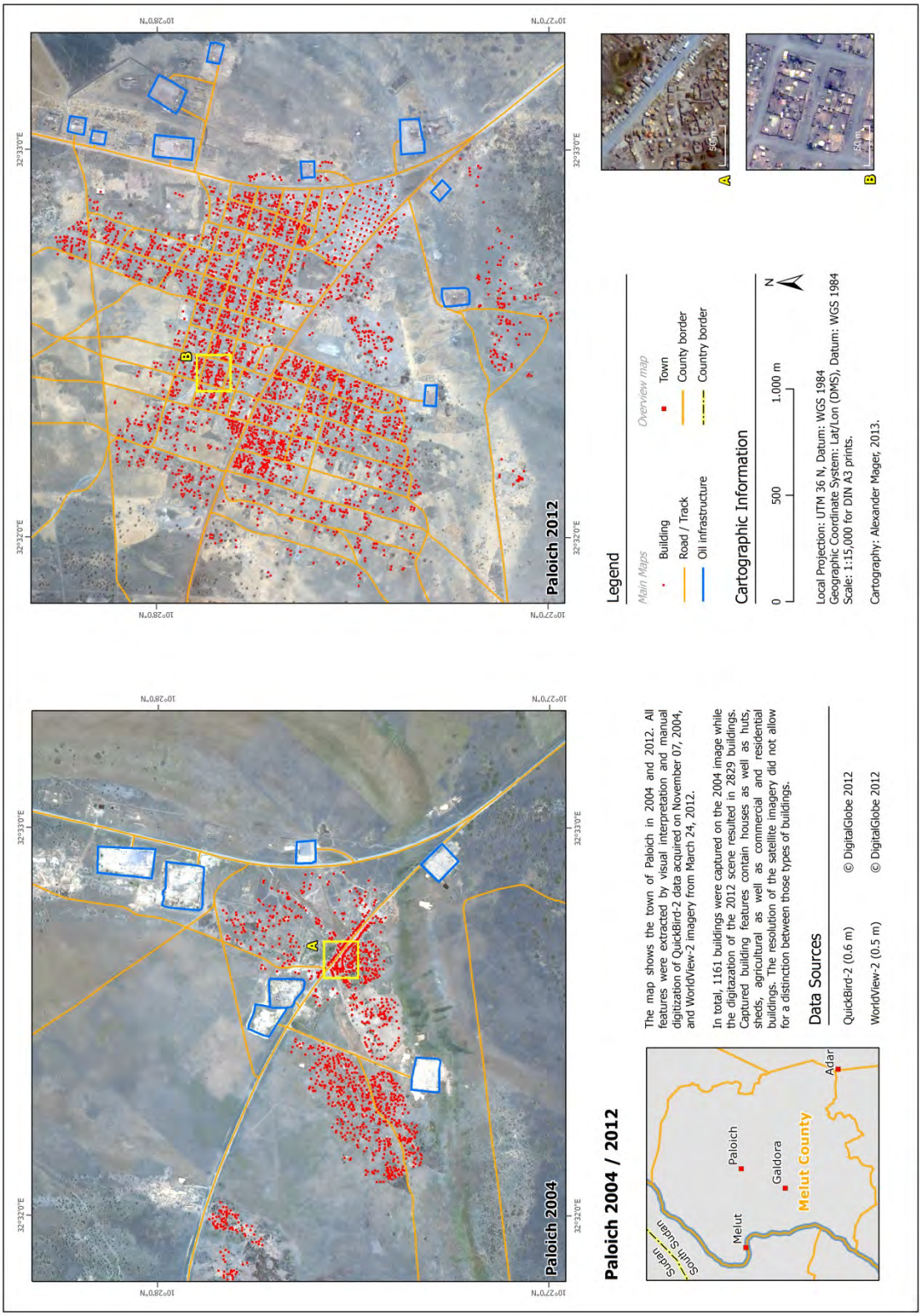

Figure 64: Paloich 2004 / 2012

8.3 Land cover data sets

Source	Year (Release)	Spatial Resolution	Data Sources	Classes present in area of interest
CDE: University of Bern, Centre for Development and Environment (South Sudan)	2008	30 m	Landsat ETM+ 7/4/2 EarthSat NatVue data (2000) QuickBird-2 (2003-2005)	1 – Sparse Vegetation 2 – Shrubby Vegetation 3 – Dense Vegetation 4 – Wetlands 5 – Surface Water / Wet Season 6 – Agriculture 7 – Outcrop / No vegetation 8 – Settlement Area
FAO Africover (Several African countries)	2003	30 m	Landsat TM (1994-1999)	10223-11971 Rainfed Herbaceous crop - Medium Fields 10282 Rainfed Herbaceous crop, Small Fields 10675-12006 Irrigated Herbaceous Crop (1 add. Herbaceous Crop), Medium Fields 20304 Open general woody with closed to open herbaceous 20389 Open low shrubs with herbaceous 10302 Rainfed Herbaceous Crop, Small Fields, Isolated 20868-15058 Open general trees with open herbaceous and sparse shrubs 21647 Closed to very open herbaceous with sparse trees and sparse shrubs 21648 Closed to very open herbaceous with sparse shrubs 10292 Rainfed Herbaceous Crop, Small Fields, Clustered 40366 Open general shrubs with closed to open herbaceous on permanently flooded land 40371 Open general shrubs with closed to open herbaceous ontemporarily flooded land 42347-R1 Closed to Open Herbaceous On Permanently Flooded Land 10296 Clustered Small Herbaceous Fields - Post Flooding / Waterlogged 5003-9 Urban area - general 8002-1-V1 River
ESA Globcover (Global)	2008	300 m	Unknown (2005)	14 – Rainfed Croplands 20 – Mosaic Croplands/Vegetation 30 – Mosaic Vegetation/Croplands 60 – Open broadleaved deciduous forest 110 – Mosaic forest – Shrubland/Grassland 120 – Mosaic Grassland/Forest – Shrubland 130 – Closed to open shrubland 140 – Closed to open grassland 180 – Closed to open vegetation regularly flooded 190 – Artificial areas 200 – Bare areas 210 – Water bodies

Figure 65: Land cover data sets I

Source	Year (Release)	Spatial Resolution	Data Sources	Classes present in area of interest
Food Policy Research Institute (Global)	2002	30 arc seconds (approx. 1 km)	Unknown	13 – Cropland / Pasture 15 – Agriculture with other vegetation 21 – Agriculture / Other mosaic 31 – Other vegetation with agriculture 40 – Agriculture / 2 other land cover types 42 – Primarily Grassland 60 –Non-vegetated / Sparsely vegetated 70 – In-land water
JRC GLC2000 (Global)	2004	1 km at equator (approx. 975 m in AOI)	SPOT Vegetation (2000)	12 – Shrub Cover, closed-open, deciduous 13 – Herbaceous Cover, closed-open 14 – Sparse herbaceous or sparse shrub cover 16 – Cultivated and managed areas 18 – Mosaic: Cropland / Shrub and/or grass cover
USGS (Africa)	2003	30 arc seconds (approx. 1 km)	Unknown (2000)	2 – Dryland, cropland and pasture 6 – Cropland / Woodland mosaic 7 – Grassland 10 – Savanna 16 – Water body 19 – Barren or sparsely vegetated

Figure 66: Land cover data sets II